Atrium Models for the Analysis of Thermal Comfort and Energy Use

A Report of Task 12
Building Energy Analysis and
Design Tools for Solar Applications

Project A.3   Atrium Model Development

Edited by
Ida Bryn and
Per Arne Schiefloe

T.12.A.3-1

March 1996

INTERNATIONAL ENERGY AGENCY
Solar Heating & Cooling Programme

PREFACE

INTRODUCTION TO THE INTERNATIONAL ENERGY AGENCY

BACKGROUND

The International Energy Agency was founded in November 1974 as a cooperation among industrialized nations to address energy policy issues. It is an autonomous body within the framework of the Organization for Economic Cooperation and Development (OECD). Twenty-one countries are presently members, with the Commission of the European Communities also participating in the work of the IEA under a special agreement.

One element of the IEA's program involves cooperation in the research and development of alternative energy resources in order to reduce excessive dependence on oil. A number of new and improved energy technologies which have the potential of making significant contribution to global energy needs were identified for collaborate efforts. The IEA Committee on Energy Research and Development (CRD), comprising representatives from each member country, supported by a small Secretariat staff, is the focus of IEA R & D activities. Four Working Parties (Conservation, Fossil Fuels, Renewable Energy, and Fusion) are charged with identifying new areas for cooperation and advising the CRD on policy matters in their respective technology areas.

SOLAR HEATING AND COOLING PROGRAM

Solar Heating and Cooling was one of the technologies selected for joint activities. During 1976 - 1977, specific projects were identified in key areas of this field and a formal implementing Agreement drawn up. The Agreement covers the obligations and rights of the Participants and outlines the scope of each project or "Task" in annexes to the document. There are now twenty signatories to the Agreement:

Australia	France	Spain
Austria	Germany	Sweden
Belgium	Italy	Switzerland
Canada	Japan	Turkey
Denmark	Netherlands	United Kingdom
European Commission	New Zealand	United States
Finland	Norway	

The overall program is managed by an Executive Committee, while the management of the individual Tasks is the responsibility of Operating Agents. The tasks of the IEA Solar Heating and Cooling Programme, their

I

respective Operating Agents, and current status (ongoing or completed) are as follows:

Task 1   Investigation of the Performance of Solar Heating and Cooling Systems, Technical University of Denmark (Completed)

Task 2   Coordination of Research and Development of Solar Heating and Cooling-Solar Research Laboratory-GIRN, Japan (Co pleted)

Task 3   Performance Testing of Solar Collectors - University College, Cardiff, UK (Completed)

Task 4   Development of an Isolation Handbook and Instrument Package - U.S. Department of Energy (Completed)

Task 5   Use of Existing Meteorological Information for Solar Energy Application, Swedish Meteorological and Hydrological Institute (Completed)

Task 6   Performance of Solar Heating, Cooling, and Hot Water Systems Using Evacuated Collectors - U.S. Department of Energy (Completed)

Task 7   Central Solar Heating Plants with Seasonal Storage - Swedish Council for Building Research (Completed)

Task 8   Passive and Hybrid Solar Low Energy Building - U.S. Department of Energy (Completed)

Task 9   Solar Radiation and Pyranometry Studies - KFA Jülich，Germany (Completed)

Task 10   Solar Materials R&D-AIST, Ministry of International Trade and Industry, Japan (Completed)

Task 11   Passive and Hybrid Solar Commercial Building-Swiss Federal Office of Energy (Completed)

Task 12   Building Energy Analysis and Design Tools for Solar Applications - U.S. Department of Energy (Ongoing)

Task 13   Advanced Solar Low Energy Buildings - Norwegian Institute of Technology (Ongoing)

Task 14   Advanced Active Solar Energy Systems - Canadian Department of Energy, Mines and Resources (Ongoing)

II

Task 15   Advanced Central Solar Heating Plants with Seasonal Storage
               (In Planning Stage)

Task 16   Photovoltaics in Buildings - KFA, Jülich, Germany (Ongoing)

Task 17   Measuring and Modelling Spectral Radiation Affecting Solar
               Systems and Buildings - KFA, Jülich, Germany (Ongoing)

Task 18   Advanced Glazing Material - U.K. Department of Energy
               (Ongoing)

Task 19   Solar Air Systems in Buildings - Swiss Federal Office of En-
               ergy (Ongoing)

Task 20   Solar Energy in Building Renovation - Swedish Council for
               Building Research (Ongoing)

Task 21   Daylighting - Danish Building Research Institute (Ongoing)

**TASK 12:   BUILDING ENERGY ANALYSIS AND DESIGN TOOLS FOR
               SOLAR APPLICATIONS**

The scope of Task 12 includes: (1) Selection and development of appropri-
ate algorithms for modelling of solar energy related materials, components
and systems within the building in which these solar elements are integrated,
(2) Selection of analysis and design tools and evaluation of the algorithms
as to their ability to model the dynamic performance of the solar elements in
respect to accuracy and ease of use, and (3) Improvement of the usability of
the analysis and design tools, through preparation of common formats and
procedures, and by standardization for input/output, default values and other
user-related factors.

The subtasks of this project are:

    A: Model Development
    B: Model Evaluation
    C: Model Use

The participants in this Task are: Denmark, Finland, Germany, Norway,
Spain, Sweden, Switzerland and the United States. The United States
serves as Operating Agent for this Task, Michael Holtz of Architectural
Energy Corporation serves as the Operating Agent on behalf of the U.S.
Department of Energy.

This report documents work carried out under Subtask A.3 of this Task
entitled Atrium Model Development.

Project A.3   Atrium Model Development

Project leader: Norway

Participants:

Denmark   Mr. Kjeld Johnsen
                        Danish Building Research Institute
                        P.O. Box 119
                        2970
                        Phone +45-42-865533, Fax +45-42-867535

Norway   Dr. Ida Bryn
                        Erichsen & Horgen A/S
                        P.O.Box 4464 Torshov,
                        N-0403 OSLO
                        Phone +47-22 02 63 00 Fax +47-22 02 63 90

Sweden   Dr. Maria Wall
                        Dr. Bertil Fredlund
                        Lund Institute of Technology
                        Department of Building Science,
                        P.O.Box 118, S-22100 Lund
                        Phone +46-46-2220000, Fax +46-46-2224719

Switzerland   Mr. Dominique Chuard
                        Mr. Pierre Jaboyedoff
                        Sorane SA
                        Route de Châtelard 52
                        CH-1018 Lausanne
                        Phone +41-21-6471175, Fax +41-21-6468876

NOTICE

IV

List of Authors/Editors

BF   **Bertil Fredlund,** Lund Institute of Technology, Department of Building Science,
P.O.Box 118, S-22100 Lund
Phone +46-46-2220000, Fax +46-46-2224719

DA   **Dario Aiulfi,** Sorane SA, rte de Châtelard 52, CH-1018 Lausanne
Phone +41-21-6471175, Fax +41-21-6468876

DC   **Dominique Chuard,** Sorane SA, rte de Châtelard 52, CH-1018 Lausanne
Phone +41-21-371-175, Fax +41-21-6468876

HK   **Hasse Kvist,** Lund Institute of Technology, Department of Building Science,
P.O.Box 118, S-22100 Lund
Phone +46-46-2220000, Fax +46-46-2224719

IB   **Ida Bryn,** Erichsen & Horgen A'S, P.O.Box 4464 Torshov, N-0403 OSLO
Phone +47-22 02 63 00 Fax +47-22 02 63 90

JR   **Johann Reiß,** Fraunhofer Institut für Bauphysik, Nobelstraße 12,
P.O.Box 80 04 69, D-70569 Stuttgart 80
Phone +49 71 1-970 3337 (0000), Fax +49-711-970 3399

KJ   **Kjeld Johnsen,** Danish Building Research Institute, DK-2970
Phone +45-42-865533, Fax +45-42-867535

KK   **Kurt Källblad**, Lund Institute of Technology, Department of Building Science,
P.O.Box 118, S-22100 Lund
Phone +46-46-2220000, Fax +46-46-2224719

KKo **Kjell Kolsaker,** Norwegian University of Science and Technology,
Department of Refrigeration and Air Conditioning, N-7034 Trondheim
Phone +47 73 59 38 60, Fax +47 73 59 38 59

KTA **Karl Terpager Andersen,** Danish Building Research Institute,
DK-2970 Hörsholm
Phone +45-42-865533, Fax +45-42-867535

MJH **Michael J. Holtz,** Architectural Energy Corporation
2540 Frontier Avenue, Suite 201, Boulder, Colorado 80301 USA
Phone +1-303 444-4149, Fax +1-303 444-4304

MW   **Maria Wall,** Lund Institute of Technology, Department of Building Science,
P.O.Box 118, S-22100 Lund
Phone +46-46-2220000, (direct line 2229662) Fax +46-46-2224719

PAS **Per Arne Schiefloe,** SINTEF Energy, N-7034 Trondheim
Phone +47 73 59 16 34, Fax +47 73 59 39 26

POT **Per Olaf Tjelflaat,** Norwegian University of Science and Technology,
Department of Refrigeration and Air Conditioning, N-7034 Trondheim
Phone +47 73 59 38 60, Fax +47 73 59 38 59

PS   **Peter Schild,** Norwegian University of Science and Technology,
Department of Refrigeration and Air Conditioning, N-7034 Trondheim
Phone +47 73 59 38 60, Fax +47 73 59 38 59

Abstract

This report describes models for thermal comfort and energy consumption in atria. These are models which have not been included in many of the commonly used building energy simulation tools today, and improvements of these programs constitute the main result of this work. The models include infiltration and natural ventilation, stratification, air flow patterns, surface film coefficients and solar radiation. Some of the models have been tested against monitored performance data. In cases were data have been unavailable, they have been obtained by use of computational fluid dynamics (CDF) models. CFD models have also been used in order to validate the simplified models developed here.

The models have been integrated in different computer programs. These are generally simplified tools, often used in the design phase of atria and other, more conventional buildings. As a result of this, these programs have become more reliable and accurate as they include new and better models.

Contents

Contents

X

Background

An atrium has become a fashionable feature to use in commercial and institutional building design. It provides a dramatic visual and spatial experience and brings light and view to the interior of the building. Saving energy is not the primary reason why atria are incorporated into the design of buildings. Nevertheless, energy has become a concern because these atrium spaces typically incorporate large areas of glazed surfaces, and the resultant solar heat gains and thermal losses may play a significant role in the overall energy performance of the building. An atrium reduces the daylight level, but due to the buffer effect, the glazing in the walls between the atrium and adjacent spaces may be increased, and the need for electric lighting reduced.

Improper design of an atrium may result in significantly higher energy costs than if the atrium was excluded from the design. However, given that atria will be incorporated into the design for non-energy reasons, it is essential that it is designed to be at a minimum energy neutral; that is, it does not adversely impact the total building energy costs. A better approach is to design the atrium to provide a net energy benefit, actually reducing the total energy costs of the building.

An atrium represents a complex thermal and luminous environment. Numerous interactions exist between the atrium, the outdoor environment and the spaces adjacent to the atrium. These interactions are dynamic and vary by time of day and season, and by the operation of the building's HVAC and lighting systems. The effective design of an atrium requires an understanding of these various thermal and luminous interactions, and an ability to assess the influence of various design configurations on them.

Apart from measuring a physical model, calculations and simulations are the only means for a designer to determine the performance variables of the building. The results of the calculations form the basis for the evaluation of the design.

XIII

Simplified design tools are to be used in an early design phase when basic parameters are set and indication of where problems may occur is important. Detailed simulation tools are used as the design evolves and more details are available to solve problems that remain. The following example shows how tools at different levels can be used when developing ideas. An architect plans a shopping centre with a glass-covered street that connects the shops. The street is to be unheated. An "outdoor" cafe is planned in connection with a restaurant. In the early design phase the designer uses a simplified design tool that calculates the monthly energy consumption in the main building, monthly average, maximum and minimum temperatures in the atrium and the main building. The results indicate that the energy consumption, minimum and average temperatures are acceptable, but that over-heating may occur in the south facade of the main building. A more detailed model is used to simulate the south facade as a temperature zone hour by hour, and a satisfactory solution is found by applying shading and night ventilation. A whole year simulation for the building is also performed as more detailed data are available. The comfort analysis in the program indicates that draught may be a problem in parts of the atrium. A Computational Fluid Dynamics model is used to study the air movements and temperatures in the atrium. A one metre high shelter is put up around the cafe increasing comfort for people sitting within this shelter.

Experience shows that simplified design tools for calculation of the thermal and energy conditions on a monthly basis are not very accurate, but they are quick and simple to understand. They provide means to give a good overview of the thermal and energy performance at an early phase of the design, but they should not be used for anything more than that. When detailed solutions are to be studied, building energy simulation programs should be used. As the building energy simulation programs can handle several temperature zones, they have been most commonly used when studying atria. Research findings show that these tools also have several limitations. The following limitations of existing tools are reported in "IEA Task XI, Passive and Hybrid Solar Commercial Buildings" (Hastings, 1994. *Passive Solar Commercial and Institutional Buildings.* Wiley, England):

> "In attempting to simulate energy performance and comfort conditions in atria, several limitations in existing analysis tools are encountered. The key problems are identified below:
>
> *INFILTRATION AND NATURAL VENTILATION: The algorithms used in most existing simulation programs to calculate infiltration and natural ventilation rates do not account for the interaction of temperature and wind pressure dependent air flow between a particular space and its surrounding spaces and environ-*

XIV

ment, or the dependence of either component of air flow on the geometric configuration of the space, mode of operation (e.g., presence of ventilation openings), or interaction with mechanical ventilation. In order to properly represent buoyancy and cross venting effects, simulation programs must be capable of predicting air flow rates in multi-zone configurations, accounting for both natural and mechanical ventilation, and including the dependence on height and temperature gradients in the space.

STRATIFICATION: Existing simulation programs calculate a single indoor air temperature in each thermal zone being analyzed. The real temperature distributions in the space are important in determining transmission heat losses; air change rate between the atrium and ambient, and between the atrium and adjacent spaces; air motion within the atrium; and comfort conditions. In order to provide a more faithful representation of thermal conditions in an atrium, the spatial distribution of air and surface temperatures must be determined.

AIR FLOW PATTERNS: None of the existing simulations account for air movements within individual zones. Air movements influence transient thermal conditions, temperature distributions, comfort conditions and energy performance. For example, none of the programs explicitly estimate the impact of "drafts" caused by downward air flow at cold surfaces on comfort conditions, or the impact of free upward convection from heating devices on heat losses through surfaces above the heater. Algorithms are needed which enable local air flow distribution to be calculated.

SURFACE FILM COEFFICIENTS: Most calculation programs provide fixed, global values for surface film coefficients, and many do not even account separately for the convective and radiant components of heat transfer at the surface. Because there are often substantial local differences of air flow and temperature conditions within atria, the magnitudes of each component can vary significantly from surface to surface, affecting heat transfer and comfort conditions.

SOLAR RADIATION: Few simulation programs use geometric models to calculate the distribution of solar radiation on surfaces internal to a zone, or solar radiation transmission through glazed partition walls to adjacent spaces. Failure to accurately account for the distribution of solar gains between the atrium and its adjacent spaces negatively impacts the reliability of daylighting and thermal calculations. Furthermore, proper accounting for the distribution of solar gains among surfaces is necessary in order to properly calculate surface temperature, and therefore air flow profiles,

convection coefficients at surfaces, interior air temperature distributions, and radiative exchange between surfaces.

All of the problems identified above are interconnected, and, to some extent, result from the basis of existing programs in heat transfer, rather than mass transfer. Various "tricks" can be used to circumvent some of the problems - at least in part. For example, temperature stratification and air flow patterns in large spaces such as atria can be approximated by sub-zoning the space into two or more adjacent zones which can be at different temperatures and between which air exchange can be modelled; this allows the spatially continuous variation in temperatures within the larger space to be approximated as discrete changes in temperature across sub-zone partitions. While this may improve the representation of the atrium in the simulation, it requires considerable engineering judgement that is typically not based on well defined facts: in the example cited above, a sub-zoning configuration must be postulated and an air flow path (typically with constant heat transfer coefficients representing a certain air velocity) must be defined. These "tricks" may improve the model, but they are not entirely satisfactory.

Other ways of dealing with mass transfer in atria should be considered. Complex simulation programs have been developed for calculating heat and mass transfer, considering turbulence effects and transient temperature dependent physical properties of the medium. A fundamental shortcoming of many of these programs in application to atria is that while they provide technically sound analyses at high air speeds, the solution of the Navier Stokes equation becomes unstable with decreasing velocities in non- -constant local fields. In addition, because of the complexity of the programs, unacceptably long computation time is required to deal with the time (e.g., annual) and spatial (e.g., tens of meters) scales of interest in atrium analysis. Furthermore, most of these programs were developed for aerospace applications where fixed boundary conditions commonly can be assumed; as a result, these programs do not account for the effect on temperature distribution and energy balances of user scheduled parameters (e.g., shading), for complex building heating, cooling, and ventilation systems and controls. In short, these more detailed methods too are seriously limited in analysis of atria."

As seen in the contents of this report, it is the limitations listed above we have concentrated on in this project.

XVI

Another problem that arise when choosing a simplified simulation program is how to identify the critical factors for the problem in question. Which principles must be studied in detail and which can be omitted? For example, is the solar energy distribution in the atrium critical for the calculation of the energy consumption in the building? and is it necessary to study the whole building or will a part of it suffice? When choosing the level of detail, it is also necessary to be aware of the availability or the accuracy of the input data. An example is the availability and accuracy of infiltration data for an atrium. Thus the problems with choosing and using models as discussed above, can be generalized in the following questions:

Model:

- Does the program have the algorithms for the principles to be studied?
- If it has the algorithms, do they "work" for the problem in question?
- Does the program offer the right time-steps to study the problems?

Data:

- Do the data exist that the program requires?
- How accurate are these data?

The correctness of the simulation results depends heavily on how positive these questions may be answered. Information to answer these questions should therefore be developed for the simulation programs and their algorithms. It is our wish that this report can answer some of these questions for researchers and designers that study atrium buildings.

XVII

1 Executive summary -problem definition

1.1 Introduction

The goal of this project was to define, describe and develop better building energy simulation models for infiltration and natural ventilation, stratification, air flow patterns, surface area film coefficients and solar radiation in atria. As these simplified models will not cover all situations, Computational Fluid Dynamics, (CFD), models were used and compared to monitored results. The CFD models are used to cover the lack of measurements and in connection to zonal models to provide input data for these. Methodology on how to use these models to study thermal comfort in atria and how to combine them with zonal models was also developed.

1.2 Thermal comfort

Extreme thermal situations (hot, cold, draught, direct sun) often occur in atria. A thermal comfort model is useful to predict the usability of the atrium. A thermal comfort model that considers air and surface temperatures and cold draughts is developed and integrated into the Norwegian program FRES.

Thermal comfort is the state when the human is satisfied with his or . her thermal environment, the person's body feels thermally neutral—not too warm or too cold. Thermal comfort is a widely used criterion when designing the HVAC system in a building.

This chapter contains a description of the ISO 7730 standard, "Moderate Thermal Environments - Determination of the PMV and PPD Indices and Specification of the Conditions for Thermal Comfort", that gives a method to evaluate the thermal comfort for the body as a whole.

In addition, limits for the following local thermal comfort parameters are given in the appendix of the ISO 7730 standard :

- Vertical temperature difference
- Warm and cold floors
- Asymmetric radiation.

The parameters that define thermal comfort are:

For the users: Activity level and clothing

For the room/area: Room air temperature, surface temperatures, solar radiation, air velocity and vapour pressure.

Room air temperature, surface temperatures, vapour pressure and solar radiation are reported from building energy simulation programs. Air velocity can be defined by a minimum value, calculated manually or by CFD programs

These values are suggested as input to ISO 7730 standard to deter m ine the thermal comfort in the area under study.

An example is shown by using the building energy simulation program FRES. It calculates thermal comfort for five situations:

Air temperature.

Air and surface temperatures.

With window surface temperature as dominant
surface temperature.

In direct sun.

With window surface temperature as dominant surface tempera ture and with draught from the window.

Operative temperature is also calculated and presented.

1.3   Stratification

Stratification occurs in atria in periods of high solar gains. The stratification is important for calculation of thermal comfort, and it is also critical for heat recovery systems that utilize the surplus heat under the ceiling. Norway and Switzerland have developed algorithms for stratification that are included in simplified calculation programs. Sweden has tested a method in DEROB.

1:2

The temperature stratification is an important characteristic of large glazed spaces such as an atrium. The stratification depends on the thermal condition, and particularly on the distribution of the solar and internal heat gains. The air movement in the atrium and between the outside or adjacent zones also have a significant influence on stratification.

The three atria presented in this chapter illustrate different situations where temperature stratification occurs, and when a homogenous temperature assumption is not far from reality. Temperature can be seen as positive for the comfort of the occupied zone at the ground level, but can also lead to overheating problems if the upper part is occupied or in adjacent offices. In winter, temperature stratification is a disadvantage because the atrium will require more heat in order to obtain comfortable conditions on the ground level. In summer, natural ventilation is often used to obtain thermal comfort. The stratification is then reduced, and a simulation tool that assumes well mixed air will give reasonable results.

For energy consumption prediction, it is probably not important to take into account the temperature stratification. Very often, heated spaces are not stratified, as for example, in the ELA building. The reason is that convectors (heat sources) and cold surfaces (glazing of the gable and the roof) are creating a strong air movement which will mix the air.

The studies conclude that the linear temperature stratification model works well in the ELA building case. This temperature profile is, however, not valid in cases where there are air vents at different levels.

When no temperature profile is assumed, but the volume **is** simply divided horizontally, the correct distribution of the solar gains in the vertical partitioning is the most important parameter for the correct temperature calculation. Simulation tools that are able in their standard form to predict this distribution, such as DEROB, give reasonable results. Other programs, such as TRNSYS, must be corrected as shown in chapter 3.11.3.

A simple flow field assumption also gives reasonable results, particularly when vents are opened and the atrium is naturally vented. Down draught problems cannot be identified with these simple flow field models.

The effect of the temperature stratification on building energy consumption seems not to be very important in most atria. But more sensitivity studies must be completed before a final conclusion can be drawn.

1:3

1.4   Natural Ventilation.

Natural ventilation is a widely used technique for cooling in atria, but problems with thermal comfort often occur in spring and autumn.

Natural ventilation can be used as a means to cool atria and the adjacent building, based on both buoyancy and wind induced natural ventilation effects. This chapter provides formulas to study natural ventilation by buoyancy and wind, separate and together. It also gives data on infiltration in existing and new atria.

A method is presented on how to calculate thermal buoyancy for two separate openings, a single vertical and a single horizontal. For two separate openings, natural axis, air velocities and ventilation capacity as a function of opening area can be studied. Required and optimum opening area can be calculated.

The influence of thermal stratification on natural ventilation is also shown. Resistance and contraction values for the openings are suggested.

Calculation of natural ventilation can be performed by hand, as a part of a CFD simulation or by a building energy simulation program.

The infiltration rate in buildings and especially in atria is hard to determine. It varies depending on climate, building shape, site and location. The infiltration rate strongly influences the thermal climate and the energy consumption in the atrium. This chapter presents monitoring results on infiltration for old and new atrium buildings in Sweden. The monitoring shows a wide variation in the infiltration rate.

1.5   Surface heat transfer coefficients

The heat loss through the glazing in an atrium varies depending on convection and long wave radiation towards the sky. The surface heat transfer is composed of radiation and convection. This chapter contains a description of the theoretical and practical interior and exterior surface heat transfer coefficients.

The principle of radiative heat transfer between surfaces is described. For interior surfaces emissivity values are suggested. For exterior surfaces sky temperature studies are presented and values suggested. The influence of surface slope is also shown.

The theory of free convection on vertical, inclined and horizontal surfaces is presented. The location of the heat source or warm surface is also discussed. Formulas are presented for both forced and combined free and forced convection.

For interior surfaces a method to combine radiation and convection coefficients into a simple coefficient is presented. Results of laboratory

1:4

and full scale measurements are shown. Recommendations are given on values for radiation and convective coefficients for warm and cold ceilings, floors and walls.

For exterior surfaces, it is suggested not to combine radiation and convection. Monitoring results are presented on wind tunnel and full scale measurements, and recommended values are given for walls and roofs.

1.6   Solar Radiation

The solar radiation into and through an atrium influences both thermal comfort and energy consumption in a building. It is hard to make estimates of the solar gains due to the building's and solar movement's geometrical complexity.

In order to take solar radiation into account, different levels of detail could be used in building energy simulation programs. The incident solar radiation should be calculated and so must the radiation transmitted through windows. The transmitted radiation has to be distributed to the different surfaces in the room and to adjacent rooms. The part of the transmitted radiation that will be absorbed should also be calculated. Each of these parts could be calculated by methods providing different levels of accuracy or treated as input data. The level of accuracy is of course dependent   on the application. For example, in an atrium building, a simple calculation method for solar radiation will give less accuracy than for an ordinary building.

The long wave sky radiation also should be calculated when studying atrium buildings. The long wave sky radiation will, especially when having glazed roofs, influence the temperature in the atrium, the level of comfort and the energy need.

The differences in the calculation methods and levels of detail concerning short wave radiation were exemplified in a study of a room with two windows, and which in some cases was connected to a sunspace. Three different sunspaces were used. The first had all the outer walls and the roof glazed. The second had only the south facade glazed. And the third had only the roof glazed. The influence of the short wave absorptivity of the inner surfaces was also studied. The four different programs evaluated, showed very large differences in calculation results. The conclusion is that if atrium buildings or other types of glazed spaces are to be studied, it is essential to base the calculations on a geometrical description of the buildings, taking into account transmission through windows, reflections, absorptivity and retransmissions through windows. It is important

1:5

to take into account the retransmission of solar radiation to the outside or into adjacent rooms as only the radiation staying in the sunspace will be a part of the energy balance used for calculation of temperatures and energy needs. Building energy simulation programs used for ordinary buildings are not automatically suitable for atrium buildings.

A simplified method to calculate how much of the transmitted solar radiation will be absorbed in a sunspace is presented. Four types of glazed spaces are studied and the influence of different parameters is evaluated. The method is based on calculations with DEROB-LTH, which is a building energy simulation program using a geometrical description of the building to calculate the solar radiation.

An example of a method calculating shadows is also presented. The method has been implemented in a PC software application, called Xsun, which can function as a stand-alone design tool or may be integrated with programs for thermal simulation of buildings or solar systems. An example is given where Xsun is integrated with the thermal simulation tool TSBI3.

1.7   Test Studies

When developing and testing models in building energy simulation programs and CFD tools, a few cases were used as example buildings. These buildings are Neuchatel University in Switzerland, Taman in Sweden, Bertholt Brecht Secondary School in Germany and the Technical University in Trondheim, Norway. Neuchatel, Taman and Technical University are existing atrium buildings where solar radiation, temperatures, air infiltration and energy consumption have been monitored. These measurements are used for comparison when simulating temperatures and energy consumption and when studying temperatures and air movements with CFD models.

Bertholt Brecht school has an open courtyard that will be covered with glazing to make an atrium. Different strategies for renovation are studied with the building energy simulation tool SUNCODE. After the renovation is performed the atrium will be monitored.

1.8   CFD models

CFD models are useful to make detailed studies of natural ventilation, stratification, air flow patterns and thermal comfort. They are also useful

1:6

when there is a lack of monitoring results. There is little experience with using such models for atrium buildings.

The principal recommendations for the CFD users are: CFD can play an important role in the HVAC design of atria, though its use demands sound engineering judgement. To keep design costs down, CFD should be used sparingly, and always together with simpler design tools. CFD should therefore generally be limited to the last stage of the design process in order to verify the proposed ventilation design. The required computational accuracy is dictated by the requirement for thermal comfort.

The k-c turbulence model is satisfactory for most ventilation design applications, though it is recommended that the k and ϵ equations include damping functions and buoyancy terms to more accurately model low-Reynolds number flow present in atria, including damping effect of stable thermal stratification.

It is important to calculate net solar gain accurately and to distribute it realistically among the atrium surfaces. This requires a geometric model of the building. It is not necessary to account for internal reflections (specular or diffuse) between surfaces; doing so marginally improves the correctness of the CFD analysis. The best surface boundary condition for absorbed solar radiation is to superimpose it as a plane heat source as described in the chapter.

Care should be taken to refine the computational grid in regions of locally steep gradients. Automatic grid generation (adaptive grid methods) makes this easier. Steady-state supply jets should be modelled using either the box method or the prescribed velocity method. This reduces the number of grid points needed to model the atrium.

It is vital to account for heat transfer by surface-to-surface radiation exchange and it is important to model the thermal capacity of an atrium's building structure. This is most simply done by carrying out a steady state CFD simulation of the worst case condition, using quasi steady-state boundary conditions taken from a dynamic model.

A more exact method is to carry out a transient CFD analysis with boundary conditions taken from coupled dynamic thermal mode. However, the computing time/costs may be prohibitive for detailed transient analysis.

1.9   Building Energy Simulation Programs

This chapter contains a short description of the Building Energy Simulation Programs used in this study. The simulation programs are DEROB-

1:7

LTH (Sweden), Fres (Norway), TRNSYS (developed in USA, used by Switzerland) and *tsbi3* (Denmark).

A building energy simulation model is a simplified description of the building. The simplification has in this case been carried out from an energy and indoor climate point of view, so that the model only describes the aspects which are relevant in this connection.

A standard list is used to describe each program to make it possible to compare the programs. For each program the following are described: Energy transmission (numerical method, heat transmission), solar radiation and distribution, shading devices and shadow, infiltration, stratification and air movements, ventilation and air conditioning, internal gains, heating and cooling, other systems (heat storage, heat pump), daylight, moisture, thermal comfort, limitations, input/output.

The building energy simulation programs can be used to study thermal comfort and energy consumption in atrium buildings to different levels of detail. If air velocities are to be studied, a CFD tool must be used.

1:8

2   Thermal comfort

2.1   Introduction

2.1.1   Thermal comfort

Thermal comfort is a prerequisite for good indoor climate. Thermal comfort is perceived when a human is satisfied with his or her thermal environment, that is when the person's body feels thermally neutral- not too warm and too cold. The person should neither feel any disturbing local cooling nor heating on the body (Fanger (1970)).

It is necessary, but not satisfactory, that the body is in thermal balance with the environment. In addition, the skin temperature and sweat should be at a level that feel neutral at a given metabolism (Fanger (1970)).

The ISO 7730 standard "Moderate Thermal Environments - Determination of the *PMV* and *PPD* Indices and Specification of the Conditions for Thermal Comfort" gives a method to evaluate the thermal comfort for the body as a whole.

In addition the appendix of the standard gives limits for the following local thermal comfort parameters:

- Vertical temperature difference
- Warm and cold floors
- Asymmetric radiation.

A method to calculate draught risk will also be included in the next edition of ISO 7730. The parameters that define thermal comfort are:

For the building users: Activity level and clothing

For the room/area: Room air temperature, surface temperatures, solar radiation, air velocity and vapour pressure.

2:1

This chapter describes problems connected to thermal comfort in atria, and defines comfort relations and simplified models to estimate draught. Finally an example shows how the thermal comfort post processor is included in a building energy simulation program.

2.1.2 Studying thermal comfort using building energy simulation programs

Thermal comfort can be calculated in a post processing unit to building energy simulation programs. Most building energy simulation programs produce data about solar gain, room air temperature and surface temperatures. Air velocity can be defined or calculated in a post processor. Together with user input on activity and clothing, this gives a basis to calculate thermal comfort as shown in figure 2.1.
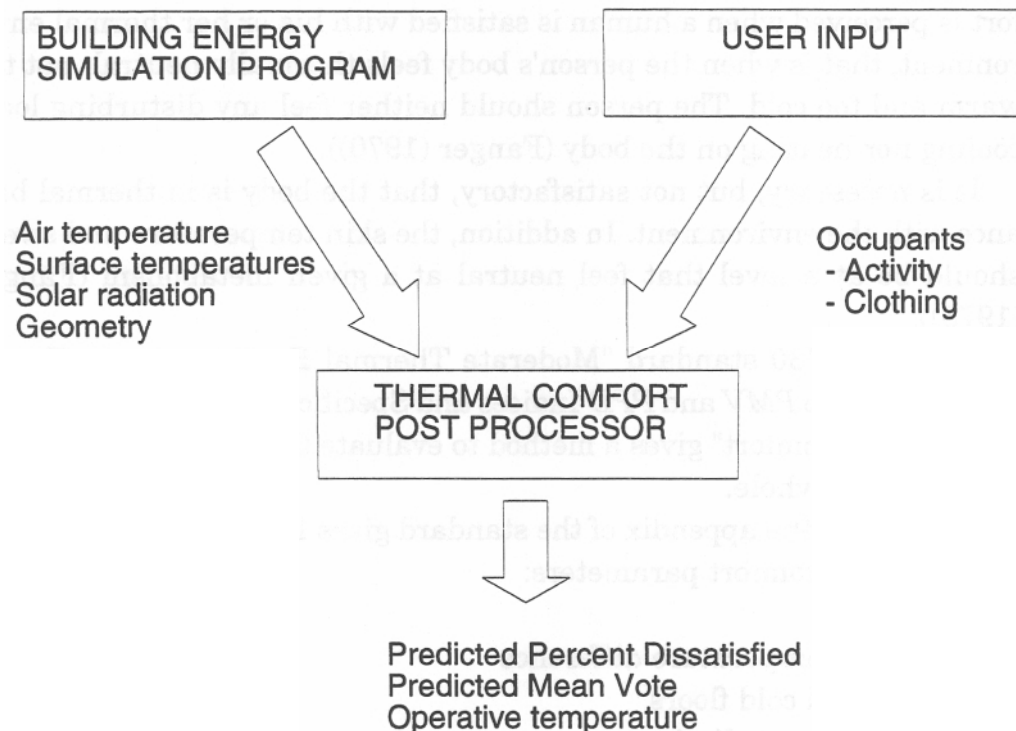

Figure 2.1   A thermal comfort post processor connected to a building energy simulation program.

2:2

2.1.3 Thermal comfort in atria

Atria are often large rooms with cold surfaces where stratification and air movements readily occur due to strong thermal forces.

When designing the atrium, it is important to clearly define its use. An atrium designed for sedentary work must be designed for narrow limits of operative temperature, while a shopping street could have a climate like a mild outdoor climate.

If narrow limits of operative temperature are required for some activities, such as in a cafe, local climatization could be a solution instead of heating the whole space.

Local climatization can include heating of floor or furnitures in the occupied area and shelters towards radiation to cold surfaces and cold down draught. Both the air movement and the temperatures in the air and at the surfaces must then be calculated to predict the thermal comfort of different architectural solutions.

Zonal models can be used to study the overall thermal comfort in an atrium. However, in order to study detailed local phenomena and local climatization, a computational fluid dynamics (CFD) model is necessary.

In most cases the thermal comfort model works as a postprocessor on the results of the zonal or CFD model. In a few cases the zonal models include possibilities to use a thermal comfort parameter like operative temperature as a control parameter.

2.2 The ISO 7730 Standard

The ISO 7730 Standard - "Moderate Thermal Environment- Determination of the *PMV* and *PPD* Indices and Specification of the Conditions for Thermal Comfort Standard" (1988) gives a method to estimate expected sensation of thermal comfort for humans as a function of physical activity, clothing, air temperature, mean radiant temperature, air velocity and air humidity. A short description of the content of the standard is given in the following.

2.2.1 The *PMV* Index

To quantify the degree of discomfort, *a PMV* (Predicted Mean Vote) index has been introduced. The *PMV* index is based on a seven point scale as a result of large scale tests on a group of subjects:

2:3

+3 hot
+2 warm
+1 slightly warm
 0 neutral
-1 slightly cool
-2 cool
-3 cold

The *PMV* is based on a heat balance of the human body. It is calculated with the following main parameters that should be within the below listed ranges:

Metabolism: $M = 46$ to 232 [W/m²], (0.8 to 4 met)
Clothing: $I_{cl} = 0$ to 0.31 [m²K/W], (0 to 2 clo)
Air temperature: $t_a = 10$ to 30 [°C]
Mean radiant
temperature: $\bar{t}_r = 10$ to 40 [°C]
Air velocity : $v_{ar} = 0$ to 1 [m/s]
Vapour pressure: $p_{da} = 0$ to 2700 [Pa]

The *PMV* value is determined from the following equation:

$$PMV = (0.303 \cdot e^{-0.036 \cdot M} + 0.028) \cdot [(M - W) - 3.05 \cdot 10^{-3}$$

$$[5733 - 6.99(M - W) - p_{da}] - 0.42[(M - W) - 58.15]$$

$$-17 \cdot 10^{-6} \cdot M (5867 - p_{da}) - 1.4 \cdot 10^{-3} \cdot M (34 - t_a) - 39.6 \cdot 10^{-9} \cdot f_{cl}$$

$$[(t_{cl} + 273)^4 - (\bar{t}_r + 273)^4] - f_{cl} \cdot \alpha_c (t_{cl} - t_a)] \tag{2.1}$$

where: (estimated by iteration)

$$t_{cl} = 35.7 - 0.028(M - W) - 0.155 \cdot I_{cl}$$

$$[39.6 \cdot 10^{-9} \cdot f_{cl}[(t_{cl} + 273)^4 - (\bar{t}_r + 273)^4] + f_{cl} \cdot \alpha_c (t_{cl} - t_a)]$$

2:4

2.2.2 The PPD index

The *PPD* (Predicted Percentage of Dissatisfied) index gives a quantita
tive predicted number of people who will not be satisfied with the ther
mal environment. The *PPD* value is therefore an appropriate and easily
understandable expression for the quality of the thermal comfort. When
the *PMV* index is estimated, the *PPD* index can be found from Figure 2.2,
eventually it can be calculated from the Eq. 2.2:

$$PPD = 100 - 95 \cdot e^{-0.03353 \cdot PMV^4 - 0.2179 \cdot PMV^2} \qquad (2.2)$$

It is important to note that the lowest value of *PPD* is 5 %, which corre-
sponds to *PMV* = O. So even if the *PMV* value predicts thermal neutrality,
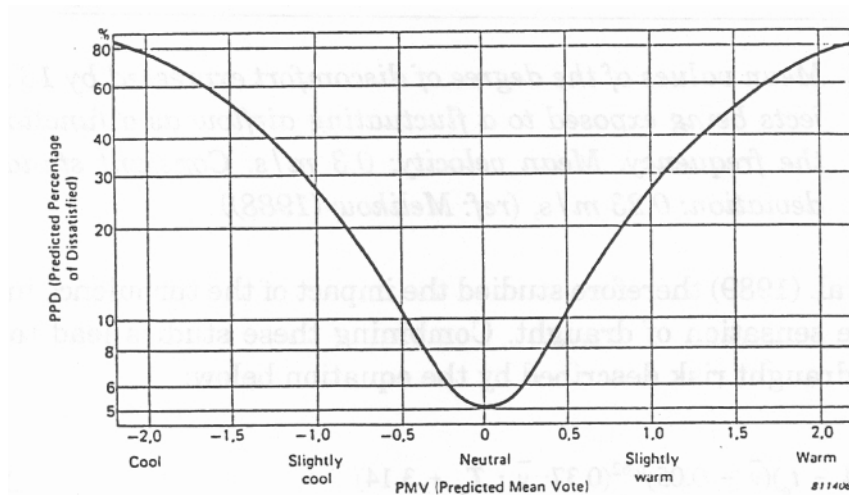a person may feel local thermal discomfort.

*Figure 2.2   The relationship between PPD (Predicted Percentage of
Dissatisfied) and PMV (Predicted Mean Vote), (ref Olesen
(1982))*

2.3   Local thermal discomfort

Local discomfort may be caused by several conditions, in this report we
deal with local convective cooling or down draught caused by cold sur-
faces, mainly window surfaces. Draught is defined as an undesired cool-
ing of the human body caused by fluctuating air flows. It has been shown
that a fluctuating air flow is more uncomfortable than a constant flow.

2:5

Figure 2.3 from Melikow (1988), shows the sensation of comfort as a function of the frequency of the fluctuating air velocity. P.O. Fanger and N.K. Christensen studied air velocities with fluctuations for ventilated spaces and derived an equation with the predicted percentage of dissatisfied occupants as a function of mean velocity and air temperature. Comparable studies have been done but the results varies significantly.
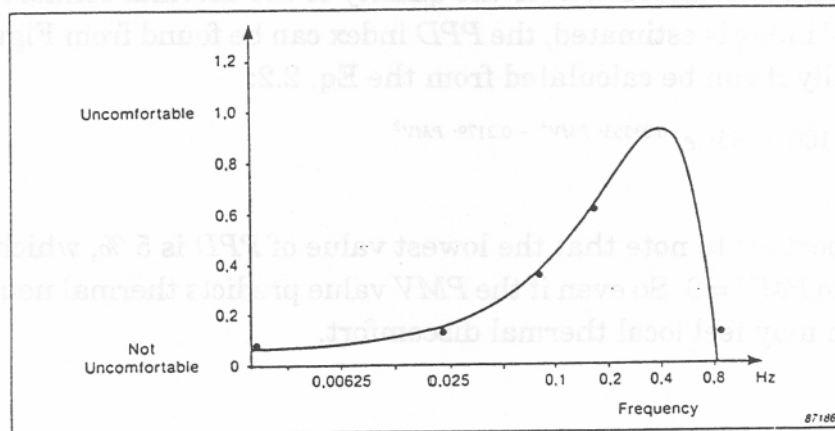

Figure 2.3 Mean values of the degree of discomfort expressed by 16 subjects being exposed to a fluctuating airflow as a function of the frequency. Mean velocity: 0.3 m/s. Constant standard deviation: 0.23 m/s, (ref Melikow (1988))

Fanger et. al. (1989) therefore studied the impact of the turbulence intensity on the sensation of draught. Combining these studies lead to the model for draught risk described by the equation below:

$$PPD = (34 - t_a)(\bar{v} - 0.05)^{0.62}(0.37 \cdot \bar{v} \cdot T_u + 3.14) \qquad (2.3)$$

for $\bar{v} < 0.05$ m/s use $\bar{v} = 0.05$ m/s
for $PPD > 100\ \%$ use $PPD = 100\ \%$

$$T_u = \frac{SD_v}{\bar{v}} \cdot 100 \qquad (2.4)$$

T_u = turbulence intensity, [%]
SD_v = standard deviation, [m/s]
$\bar{v}$ = mean air velocity, [m/s]

2:6

Figure 2.7 shows the relationship between the mean air velocity and the turbulence intensity.

2.4 Draught due to cooled air falling down along cold surfaces

Draught is usually caused by convective air currents along windows. Especially during the winter, natural downward convective air currents along windows may create considerable velocities in the occupied zone. Skåret (1986), shows that no great errors are made, estimating the maximum velocity, U_{max}, by using the same equation on both steady state and turbulent convective air flow. Given that the flow is self-conserving and independent of width, and that there is a constant window surface temperature and the pressure is equal to the surrounding air pressure, using Reynolds analogy for turbulent flow over a flat plate (Kreith and Black (1980)), and Blassius theory, yields:

$$ U_{max} = 0.54 \cdot (g \cdot \beta_T \cdot \Delta T_f)^{0.5} \cdot x^{0.5} \tag{2.5} $$

g	=	Acceleration of gravity, [m/s²]
β_T	=	Volumetric thermal expansion coefficient, [°C⁻¹]
ΔT_f	=	Temperature difference between the window surface and the ambient air, [K]
x	=	Height of window, [m]
U_{max}	=	Velocity at the lower edge of the window [m/s]

This formula gives the air velocity of draught from windows and can be used as input to calculate draught risk in formula 2.3.

2.5 The PPD comfort models incorporated in FRES

FRES, version 2.0, a building energy simulation program described in chapter 9, contains 5 different models for estimating the PPD value. This description of the five models is based on Frydenlund and Rømen (1992).

2:7

In each case the *PPD* value is estimated from the correlation equation between the *PMV* and the *PPD* index (Eq.2.2) and the formula for the PMV value (Eq. 2.1). Seven parameters are used to calculate the *PPD* values.

$$M, W, I_{cl}, t_a, \bar{t}_r, v_{ar}, p_{da}$$

Metabolism, *M,* external work, *W,* thermal resistance of clothing, I_{cl}, and the ambient air vapour pressure, p_{ar}, are inputs selected by the user depending on expected activity level, clothing level and indoor climate of the building.

The air temperature, t_a, obtains the instantaneous air temperature value estimated by the FRES simulations. However, there is one exception. If the stratification model in FRES, shown in figure 2.4, is used, the temperature *Y* metres above the floor is calculated and used in the *PPD* estimation. This stratification model has been experimentally verified by Mathisen (Kolsaker and Mathisen (1991)), and it shows that the profile in many cases becomes more or less linear. For most *PPD* models in FRES, the relative air velocity, v_{ar}, is set equal to zero. However, the exception is when calculating the down draught using Eq. 2.5.
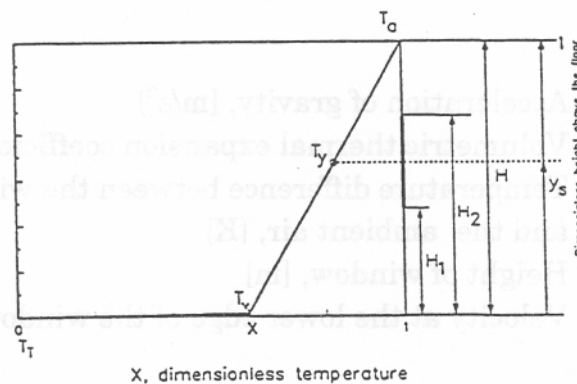

Figure 2.4   The stratification model implemented in FRES, (ref Kolsaker and Mathisen (1991))

2.5.1 Calculation of mean radiant temperature

"The mean radiant temperature related to a person in a given body posture and clothing placed at a given point in a room, is defined as that uniform temperature of black surroundings which will give the same radiant heat loss from the person as the actual case under study", Fanger (1970). The mean radiant temperature in relation to a human being

2:8

depends on the person's location and orientation in the room. This must be known to calculate exact values. To evaluate the mean radiant temperature, it is therefore necessary to calculate the angle factors between the body and the surrounding surfaces, as shown in figure 2.5. To estimate the angle factors, it is further necessary to know the right geometrical form, size and distances. In FRES, there are no defined geometrical relationship or geometrical connection between the different surfaces, so the computer program does not have any geometrical ¨picture¨ of the rooms or the building. The way the mean radiant temperature is calculated, is therefore simply by using the mean surface area temperature, $\bar{t}_r^*$, according to the equation below.
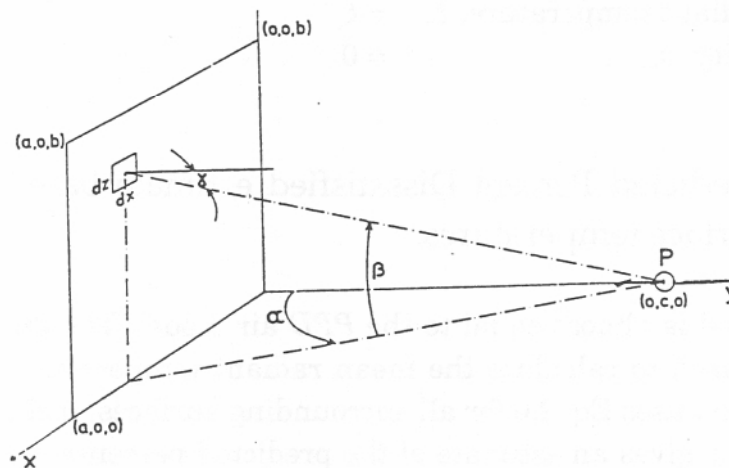

Figure 2.5   *Diagram for the development of the evaluation of the angle factor between a person (center in P and facing towards the center of the coordinate system) and a rectangle (a x b) in the x-z plane, ref. Fanger (1970)*

$$\bar{t}_r^* = \frac{\sum_{i=1}^{\infty} A_i \cdot t_i}{\sum_{i=1}^{\infty} A_i} \tag{2.6}$$

$\bar{t}_r^*$ = mean surface area temperature, [°C]
A_i = ith surface area, [m²]
t_i = ith surface temperature, [°C]

2:9

2.5.2 Predicted Percent Dissatisfied estimate based on air temperature

This model calculates the *PPD* value with regard to the air temperature, t_a, either directly or estimated from the simple linear stratification model. Relative air velocity, v_{ar}, is equal to zero, and the mean radiant temperature, $\bar{t}_r$, is set to be equal to the air temperature. This identifies the quantity of dissatisfied people for the simulated building with a given metabolism, external work and clothing, just influenced by the air temperature.

Parameters:

Air temperature, t_a	= estimated by FRES
Mean radiant temperature, $\bar{t}_r$	$= t_a$
Air velocity, v_{ar}	$= 0$

2.5.3 Predicted Percent Dissatisfied estimate based on air and surface temperatures.

This model is almost equal to the *PPD* air model. The difference is the method used to calculate the mean radiant temperature, $\bar{t}_r$. The *PPD* room model uses Eq. 2.6 for all surrounding surfaces, including the windows. This gives an estimate of the predicted percentage dissatisfied of the people seated in the middle of the room, influenced by the air temperature and the temperature of the surrounding surfaces.

Parameters:

Air temperature, t_a	= estimated by FRES
Mean radiant temperature, $\bar{t}_r$	$= \bar{t}_r^{*}$, derived from temperatures calculated by FRES.
Air velocity, v_{ar}	$= 0$

2.5.4 Predicted Percent Dissatisfied close to a window without considering draught.

This model is a more extreme variant of the *PPD* room model. Instead of estimating a mean surface temperature, the mean radiant temperature is said to be equal to the window temperature, t_w, calculated by FRES. This will give an indication of the thermal comfort influenced by the asymmetric radiation for people seated close to the window.

2:10

Parameters:

Air temperature, t_a = estimated by FRES

Mean radiant temperature, $\bar{t}_r$ = $\bar{t}_w$, window surface temperature estimated by FRES.

Air velocity, v_{ar} = 0

2.5.5 Predicted Percent Dissatisfied when exposed to sun

This model estimates the PPD value for people seated in the middle of the room exposed by direct solar radiation. Using Eq. 2.7 from Fanger (1970), the mean radiant temperature is calculated.

$$(T_r + 273)^4 = (\bar{t}_r^* + 273)^4 + (const \cdot f_p \cdot \alpha \cdot Q_{sun}) \tag{2.7}$$

T_r = total mean radiant temperature incl. solar radiation, [K]
const = $1/0.97\sigma$
σ = $5.77 \cdot 10^{-8}$, Stephan Boltzman's constant, [W/m²K⁴]
f_p = projected area factor
α = 0.6, absorption factor

$$Q_{sun} = \frac{I_{tot}}{\sin(\beta)} \cdot \alpha_k \tag{2.8}$$

I_{tot} = horizontal total radiation per unit area, [W/m²]
β = altitude, [°]
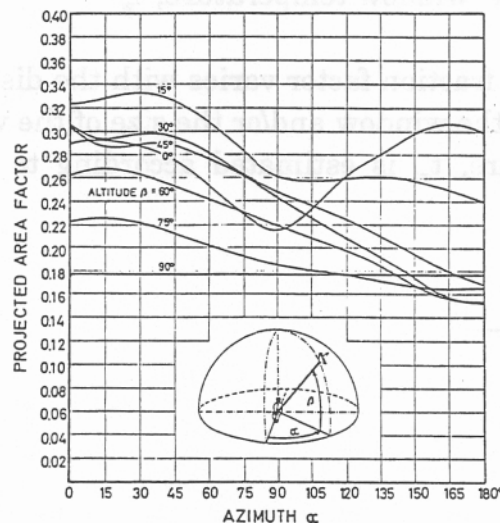α_k = shading factor

Figure 2.6   Projected area factor for seated persons, nude and clothed, Fanger (1970)

2:11

It should be noted that reflected solar radiation has a considerable effect. Figure 2.6 shows the projected area factor as a function of azimuth and altitude angle used to estimate f_p in Eq. 2.7. The graph in figure 2.6 is tabulated in FRES for $\alpha = 0$.

Parameters

Air temperature: t_a,   = estimated by FRES

Mean radiant temperature, $\bar{t}_r$ = estimated by FRES, Eq. 2.7

Air velocity, v_{ar} = 0

2.5.6 Predicted Percent Dissatisfied when draught from the window is considered.

This model calculates the *PPD* value in two ways. In both cases the relative air velocity is equal to the maximum air velocity estimated from Eq. 2.5, caused by cold window surfaces. The mean values of the three curves between the air velocity and the turbulence intensity in figure 2.7 is tabulated in FRES. Using Eq. 2.3 alone and Eq. 2.1 and 2.2 together, the two *PPD* values are estimated. FRES always displays the most critical value of the two. The critical area for local discomfort caused by down draught, is the ankles. The air temperature, t_a, used in the equations is therefore replaced by an ankle temperature, t_{ank}, described by Eq. 2.9.

$$t_{ank} = \alpha_f \cdot t_w + (1 - \alpha_f) \cdot t_a \tag{2.9}$$

α_f =   the down draught fraction factor
α_f =   0, gives the air temperature, t_a
α_f =   1, gives the window temperature, t_w

The down draught fraction factor varies with the distance between the seated person and the window and/or the size of the window. The mean radiant temperature, $\bar{t}_r$, is estimated according to the two following equations.

$$\bar{t}_r^{**} = \frac{\sum\limits_{i=1}^{\infty} A_i \cdot t_i - A_w \cdot t_w}{\sum\limits_{i=1}^{\infty} A_i - A_w} \tag{2.10}$$

2:12

$$\bar{t}_r = \frac{\bar{t}_r^{**} + t_w}{2} \qquad (2.11)$$

$\bar{t}_r^{**}$ = mean surface area temperature, not including windows [°C]

A_w = total window area, [m²]

t_w = window temperature, [°C]

The window temperature constantly count the same as the rest of the surrounding surfaces.

Parameters:

Air temperature, t_a = estimated by FRES

Mean radiant temperature, $\bar{t}_r$ = $(\bar{t}_r^{**} + t_w)/2$
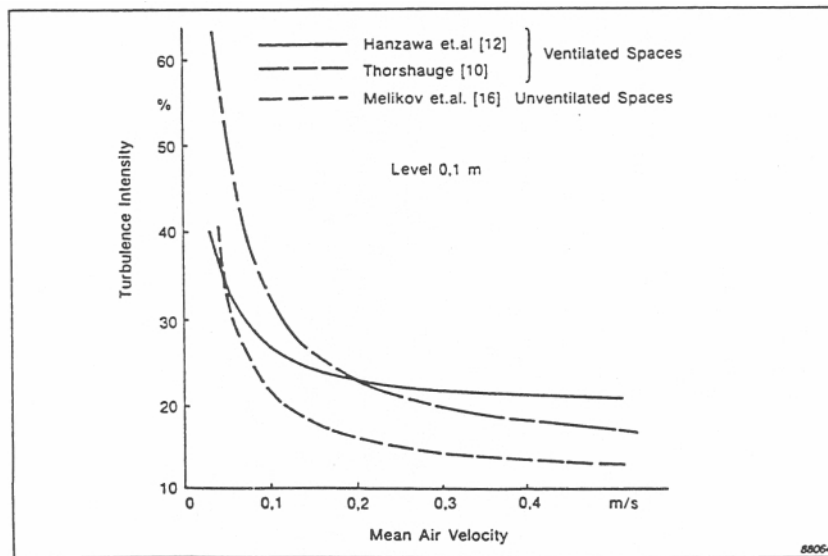
Air velocity, $v_{ar} = \bar{v}$ = U_{max}

Figure 2.7   Relationship between turbulence intensity (Tu) and mean velocity (v) in ventilated spaces and heated rooms without mechanical ventilation (unventilated spaces), (ref Melikow (1988))

2.5.7 Operative temperature

The operative temperature, t_0, is often used as a measurement of the thermal comfort in a building. The operative temperature in relation to

2:13

a person in a given body posture and clothing placed at a given point in a room, is defined as the mean value of a uniform temperature of black surroundings and the air temperature, which will give the same radiant and convective heat loss from the person as the actual case under study. The operative temperature is described by the Eq. 2.12 for thermal comfort mainly at low activity level.

$$t_o = \frac{t_r + t_a}{2} \qquad\qquad (2.12)$$

t_r (mean radiant temperature) and t_a (air temperature) are derived from the simulation results with the level of detail corresponding to the simulation model.

The air- and the operative temperature are graphically presented together with the PPD values for the room or building.

2:14

2.6   Summary and conclusions

Thermal comfort is the state when the human is satisfied with his or her thermal environment, that the person's body feel thermally neutral- not too warm and too cold. Thermal comfort is a widely used criterion when designing the HVAC system in a building.

This chapter contains a description of the ISO 7730 standard "Moderate Thermal Environments - Determination of the PMV and PPD Indices and Specification of the Conditions for Thermal Comfort" that gives a method to evaluate the thermal comfort for the body as a whole.

In addition, the appendix of the standard gives limits for the following local thermal comfort parameters:

- Vertical temperature difference
- Warm and cold floors
- Asymmetric radiation.

The parameters that define thermal comfort are:

For the users: Activity level and clothing
For the room/area: Room air temperature, surface temperatures, solar radiation, air velocity and vapor pressure.

Room air temperature, surface temperatures, vapor pressure and solar radiation are output from building energy simulation programs. Air velocity can be defined by a minimum value, calculated manually or by computational fluid dynamics programs

These values are suggested as input to ISO 7730 standard to determine the thermal comfort in the area being studied.

An example using the building energy simulation program FRES is given. Thermal comfort for five situations are calculated:

- Air temperature.
- Air and surface temperatures.
- With window surface temperature as dominant surface temperature.
- In direct sun.
- With window surface temperature as dominant surface temperature and with draught from the window.

Operative temperature is also calculated and presented.

2:15

2.7 Symbol list

M	=	Metabolism
W	=	External work
I_{cl}	=	Thermal resistance of clothing
t_a	=	Air temperature
$\bar{t}_r$	=	Mean radiant temperature
$\bar{t}_w$	=	Window surface temperature
v_{ar}	=	Air velocity
p_{da}	=	Vapour pressure
T_u	=	turbulence intensity, [%]
SD_v	=	standard deviation, [m/s]
v	=	mean air velocity, [m/s]
g	=	Acceleration of gravity, [m/s^2]
β_T	=	Volumetric thermal expansion coefficient, [°C^{-1}]
ΔT_f	=	Difference in temperature between the window surface and the ambient air, [K]
x	=	Height of window, [m]
U_{max}	=	Velocity at the lower edge of the window
$\bar{t}_r$	=	mean surface area temperature, [°C]
A_i	=	ith surface area, [m^2]
t_i	=	ith surface temperature, [°C]
t_{rad}	=	total mean radiant temperature including solar radiation [°C]
σ	=	5.77 •10^{-8}, Stephan Boltzman's constant, [W/m^{2o}K^4]
f_p	=	projected area factor
α	=	0.6, absorption factor
$E_{tot}\beta$	=	horizontal total radiation per unit area, [W/m^2]
	=	altitude, [°]
α_k	=	shading factor
α_f	=	the down draught fraction factor
α_f	=	0, gives the air temperature, t_a
α_f	=	1, gives det window temperature, t_w
$\bar{t}_r{}^{**}$	=	mean surface area temperature, not including windows, [°C]
A_w	=	total window area, [m^2]

2:16

2.8   References

Fanger, P.O. (1970). *Thermal comfort.* (Analysis and Applications in Environmental Engineering). Danish Technical Press. Copenhagen. Denmark.

Fanger, P.O. et.al. (1989) Turbulens *og trekk. (Eng: Air turbulence and sensation of draught).* (Norsk VVS No 2). Oslo. Norway.

Frydenlund, F., Rømen, B.H. (1992). *Thermal Comfort Simulation using FRES.* (SINTEF Report no STF A92014). Trondheim. Norway.

ISO 7730 Standard (1988) *Moderate thermal environment- Deter mination of the PMV and PPD indices and specification of the conditions for thermal comfort.*

Kolsaker, K. and Mathisen, H.M. (1991) *Computer simulation of energy use and thermal climate in glazed spaces.* (STF 15 A92056). SINTEF Applied Thermodynamics. Trondheim. Norway.

Kreith, F. , Black, W.Z. (1980) *Basic Heat Transfer.* Harper & Row Publishers. New York. USA.

Melikow, A.K. (1988) *Quantifying draught risk. (Brüel* & Kjær Technical Review No.2). Nærum. Denmark.

Olesen, B.W. (1982). *Thermal comfort. (Brüel* & Kjær Technical Review No. 2). Nærum. Denmark.

Skåret, E. (1986). *Ventilasjonsteknikk.* NTH. Trondheim. Norway.

3.   Stratification of the Temperature in Atria

3.1   Introduction

One important characteristic of large glazed spaces such as atrium is that the air temperature is not always homogeneous but can increase with the height of the atria. This phenomena is called temperature stratification. Depending on the thermal situation, we can define four main temperature distributions in large enclosures.

1. Constant in the height
2. Increasing linearly
3. No linear profile, increasing rapidly in the lower part
4. No linear profile, increasing rapidly in the upper part
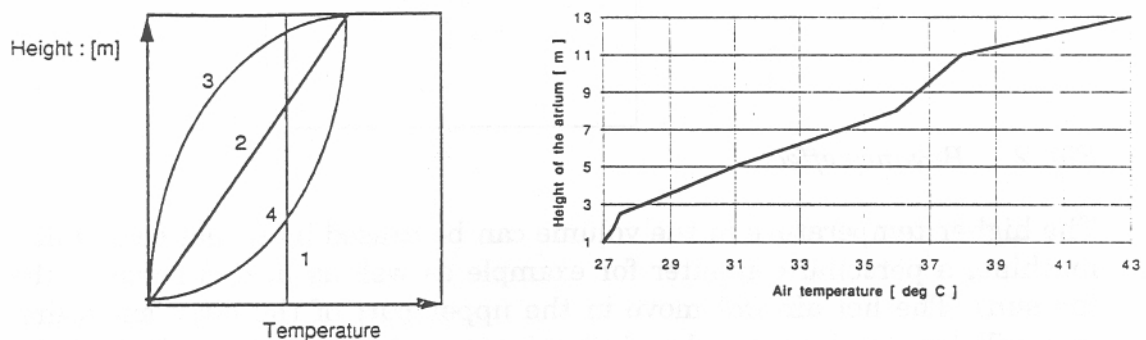
Fig. 1   *Typical vertical temperature profiles*   *Real Case : ELA*

Profile 1 is typical for complete mixed situation

Profile 2 is typical in atria where the heat sources are uniformly distributed in the space and its surfaces.

Profile 3 represents the common case where either central heat source or sources generates a column of heated air which rises rapidly to the roof prior to mixing and tends to pool at the upper level, or heat sources are distributed only in the upper part (internal shading under the roof for example).

Profile 4 represents the case where heat sources are close to the floor level.

These temperature distributions are caused by different thermal effects which will be explained later. It is important to notice that on the horizontal   direction   the temperature of the air is always quite homogeneous.

3:1

3.2 Physical theory

The temperature stratification in large enclosures is due to the following effects :

A volume of air which is heated and then reaches a higher temperature than its surrounding will be affected by a driving force, due to density differences between the warm air and the cold air (the warm air is lighter than the cold one), which will tend to displace it in the vertical direction.
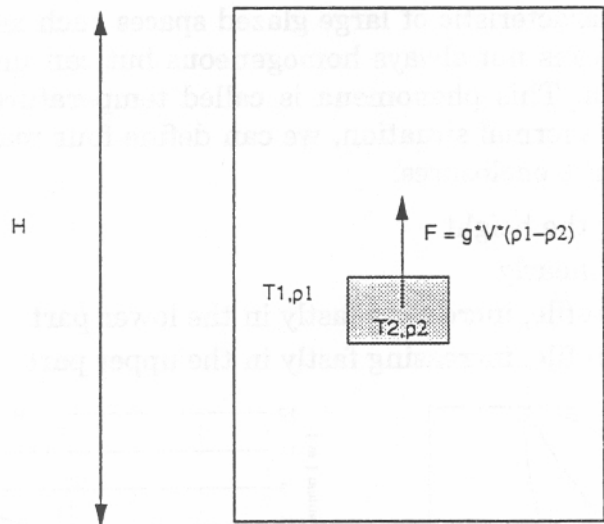

H

$F = g^*V^*(\rho 1 - \rho 2)$

$T1, \rho 1$

$T2, \rho 2$

Fig. 2   Buoyancy effect

The higher temperature in the volume can be caused by a heat source of a machine, a personal computer for example as well as heated surfaces (by the sun). The hot air will move in the upper part of the large enclosure, this will tend to increase the air temperature in that region. But as the warm air going up must be replaced by surrounding air, a back flow will take place which will create some mixing.

If the heat source is placed at the floor level there will be no relevant stratification (see fig. 3). In the other hand if the heat source is placed in the middle of the space some temperature stratification will occur.
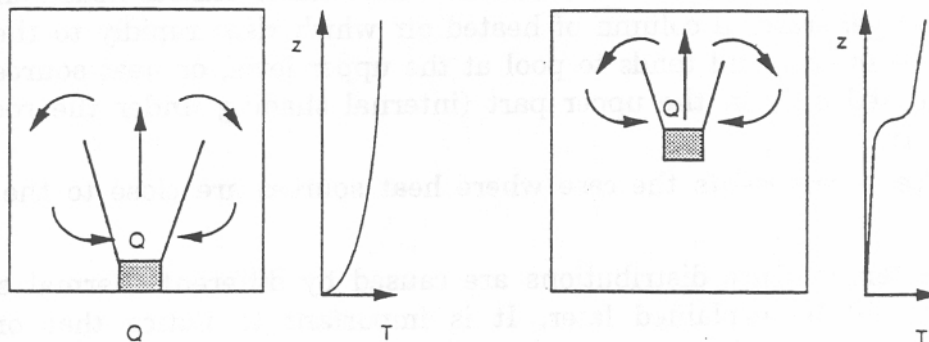
Fig. 3   Position of the heat source and effect on the stratification

3:2

3.3   When is stratification important ?

The stratification of the temperature is relevant when the following conditions are fulfilled:

- Height of the volume is important

- Heat transfer to the air from the heat source in the upper part or linearly distributed   through the height of the volume.

- Hatches (vents) not opened (or only partially)

- Volume with small air movements

- The internal shadowing devices will tend to create some stratification.

In order to illustrate the problem, different typical atria situation are shown in the following figures.

a)
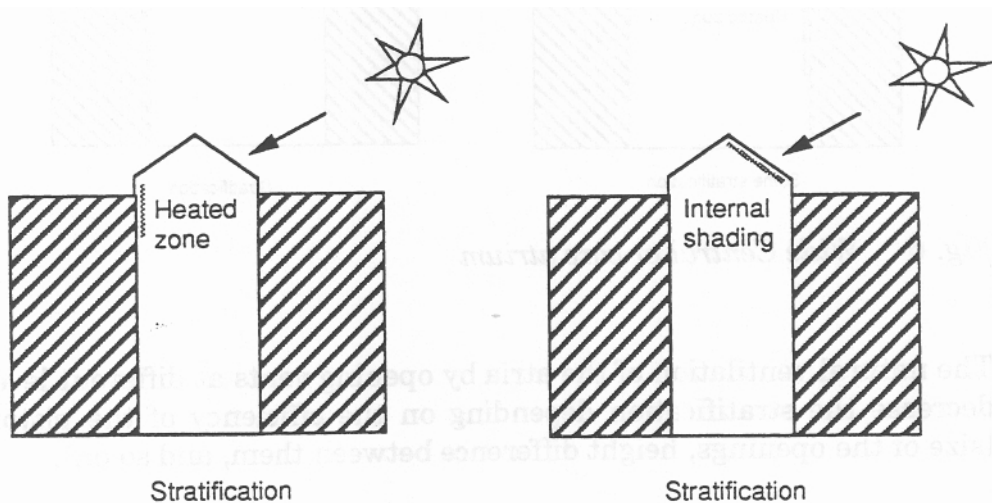
Fig. 4   Central or core atrium

b)
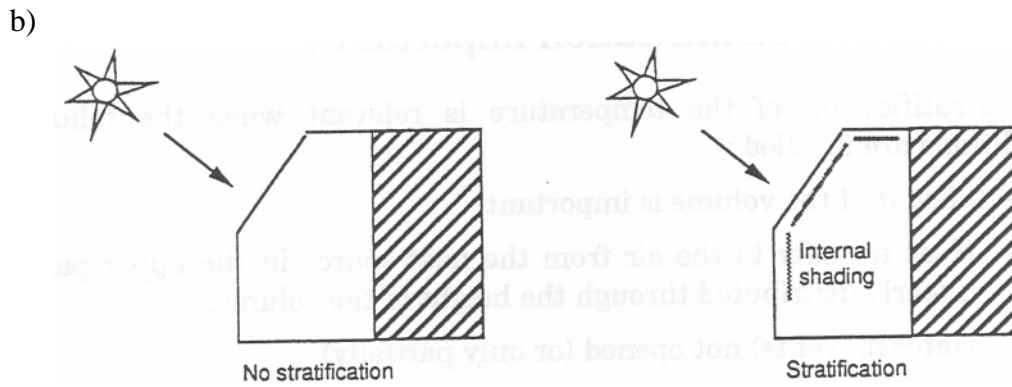
Fig 5   Attached atrium

c)
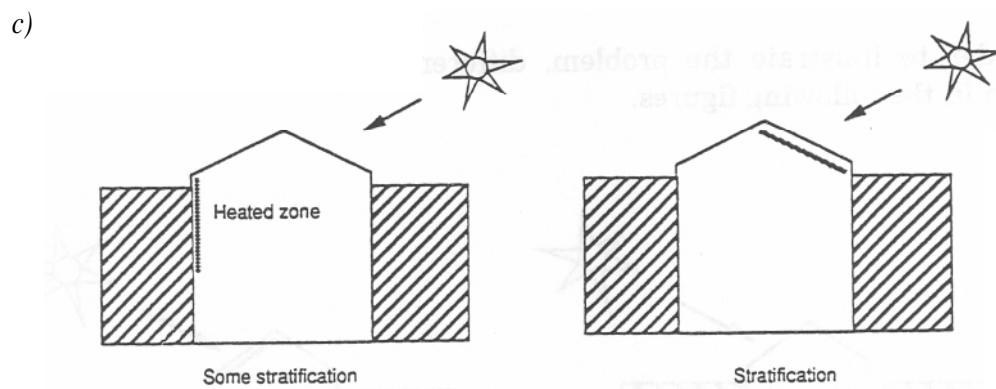
Fig. 6   Wide Central or core atrium

The natural ventilation of the atria by opening vents at different levels will decrease the stratification depending on the efficiency of the piston flow (size of the openings, height difference between them, and so on).
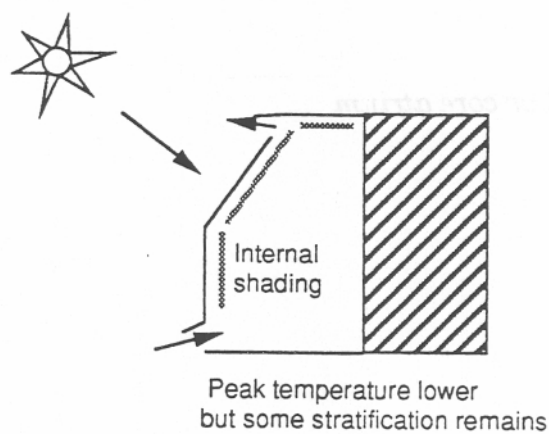
Fig. 7   Attached atrium naturally ventilated

3:4

3.4   Examples of existing atria

To illustrate the temperature profiles of existing atria three examples are shown:

- Atrium of the university of Neuchâtel   (CH)   type b of p.3.4
- Atrium of the university of Trondheim   (N)   type a of p. 3.3
- Glazed courtyard at Tärnan   (S)   type c of p. 3.4

In the first two examples, the temperature profile was stratified, in the last one no relevant stratification has been measured. All the three atria are naturally ventilated in the summer.

3.4.1   Atrium of the University of Neuchâtel (Nuni)

The new building of the faculty of literature of the University of Neuchâtel has an attached sunspace. A detailed description of this atrium can be found into chapter 7.1.

The temperature profile that can be encountered in such an attached atrium are summarized by the three typical days represented in figure 8.
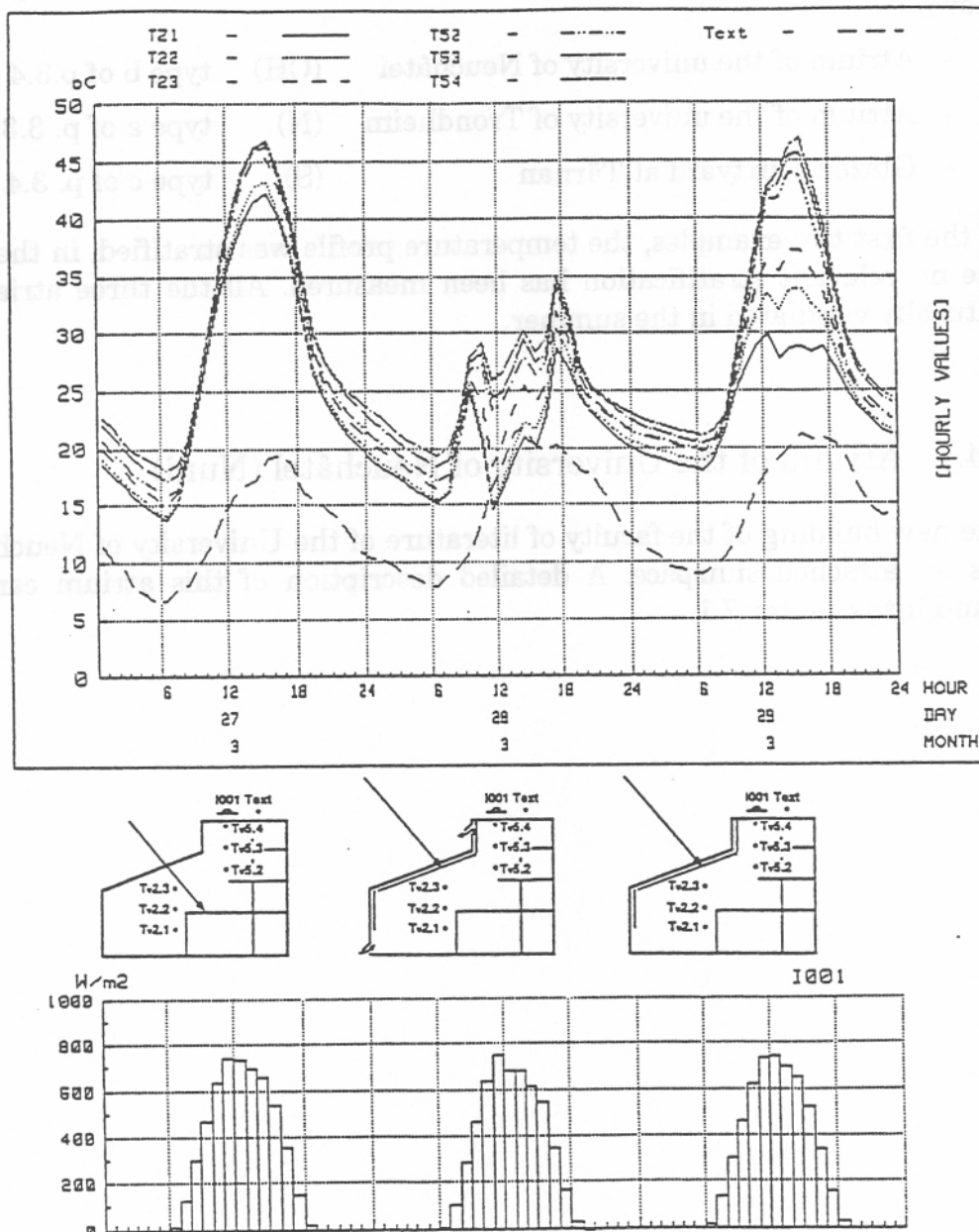
Fig. 8   Measured temperature profiles for three typical days

First day

- No internal shading is used
- The hatches are closed

    The air stratification is not relevant (only 4°C), because the solar gains are heating also the lower part of the atrium (ground, walls), and create in this way a mixed temperature condition.

Second day

- The hatches are opened
- The internal shading devices are used

    The air stratification is reduced in comparison of the third day (8-10°C), the average temperature in the atrium is also reduced and the occupied zone becomes comfortable.

Third day

- The hatches are closed
- The internal shading devices are used

    The air stratification is important (15°C) ! The upper shading devices are intercepting the main part of the solar gains and do not allow them to reach the lower part of the atrium (or at least only small amounts). In the lower part of the atrium the vents are opened briefly (point 7) and a wide mobile wall is opened. The lower part of the atrium is exchanging air with the building which is 20°C.

3:7

3.4.2 Atrium of the University of Trondheim (ELA)

A field study has been conducted in Trondheim on a glazed atrium of the university. The dimensions of this large enclosure are 46 m x 10 m x 17 m (high).

A detailed description can be found in chapter 7.4.

Figure 9 shows the effect on the internal air temperature when opening the ventilation hatches at two heights inside the atrium in the summer.

The first 3 days represent opened hatches during which the maximum temperature difference at 13 m and 1,7 m above the floor was only 3 degrees. In the last 2 days during which the hatches are closed a temperature difference as high as 16°C (max. temperature at roof level : 46°C) was recorded.
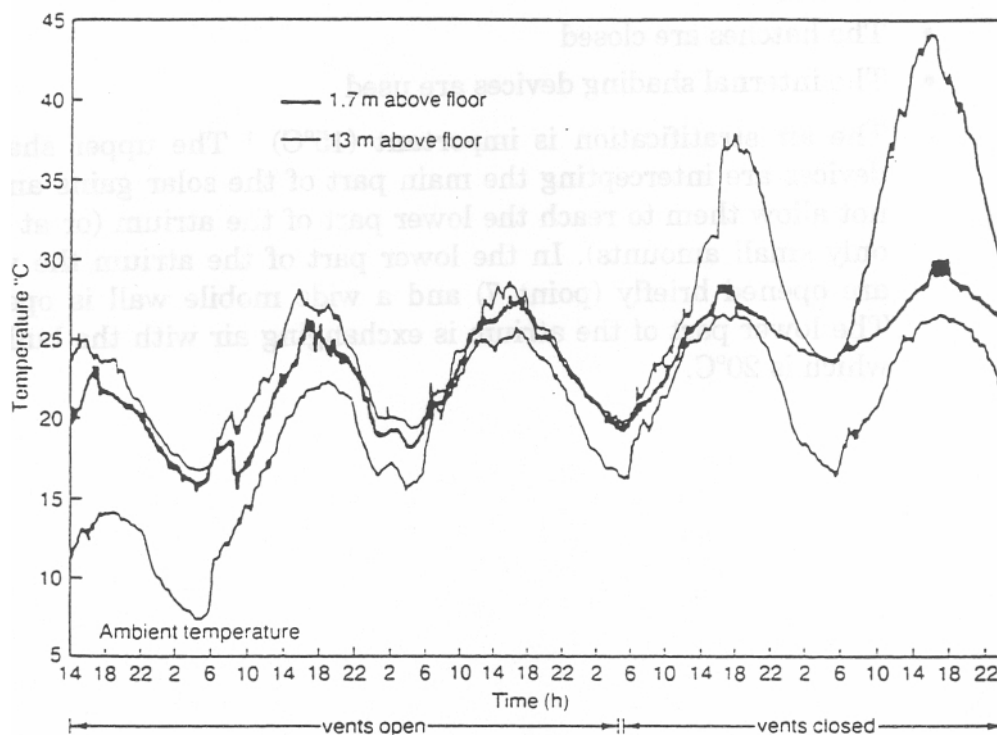
Fig. 9   Measured air temperature at two levels in a glazed atrium with and without passive ventilation

3:8

3.4.3 Glazed courtyard at Taman

Also here a detailed description of this atrium can be found in chapter 7.2.

The temperature measurement at different level during a sunny week in May are presented in the next figure.

This week, the curtains were used as insulation during the nights and as sun shades during parts of the days. The vents were open parts of the day during all days except the last one which was cold and cloudy and no curtains were used during daytime.
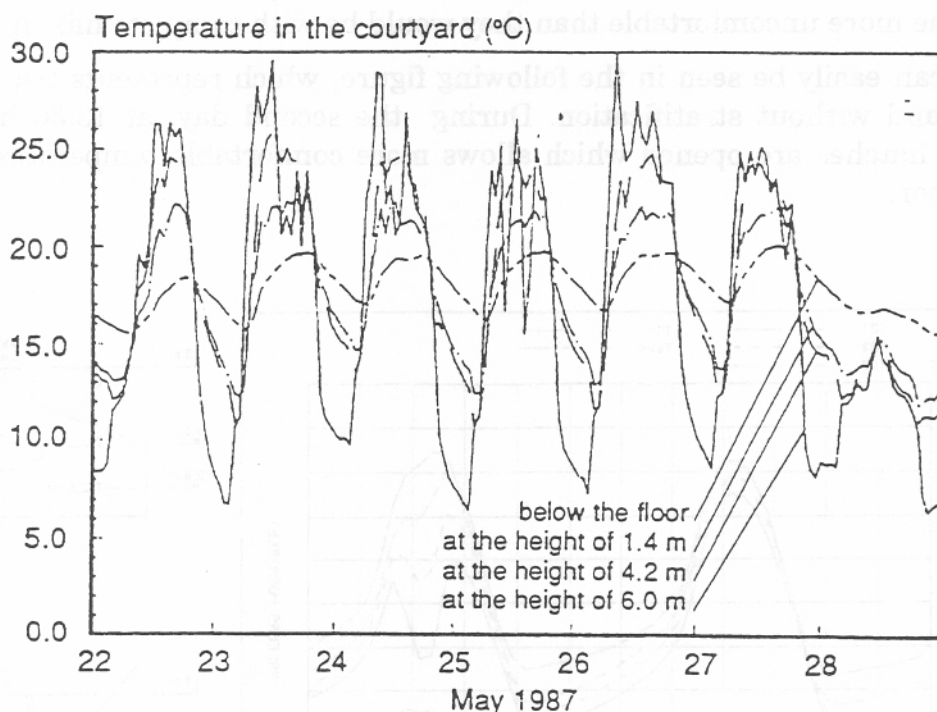

Fig. 10 *The temperature at different levels in the glazed courtyard during a week in May 1987*

As can be seen, there is not a big stratification between 1,4 m and 6 m height. The irregular shape of the temperature is due to the changes in the shading devices and opened hatches.

In such an atrium configuration (type c p.4) with a small height (~ 6 m) no important stratification is taking place, especially when the vents are opened and the space naturally ventilated.

3:9

3.5 Influence of the temperature stratification on thermal comfort and energy consumption

3.5.1 Thermal comfort

During the summer, temperature stratification can be seen as positive for the comfort of the occupied zone at the ground level.

If the peak temperature of the upper part of the atrium is not increased by the internal shading devices which tend to create stratification, the upper occupied zone or the rooms at that level of the adjacent building will not become more uncomfortable than they would be with complete mixing.

This can easily be seen in the following figure, which represents two days with and without stratification. During the second day, at 13.30 h; the lower hatches are opened which allows more comfortable temperature on the floor.
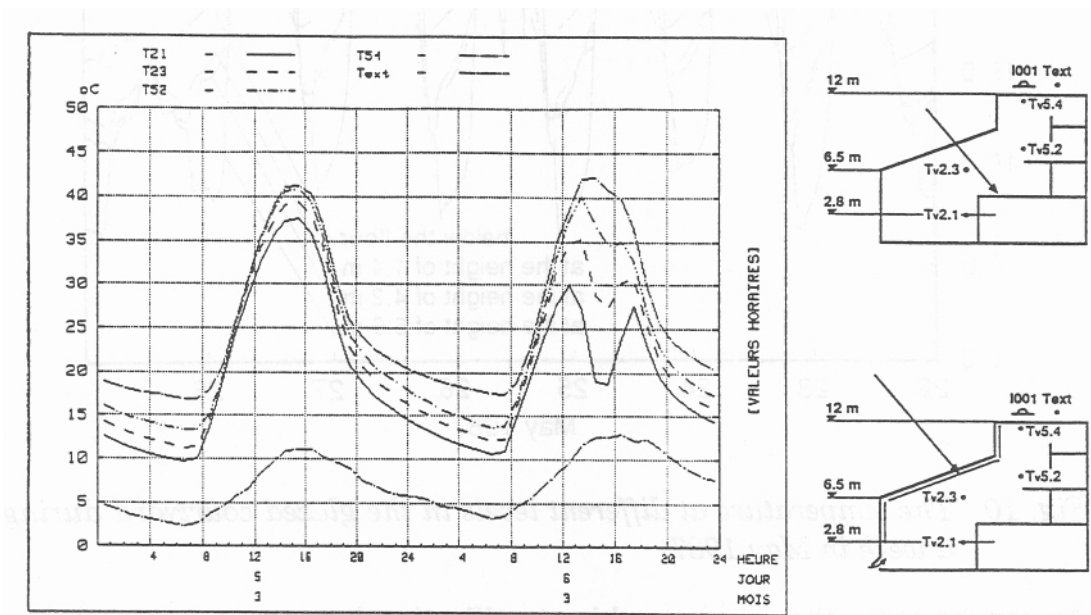
Fig. 11   Temperature profiles with and without stratification for the March 5 or 6 1989 in Neuchâtel

3:10

In fact, stratification of the temperature in the summer is not very often sufficient to provide comfortable conditions at the ground level and natural ventilation must be used. It is also important to notice that the atrium configuration which tend to produce a temperature profile of the type 3 (fig .1) will be better for the comfort if there is some occupied zones at different levels. The same remark is valid for the adjacent buildings room especially if they have openable windows to the atrium.

Winter time

In winter time, especially in heated atria, temperature stratification is a disadvantage, because it will require the heating system to overheat the upper part of the atrium to obtain comfortable conditions in the occupied zone (lower part of the atrium).

3.5.2 Energy consumption

For the comfort point of view it is important for the designer to be able to predict the temperature stratification in the atrium. On the other hand : it is not quite clear if it is very important to take into account the temperature stratification in the annual energy consumption of the atrium and the adjacent building.

In order to illustrate the problem three type of calculations have been done with the atrium of the University of Neuchâtel (Nuni).

1. The first calculation assumes that the air temperature of the atrium is fully mixed, and that the use of the shading devices and of the vents are controlled using this mixed air temperature. When the air temperature is greater than 26°C the shading devices are used and the vents opened.

2. The second calculation takes into account the temperature stratification using the model presented in chapter 6.5. The use of the shading devices and of the vents (opening for natural ventilation) is controlled using the temperature of the first zone (ground level). The shading devices and the vents are used when this temperature is greater than 26°C.

3. The third calculation is the same case as number two except for the control value which is not the first zone any more but the last one (top of the atrium).

3:11

In the three calculations the control temperature for heating is 16°C. The outside glasses of the atrium have a U value of 1.5 W/m^2,K
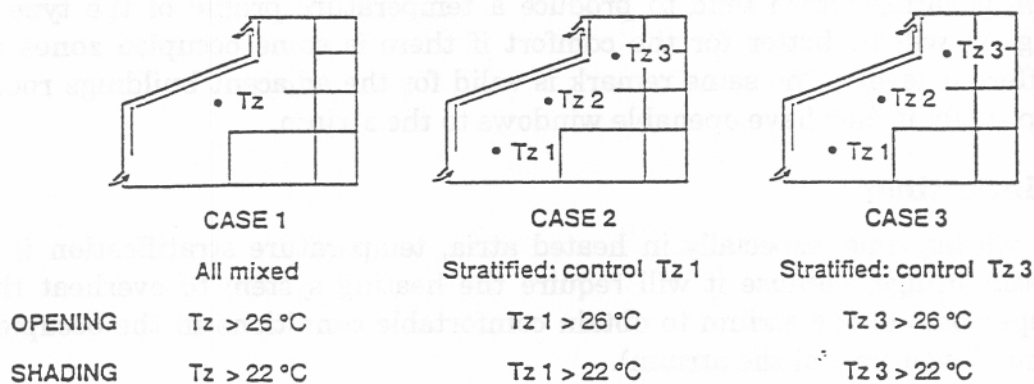

CASE 1	CASE 2	CASE 3
All mixed	Stratified: control Tz 1	Stratified: control Tz 3
OPENING Tz > 26 °C	Tz 1 > 26 °C	Tz 3 > 26 °C
SHADING Tz > 22 °C	Tz 1 > 22 °C	Tz 3 > 22 °C

Fig. 12 Energy consumption calculation ***with three different control** strategies for the opening of the vents*

For a cold day without the stratification there will be no difference between the three calculations. For a sunny day with reasonable outside temperatures the calculation number 3 will open the vents more rapidly if stratification occurs. The number 2 is the one which will open the vents latest, the number 1 being in between.

The results of the heat consumption of the atrium and of the adjacent building for the three calculations are given in the next table. The simulation have been done for a year.

	1. Mixing		2. Stratification : Control based on lower zone temp.		3. Stratification : Control based on upper zone temp.	
	Total	Atrium	Total	Atrium	Total	Atrium
kWh	324608	9979	323398	9467	325968	10565
%	100	100	100	95	100	106

The differences are not very important if we are interested in the total energy consumption of the building. So that in the case of Nuni, we can conclude that for the energy calculation it is not important to be able to model the temperature stratification. The mixed assumption give already a good result. Of course if one is interested only in the atrium consumption we have a difference of 6 % between the case 1 and 3.

In other atrium types (higher thermal mass, core or central atrium) the differences could be more significant.

3.6   Simplified models

3.6.1   Definition of the simplified models

Existing simulation programs calculate a single indoor air temperature in each thermal zone being analyzed. The real temperature distributions in the space are important in determining transmission heat losses, air change rate between the atrium and ambient, between the atrium and adjacent spaces, air motion within the atrium and comfort conditions. In order to provide a more faithful representation of thermal conditions in an atrium, the spatial distribution of air and surface temperatures must be determined.

The simplified model (S.M.) should be able to be incorporated in a dynamic building energy simulation program in order to overcome the lack of information of the single indoor air temperature model.

3.6.2   Modeling approaches

During this IEA task, different approaches have been used by the participants. They will be briefly presented :

1. Linear model (Norway)

2. Superposition of standard single zone model of a building simulation program (Sweden + Switzerland)

3. Single volume with different air nodes and wall temperatures in the vertical direction (Switzerland)

Each approach will be briefly presented, and some comparison with measurements in atrium will be shown.

3.7   Linear model

All the information from this chapter is coming from the paper of K. Kolsaker and H.M. Mathisen presented in Roomvent 92.

3.7.1   Background

The use of glazed atria has become more common during the last years. One typical characteristic of these type of premises is that the air stratifies with a temperature increasing with the height. The displacement ventilation system, which has the same quality has also become common in use. It is therefore a demand for simulation programs for calculation of the annual energy use and peak loads in such situations.

In glazed atria the ventilation airflow rate is often zero. Consequently, if we have the infiltrations the temperature stratification is maintained only by the convection flows, i.e. flows from heat sources like windows and other surfaces heated by the sun and flows directed downwards due to surfaces with a temperature lower than the room air temperature.

If the atrium is ventilated by air blown in with an impulse strong enough to cause <u>mixing</u> of the air, a uniform temperature will be the result.

The dominant heat losses in an atrium is due to transmission losses through glazing and infiltration losses.

Accordingly :

Under conditions with complete mixing (heating in the lower part and/or significant down draft, no solar radiation) simulations with programs using one node to represent the air temperature, should give adequate results for air temperature and energy demand for potential heating. During the hours of the year when there is some solar radiation and a heating demand, (i.e. some stratification), these simulations will under-estimate the heating demand. Heat of the lower part of the atrium will be necessary in spite of that the upper part is thermally comfortable.

Under conditions with poor mixing, the simulated air temperature will represent the temperature in the upper part of the atrium (more so in a linear and a core atrium than in an attached and envelope atrium). The calculated thermal climate gives us little information about the climate at floor level.

3.7.2   Linear temperature stratification model

As mentioned, simple algebraic calculation of convection flows in rooms with a changing vertical gradient is difficult. Experiments and field measurements have shown that the profile in many cases becomes more or less linear, as shown in principle in figure 13.

The reason is that the heat sources are distributed by radiation to the surfaces in the room. Thermal transmission through walls and windows may also influence on the thermal stratification.
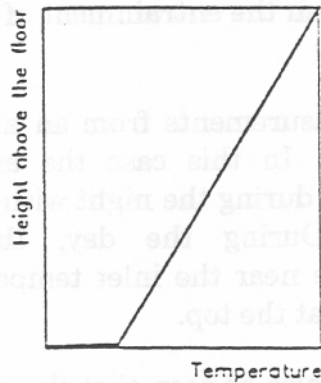

Fig. 13   Temperature profile in rooms with weak and distributed heat sources and little mixing of the air

An air temperature distribution dependent on the level above floor level and some characteristics about the room is also an interesting alternative, and may be more simple to implement than a two or multi-zone model.

In figure 14 examples from measurements in a test room with displacement ventilation are shown. The dimensionless temperature $\frac{T_{actual}-T_{supply}}{T_{exhaust}-T_{supply}}$ is plotted against the height above the floor. The temperatures were measured from the surface of the floor to a point close to ceiling.
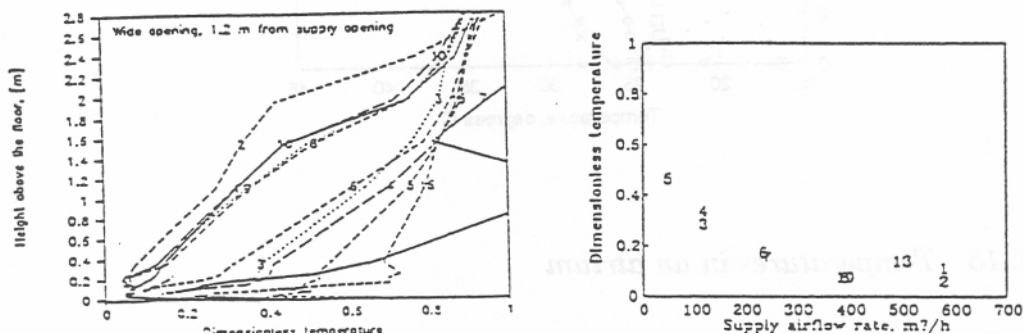
Fig. 14 a) dimensionless temperatures in a room with displacement ventilation plotted against the height above the floor. b) dimensionless temperatures plotted against the supply flow rate. The numbers in a) refer to the numbers in b)

It can be clearly seen from Fig. 14 that the shape of the profile varies from test to test. If the curves are related to the airflow rates as shown in Fig. 14 it is obvious that the shape of the curves depends on the airflow rate. What actually happens is that when the supply airflow rate is reduced the height of the lower zone decreases when the entrainment of the convection flow is constant.

The profiles in fig. 15 are measurements from an atrium under different solar and thermal conditions. In this case the air flow rate is quite constant. The gradient is small during the night with a small heat load and low surface temperatures.   During the day, the gradient can be considerable, with temperature near the inlet temperature near the floor and a high temperature (45°C) at the top.

From experimental data it can also be seen that the shape of the profiles is almost the same in all positions. This is due to the poor entrainment of ambient air in the flow. However, the quality and the position of the heat sources and the ceiling height plays an important role for the shape.
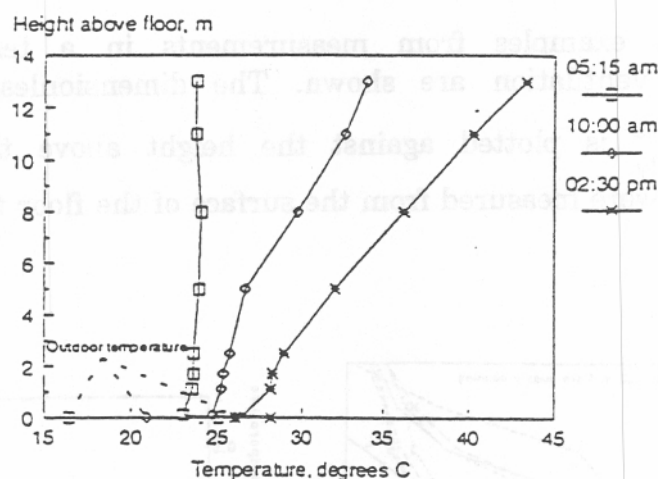
Fig. 15   Temperatures in an atrium

FRES (Flexible Room climate and Energy Simulator see chap 9.) is a dynamic simulation program for multi-zone buildings developed at SINTEF Division of Heating and Ventilation. The program is a tool for HVAC consultants and building designers, widely used in Norway. The objectives are to implement a simple and still reliable model that can improve the existing single-temperature zone model and make it a better tool for atrium simulation.

3:16

The proposed linear stratification model is implemented in FRES as described in the previous sections. For calculation of heat transfer between room air and room surfaces, the temperature difference between surface and room air at the mean height of each surface is used.

The convective heat flow to each surface is calculated for the stratified case, ensuring the correct heat balance for the whole building. The stratification will for example make floor and ceiling "feel" different air temperatures. To take care of this, the equation for convective heat flow is modified, taking into account the linear stratification model. This is quite simple, as will be shown here.

a)   Heat balance   b)   Definitions
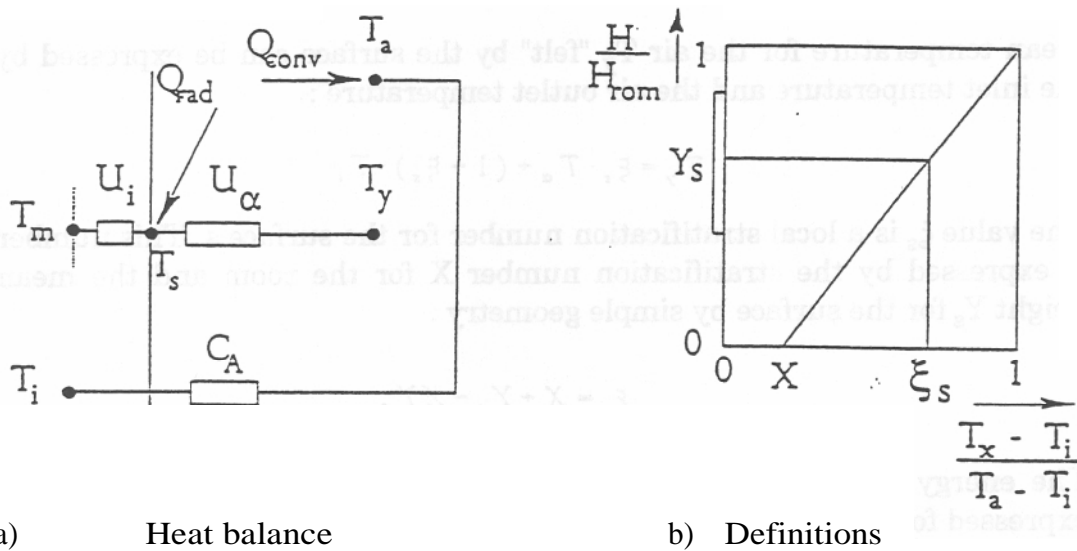
Fig 16   The model implemented in FRES

The temperature T_X near the floor is given by the equation

$$T_x = X T_a + (1 - X) T_i$$

where X = Dimensionless temperature near the floor; $X = \frac{T_x - T_i}{T_a - T_i}$

T_a = Temperature in air outlet
T_i = Temperature in air inlet

By geometry, mean dimensionless height of a rectangular surface can be expressed by

$$Y_s = \frac{H_1 + H_2}{2H}$$

where H_1 = Height of lower side of rectangle
          H_2 = Height of upper side of rectangle
          H = Height of room

Mean temperature for the air T_y "felt" by the surface can be expressed by the inlet temperature and the air outlet temperature :

$$T_y = \xi_s \cdot T_a + (1 - \xi_s) \cdot T_i$$

The value ξ is a local stratification number for the surface s. This number is expressed by the stratification number X for the room and the mean height Y_s for the surface by simple geometry :

$$\xi_s = X + Y_s - XY_s$$

The energy balance for an air volume with one single surface s can be expressed for the surface and the air volume by the equations.

$$U_i(T_m - T_s) + U_a(T_y - T_s) + F_r Q = 0$$

$$C_a(T_i - T_a) + U_a(T_s - T_y) + (1 - F_R)Q = 0$$

where

T_m	=	The neighbour temperature inside the wall	[°]
T_s	=	The surface temperature	[°]
T_i	=	Air inlet temperature	[°]
T_y	=	Air temperature at level Y = Ys (mean surface height)	[°]
T_a	=	Air temperature at level Y = 1 (Air outlet)	[°]
Q	=	Room heat load	[W]
U_i	=	Heat conductance from surface to nearest wall node	[W/°]
U_a	=	Convective heat transfer coefficient for the surface	[W]
C_a	=	Heat capacity rate of inlet air	[W/°]
F_r	=	Fraction of radiation for room heat load	[W]

3:18

This model uses the temperature $(T_y - T_s)$ instead of $(T_a - T_s)$ as the driving force for the convective heat transfer between room air and the surface. If for example a room faces to the upper part of an atrium and another room faces to the lower part of the same atrium, the model will catch the different conditions of these two rooms.

A combination of the previous equations results in the following equation system, which can be extended to multiroom models with a variable number of walls and a free air flow pattern :

$$\begin{bmatrix} -U_i + U_a & U_a \xi_s \\ U_a & -\xi_s U_a + C_a \end{bmatrix} \begin{bmatrix} T_s \\ T_a \end{bmatrix} + \begin{bmatrix} U_i & U_a(1 - \xi_s) \\ 0 & C_a - (1 - \xi_s)U_a \end{bmatrix} \begin{bmatrix} T_m \\ T_i \end{bmatrix} + \begin{bmatrix} F_r \\ 1 - F_r \end{bmatrix} Q = 0$$

The local stratification number ξs must be calculated for every surface in the room for a given X. You will see that ξs = 1 for the ceiling for all values of X. For the floor, ξs = X. Further, the case X = 1 (no stratification) result in ξ = 1 for all surface positions. This case reduces the problem to a normal single zone model.

As discussed in the previous section, X is a function of both the airflow rate and the heat load. At the moment, a constant value of X is used. A model for correlation to the floor temperature is implemented as an option. the model is proposed by Mundt, based on a simple energy balance for the air volume close to the floor, neglecting induction of room air into inlet air :

$$C_a(T_i - T_x) + U_a(T_{floor} - T_x) = 0$$

where T_{floor} is the floor surface temperature. This equation is solved for the air temperature T_x near the floor using a mixed air inlet temperature for all air inlets and the floor temperature calculated by FRES. The calculated air temperature T_X is used in the calculations.

3.7.3 Simulations and discussion

An atrium within, the ELA building at the Norwegian Institute of Technology in Trondheim has been simulated over a period and compared to measurements.

A single atrium was modelled. Solar radiation and other climatic data are measured over a 3 day period with quite warm weather and clear sky conditions. Three simulations are presented :

- Ordinary one zone model, X = 1.0
- Constant air stratification, X = 0.2
- Variable air stratification, X = f, calculated according to Mundt's model

The simulations use measured outdoor temperature over a 3 day period as input. A Cloud Cover Factor is chosen so the calculated total radiation on a horizontal surface during a day is close to the measured valued.

The results are presented in the figures 17 a, b, c and d. The simulated period is a quite warm period with day temperatures over 20°C, preceded by a colder period. There was no heating demand except during the first night. The controller setpoint in the atrium is 15°C.
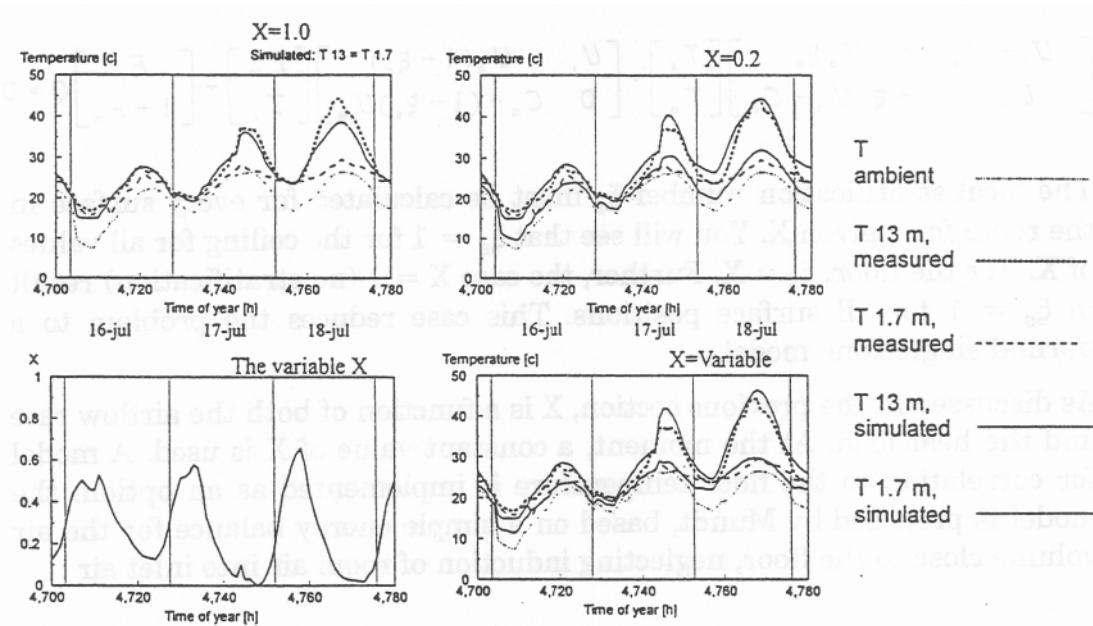

Fig. 17   The simulation results

Fig. 17 shows the temperature using X = 1.0. This simulation is identical to a one zone simulation with no air stratification model. The thick line is the simulated air temperature. You can observe the effect of heating during the first night. The air hatches were fully open the first period, using a measured air exchange rate of about 4 ach. At the time t = 4743 h, and the rest of the period, the hatches were closed, using a measured air exchange of about 0.45 ach. This results in a temperature rise of 6-7° C which can be found in the graph. In the period with closed hatches, the simulated temperature is slightly lower than the measured value.

Fig 17 shows a simulation with constant X = 0.2. This results in two simulated temperatures, one corresponding to the upper level and another corresponding to a level 1.7 m above the floor. The upper level temperatures are higher than the temperatures from the previous simulation with X = 1.0, due to the fact that convective heat transfer is connected to the average air temperature outside each surface.

3:20

Since this temperature is lower than the upper level air temperature, the calculated heat loss is lower. This results in a higher temperature in the latter case.

The calculated temperature at a level of 1.7 m is too low in the night and too high in the day. The reason for this is that the stratification is connected to the solar load, which varies from zero in the night to a significant value in the day. To correct for this, a model which includes the heat load should be applied.

Fig. 17 shows a simulation using such a model with variable X. The model is described in the previous chapter, and the resulting value of X is presented in fig 17. It varies from close to zero in the day and about 0.6 during the night. The simulated temperature at the 1.7 m level is now much closer to the measured value.

Conclusions

In buildings with stratified room air temperature, improved accuracy in calculated annual energy consumption and air temperatures should be obtained by including a two zone or linear temperature stratification model in building energy simulation programs.

Measurements show that stratification with two separate zones with homogeneous temperature are seldom found. The reason is that heat sources are distributed by radiation to the surfaces in the room. In addition, such a situation is difficult to model.

The proposed model with a linear temperature stratification shows good results using a single example. The model as implemented in FRES is quite robust and flexible, and allows an arbitrary number or surfaces and air flow patterns in the building. Even with a simple correlation of X, the model seems to behave well in a case with variable conditions. A few other cases have also been tested, but more testing work remains before the model can be released.

3.8 Use of standard building dynamic simulation program

The second approach used to model temperature stratification is to divide vertically the atria into different volumes. In each of these volumes the temperature is assumed homogeneous. This method has been used in two dynamic building energy simulation programs without any modifications of the source code :

- TRNSYS →   Nuni atrium, ETA atrium (chap 3.10/3.11)
  DEROB →   Taman Courtyard (chap. 3.9)

3:21

The principle problem with this method is that the different volume must be separated by a wall (surface) within DEROB and TRNSYS. This means that the infrared radiation exchanges are not taken into account in the right way.

With TRNSYS the situation is even worse because the surface which separates the two air zones (volume) can not be defined as a glass panel with 100 % transmission. The solar radiation is then intercepted in this volume and distributed on the surfaces following a surface ratio rule.

A mass transfer between the volumes is possible in the two cases, but the model that calculates it is either very simple (DEROB) or must be implemented (TRNSYS).

3.9 Glazed courtyard at Taman simulated with DEROB-LTH

3.9.1 Description of the analytical model

When the glazed courtyard at Taman was simulated, the model was divided into six different volumes. The courtyard is described by means of four volumes which divide the courtyard vertically. This allows temperatures to be studied at different levels and to compare these with measurements. The lowest volume extends to the level 3.2 m, and the second between 3.2 m and 5.7 m. The two top zones form the volumes just below the roof are triangular in cross section, see figure 25. the two rows of terrace houses along the south and north sides of the courtyard are described in a highly simplified manner as two volumes. In this report no study is made of the energy balances of the surrounding houses, but only of the effect these have on the energy balance in the glazed space. The walls between the surrounding houses and the courtyard are therefore described accurately,   while great simplifications have been made in describing those on the outside. Owing to the limitations of the computer program, if the surrounding buildings are to be studied the glazed courtyard must be described in a more schematic manner, for instance without division into several different zones.

3:22
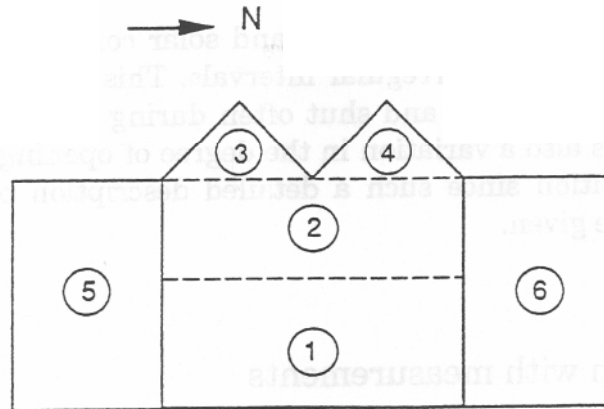
Fig. 18   Division of the analytical model into volumes

In larger volumes temperature stratification may occur, and for this reason it is desirable to have the facility to calculate the temperature at different levels. There is no facility incorporated in DEROB whereby a volume can be divided into different zones. The program makes the temperature equal in the entire volume. In order therefore that it may nevertheless be possible to calculate temperatures at different levels, the glazed space has been divided into a number of volumes, for each of which the program calculates a separate air temperature. Each volume must be delineated by surfaces, and it is therefore desirable that the horizontal division between volumes 1 and 2, volumes 2 and 3 and volumes 2 and 4 should have no effect on the energy balance. The nearest approach that can be made to this is to divide the volumes by a single pane of glass which has 100 % transmission of direct radiation (the transmission of diffuse radiation is then 92 %). By simultaneously allowing air to move between the volumes with the assistance of the thermal driving forces, a model is obtained which gives the best possible description of the glazed courtyard. The long wave radiation between surfaces in the glazed courtyard is not treated entirely correctly, since each volume is calculated separately.

The use of vents and solar control curtains can have a significant effect on the temperature in the glazed space. These must therefore be taken into account in the calculations. The measurements record whether the vents are open   and what the positions of the curtains are. Variation in ventilation is represented in DEROB by giving the number of air changes per hour with the external air. The curtains are located horizontally near the roof at the boundary between volumes 2 and 3 and between volumes 2 and 4. In DEROB it is possible to specify variable insulation by stating at what times it is used. Transmission of short wave radiation cannot be stated as input data, and it is at all times 0 %. When the curtains are used for solar control purposes in the calculations, their effect is exaggerated. The measurements show that the curtains transmit about 40 % of global radiation.

3:23

As a result of automatic control of vents and solar control curtains, their setting is altered often and at irregular intervals. This applies particularly to the vents which are opened and shut often during the warmer part of the year, and there is also a variation in the degree of opening. This causes difficulties in simulation since such a detailed description of changes in ventilation cannot be given.

3.9.2   Comparison with measurements

As it can be seen in the chapter 3.4.3, there is no big temperature stratification in this atrium. So that this example is not the best case for the performance evaluation of a model which calculate the temperature stratification. In addition the vents situated on the roof of the atrium were often opened during this period. The air exchange rate with outside has been estimated. This constitute a source of error in the calculation which have nothing to do with the temperature stratification model.

The results obtained with this method are represented in the next six figures.
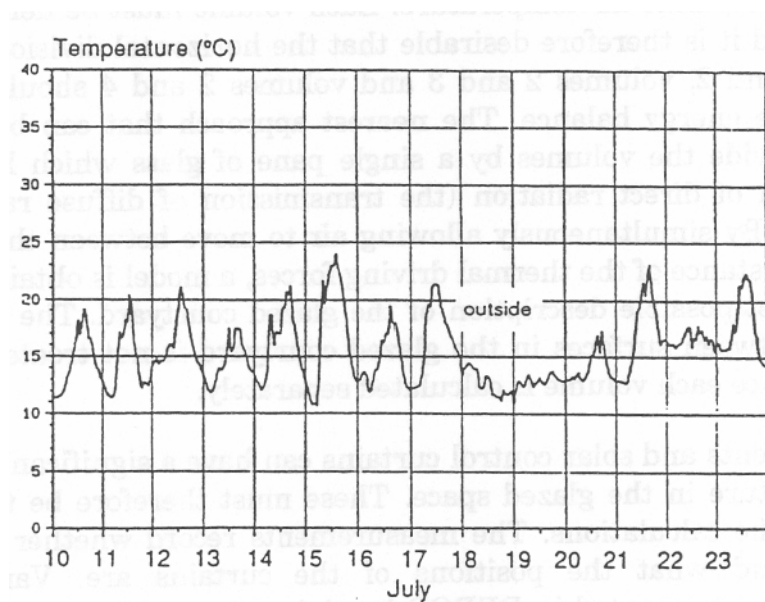
Fig. 19   Outside temperature measured during two weeks in July 1987

3:24
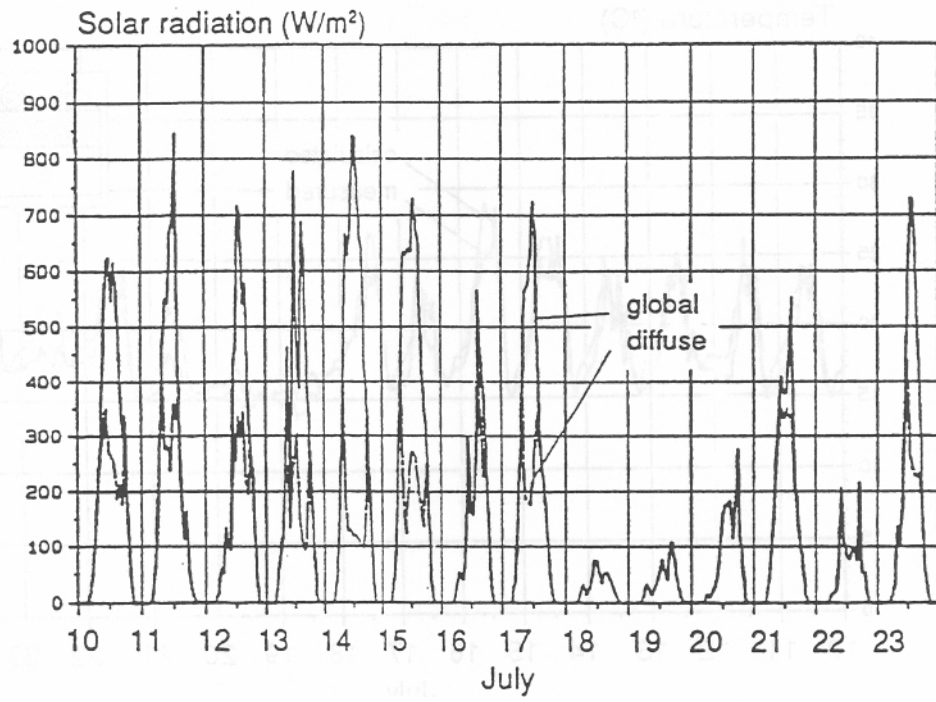
*Fig. 20 Solar radiation on a horizontal surface measured during two
weeks in July 1987*
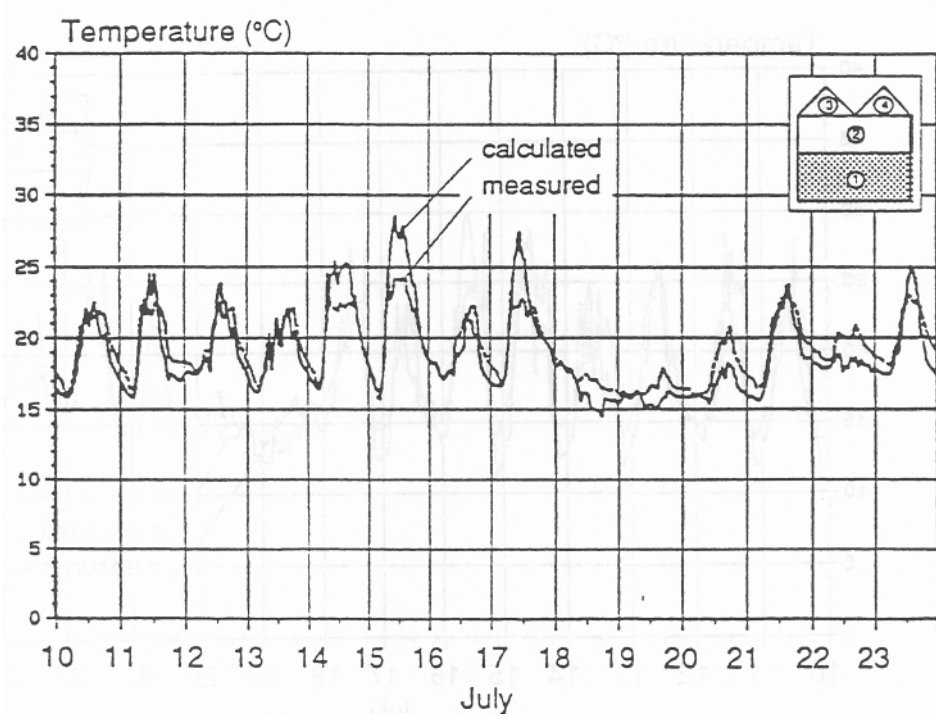
*Fig. 21   Calculated and measured temperature in volume 1 during two
weeks in July 1987*

3:25
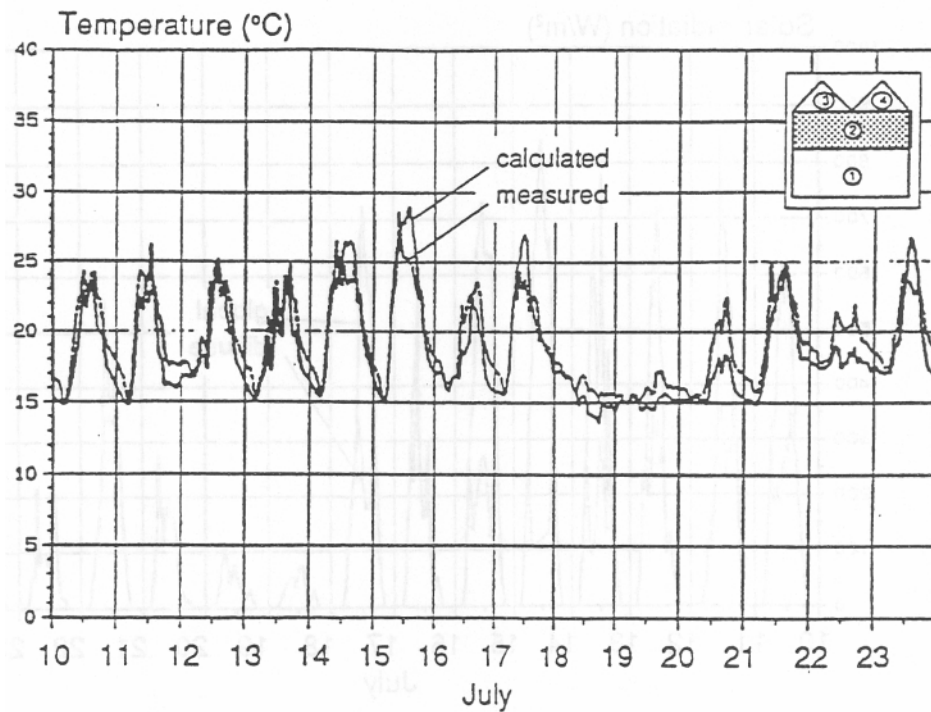
Fig. 22   Calculated and measured temperature in volume 2 during two weeks in July 1987
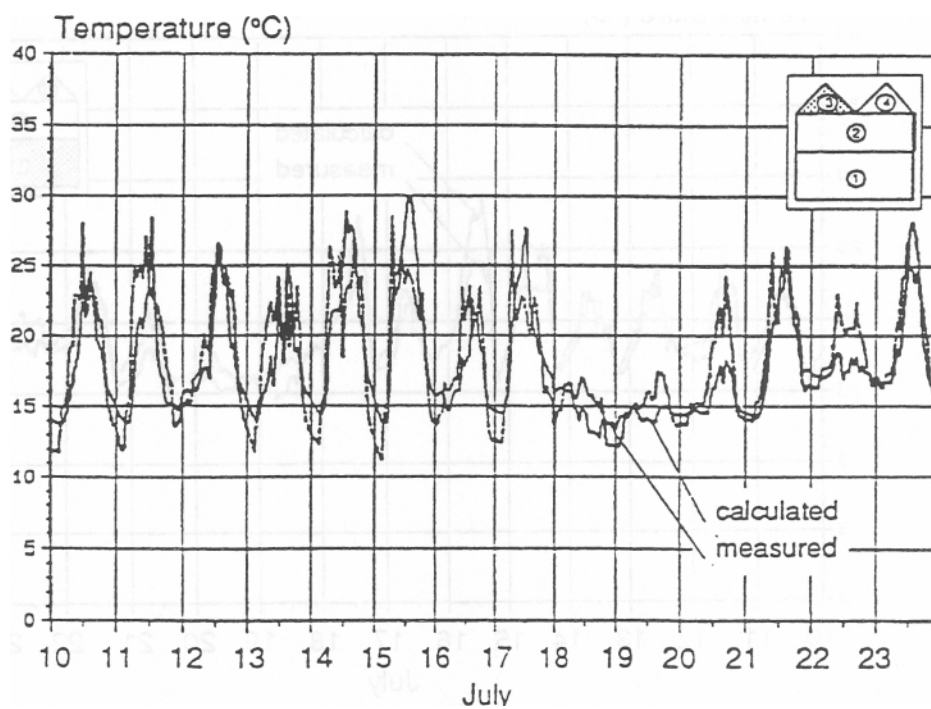
Fig. 23   Calculated and measured temperature in volume 3 during two weeks in July 1987

3:26
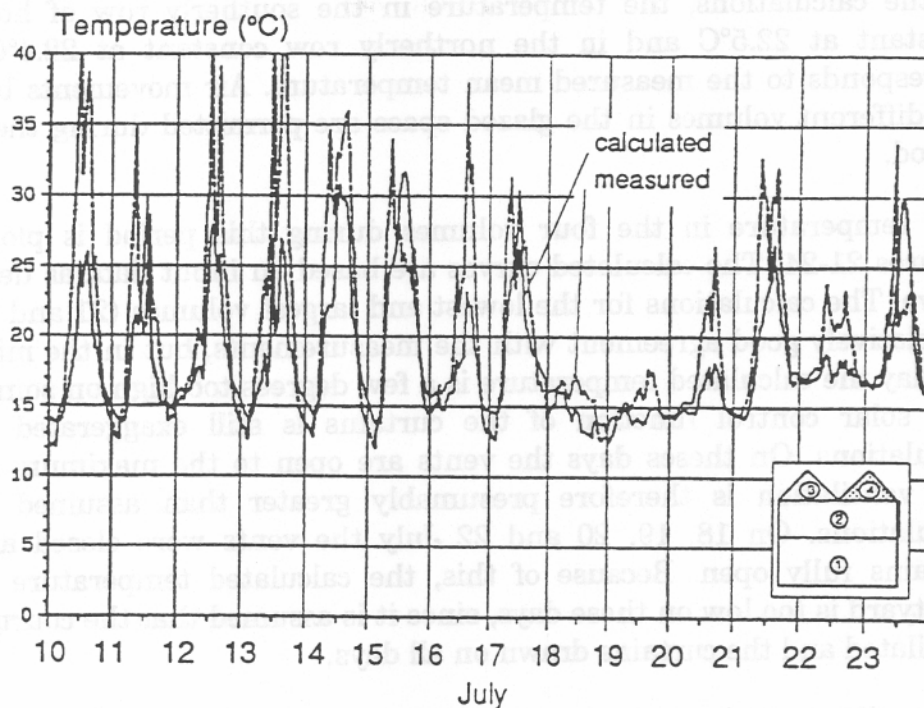
Fig. 24   *Calculated and measured temperature in volume 4 during two weeks in July 1987*

This period is very difficult to simulate, since the vents and curtains were altered often and with no set pattern. In the calculations ventilation in the lowest volumes i.e. up to a level of 5.7 m, was estimated at 5 air changes per hour between 1000 and 1800 hours and at 2 air changes per hour at other times. The roof vents were fully open during a large part of the day, and it was therefore assumed that in volumes 3 and 4 the air change rate was 10 per hour between 1000 and 1800 hours and 2 per hour at other times. The difficulty is that in reality the opening angle of the vents varied a lot from day to day, and on 18, 19, 20 and 22 July the vents were fully closed. The calculations cannot taken account of this, and it has to be assumed that ventilation is the same every day. Unfortunately, it is impossible to find a warm and sunny summer period during which regulation of the curtains and vents is the same every day over a longer period.

In spite of the fact that it was summer, the curtains were drawn in a double layer during the night. During the day the curtains were drawn in a single layer at varying times. As an average, it was decided to have them drawn between 1200 and 1700 hours as input data for the calculations. Note that in the calculations the curtains do not let through any solar radiation, either diffuse or direct. in reality, the transmittance of the curtain for global radiation is approx. 40 %.

3:27

In the calculations, the temperature in the southerly row of houses is constant at 22.5°C and in the northerly row constant at 22.4°C. This corresponds to the measured mean temperature. Air movements between the different volumes in the glazed space are permitted during the entire period.

The temperature in the four volumes during this period is plotted in Figures 21-24. The calculated curves are based on input data as described above. The calculations for the lowest and largest volumes (21 and 22) are in relatively good agreement with the measurements, but in the middle of the day the calculated temperature is a few degrees too high on some days. The solar control function of the curtains is still exaggerated in the calculations. On theses days the vents are open to the maximum extent, and ventilation is therefore presumably greater than assumed in the calculations. On 18, 19, 20 and 22 July the vents were closed and the curtains fully open. Because of this, the calculated temperature in the courtyard is too low on these days, since it is assumed that the courtyard is ventilated and the curtains drawn on all days.

When allowance is made for the difficulty of simulating such a volume, agreement between measurements and calculations is fairly good in the southerly roof volume, figure 23 In the northerly roof volume, figure 24, the measured temperature is very high during the day and it varies a lot. During some hours the temperature according to the measurements can be 10-15°C higher than the calculated values. It is evident that air movements here have a significant effect on temperature. The large difference may to some extent be due to the fact that the hot air from the lower volumes actually rises along the hottest facade which has a southerly orientation and reaches the roof in volume 4. This is not treated correctly in the calculations. To some extent, the reason for the difference is presumably that the measurement point has no radiation protection and is exposed to powerful insolation.

At the times when the calculated temperature in volume 4 is higher than that measured, this is presumably due to the fact that the vents are in reality fully open on both the leeward and windward sides. This gives rise to a strong draught, and the temperature can suddenly drop to values near the outside temperature.

On the whole, it is difficult to state with certainty why the calculations are different from the measurements. It is very likely that the reason is a combination of the parameters discussed above. One of the most difficult factors to judge is how extensive ventilation is and how it varies in time. This holds not only for this glazed space but for all types of glazed spaces.

If the solar control curtains are not drawn between 1200 and 1700 hours, the calculated temperature in the two lowest volumes is still higher while the roof volumes have a lower temperature, which seems reasonable.

Having the curtains drawn at night in a double layer appears unnecessary in the summer, and can give rise to unnecessarily high temperatures during the day. After all, the idea of having night insulations is to reduce fabric losses to the outside, so that the stored heat remains in the courtyard and raises the temperature level.

In most cases, this is undesirable in the summer. What should be done instead of this is to open the vents at night when the outside temperature is lower so as to reduce the temperature. At Taman this is not so important since there are no problems due to excessive temperatures, but in other glazed spaces where it is difficult to achieve a tolerable temperature level it is important that regulation of curtains and vents should be properly thought out.

3.10 Attached atrium of the University of Neuchatel simulated with the type 56 of TRNSYS

3.10.1 General approach

In order to calculate the vertical temperature profile in an atrium the space is divided vertically in different elements. Each element or volume is assumed as perfectly mixed (homogeneous temperature). Between these "zones" a fiction wall (surface) must be defined, this is the main disadvantage of this method :

- The fiction wall will not allow the floor of the atrium to exchange IR radiation with the ceiling of the atrium for example.

- The solar radiation which is entering volume Nr 3 (figure 25), for example, will be distributed according to the surface ratios to the surfaces of the volume Nr 3. No solar radiation will directly effect volume Nr 2 and Nr 1, except the radiation which is coming in through their own windows.

3:29

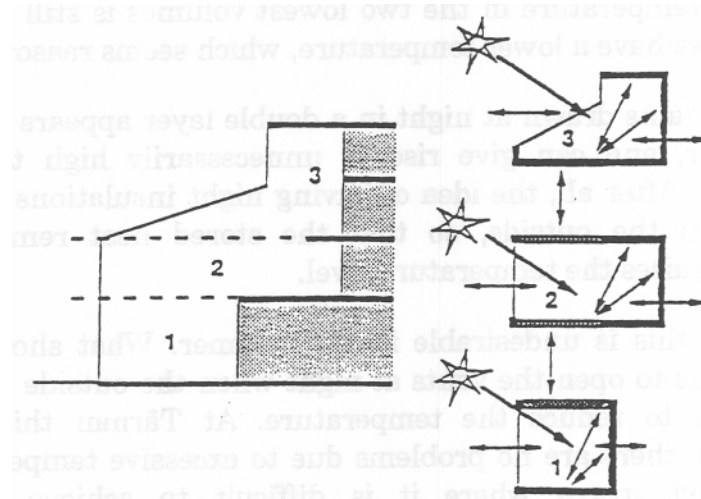The problem is illustrated in the next figure

Fig. 25 Zones definition with the TRNSYS standard approach

A mass transfer (air exchange) between the adjacent zones is possible but must be calculated separately by another subroutine.

In order to investigate this method, the three typical days presented in fig. 8 of this report have been used for the comparison.

3.10.2 Third day with temperature stratification (closed hatches, internal shading devices cases)

The volume of the atrium is divided as it is shown in fig. 25.

The first figure gives the temperature evolution of the ground level and of the upper zones (Nr 1 and 3).
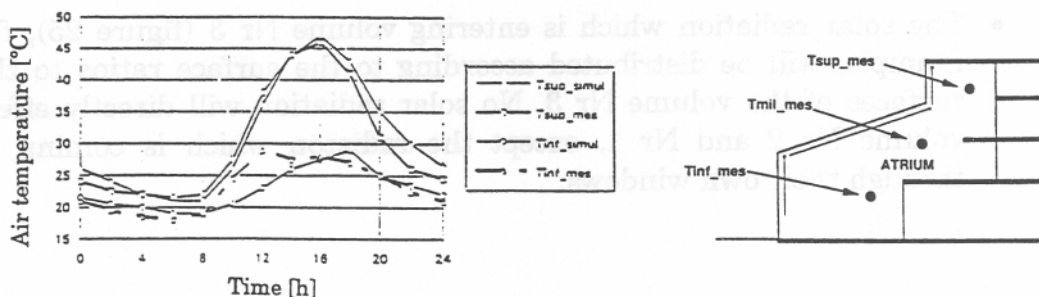
Fig. 26   Comparison between measurements and calculations

3:30

The upper zone temperature is calculated very well. The ground zone temperature is reasonably simulated although, there is a clear inertia problem. The measured temperature in this zone is increasing more rapidly than the one calculated. This can be explained on one hand by the light elements (chairs, tables, metallic structure) which are intercepting solar radiation and gives heat very rapidly to the air and on the other hand by a wrong amount of calculated solar heat gains (too small) applied in this volume. The effect of the light furnitures has not been taken into account in the calculation as the sun is being distributed on the surfaces and especially on the ground (heavy floor D. This failure can be partly eliminated by introducing light "internal" wall as in the zone Nr 1, a part of the solar gains being distributed also on these light surfaces which would play the role of the tables for example.

The second problem due to the wrong calculated amount of solar gains comes from the partitioning of the space. Some solar gain entering through the glasses of zone 3 and 2 will also effect zone 1.

There is also another element which has not been taken into account in the calculation. In fact at about 12 o'clock the lower vents have been opened for half an hour and the mobil wall N° 3 all the afternoon, see figure 27.
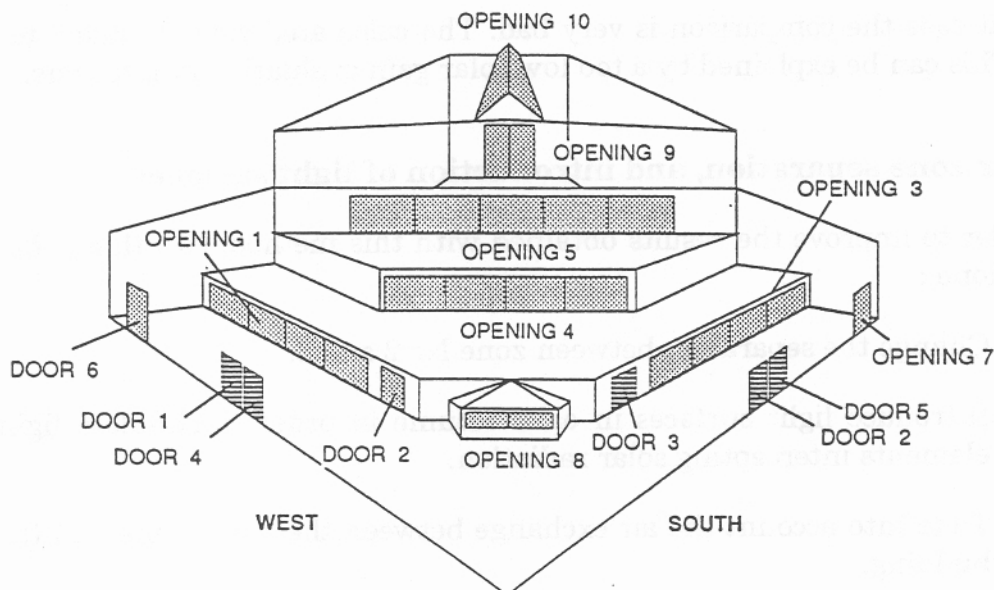
Fig. 27   General view of the openable element against the building

This element explain why the lower space of the atrium remain under 30°C. The air exchange with the building (air at about 20°C) is very important.

3:31

The difference between the measurements and the calculations seems not very important, this is due to a compensation effect less solar heat gains but not transfer of air with the building. Of course, this is not acceptable and must be corrected, otherwise the method will be not useful for a designer.

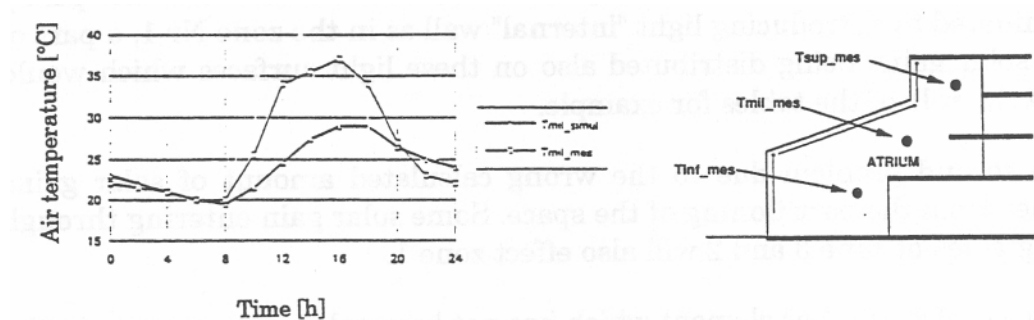The next figure illustrates the comparison of the element in the middle (Nr 2).

Fig. 28   Comparison between measurements and calculations

In that case the comparison is very bad. The calculated value is much too low. This can be explained by a too low solar gain evaluation in this zone.

Better zone separation, and introduction of light surfaces

In order to improve the results obtained with this method, two things have been done :

a. Change the separation between zone Nr 2 and 3.

b. Introduce light surfaces in each volume in order to simulate light elements   intercepting solar radiation.

c. Take into account the air exchange between the lower zone and the building.

3:32

a. New zone partitioning

With the first division of the space, zone Nr 3 had a volume of 195 m^3 and the zone Nr 2 316 m^3. The glazed surface of the volume Nr 3 was 134 m^2 and the on of the zone Nr 2 only 53 m^3.

It is clear that the proportion between the volume and glazed surface is not keeped, especially with the geometry of the atrium a lot of sun coming through the glazing of the zone Nr 3 will effect the zone Nr 2. The division of the space has therefore been changed in the following way :

Zone Nr 3	Volume	=	100 m^3
	Glazed surface	=	83 m^2
Zone Nr 2	Volume	=	406 m^3
	Glazed surface	=	104 m^2

Half of the inclined glazed surface is incorporated in the second zone!

The new separation is represented in the next figure.
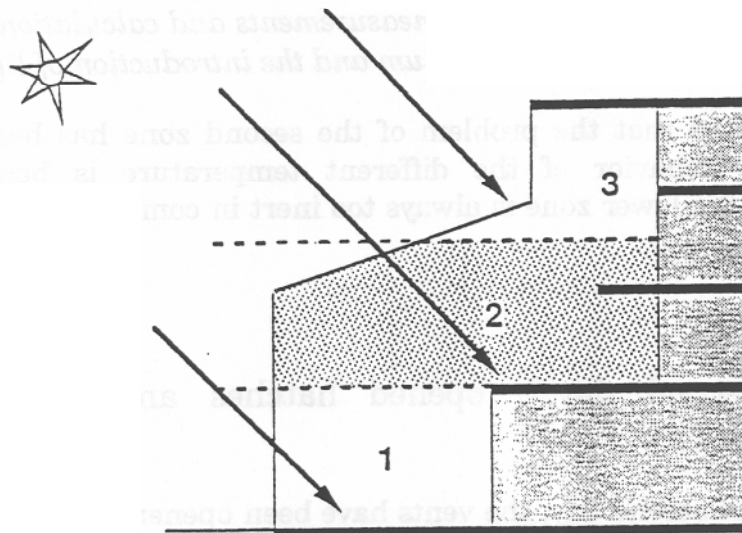
Fig. 29   New space division

b. Introduction of light surfaces

The aim of this introduction is to distribute some part of the solar gain on surfaces with low inertia. These surfaces will be heated very rapidly and will by convection give back some heat into the air rapidly.

The new comparison is presented in the next figure.
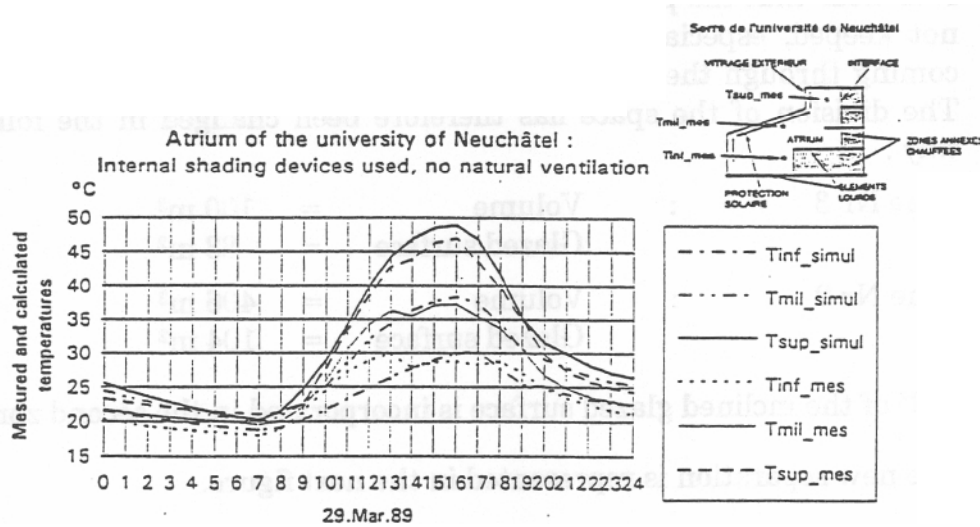
Fig. 30   Comparison between measurements and calculations with the new partitioning of the atrium and the introduction of light surfaces.

It is evident that the problem of the second zone has been solved. The transient behavior of the different temperature is better simulated, although the lower zone is always too inert in comparison to the measured value.

3.10.3 Second day : opened hatches and internal shading devices

During the second day, the vents have been opened from about 11 o'clock since 18 o'clock, and the shading devices were used.

The natural ventilation has been taken into account with the following model :

1. Piston flow : the air coming from the outside through the lower vents is going up to the second volume and finally to the third volume were it leaves the atrium through the upper vents.

Simplified flow field assuming an ideal piston flow

Air exchanges in the atrium

Recirculation due to turbulences

Air flow which is ventilating the atrium

Main air flow through the atrium
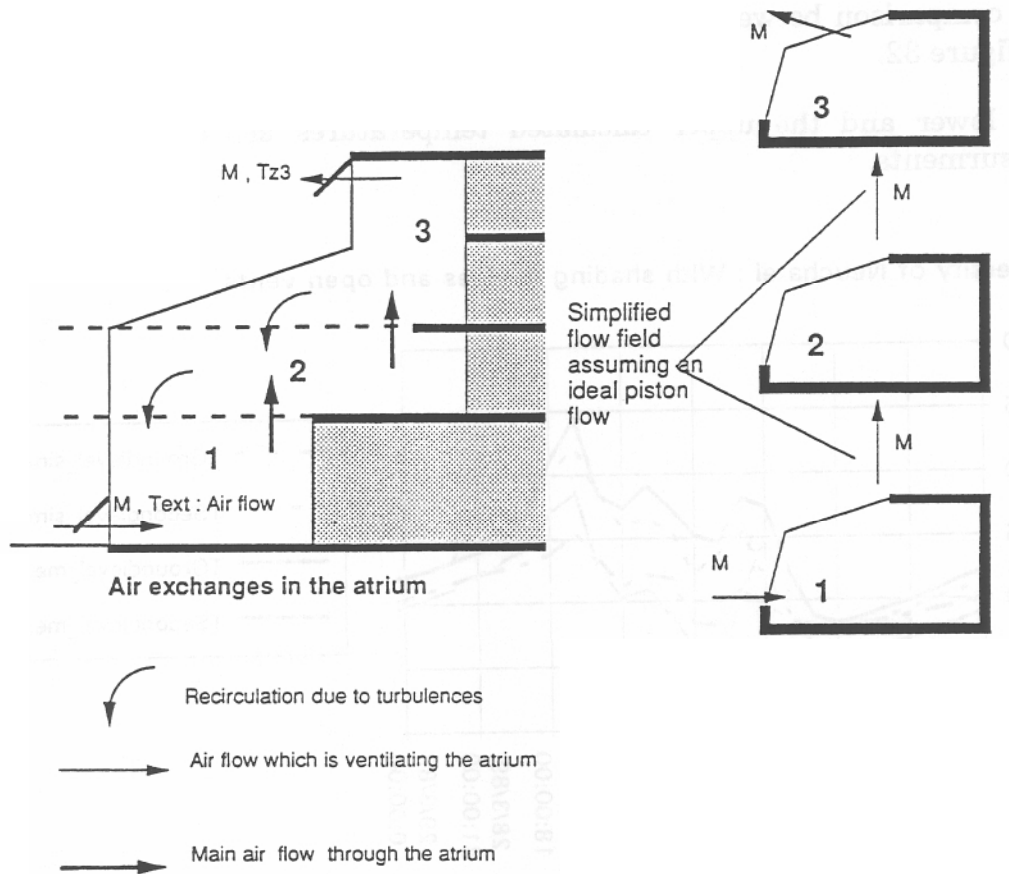
Fig. 31   Piston flow

2. The air exchange rate is calculated in the following way :

- Use of the average internal air temperature $T_{int} = (T_1 + T_2 + T_3)/2$

    Air exchange rate :

$$V = S_B \, CD_B \sqrt{\frac{2 \times g \times H \, |T_{int} - T_{ext}|}{T_{int} + T_{ext} \dfrac{S_B \times CD_B}{S_H \times CD_H}}} \quad [m^3/s]$$

where CD_B and CD_H are respectively the discharge coefficient of the lower and upper vents, the g the gravity, H the difference between the opening height, S_B and S_H respectively the surface at the lower and upper openings.

The comparison between the simulation and the measurement   is shown   in the figure 32.

The lower and the upper calculated temperatures are compared with measurements.

University of Neuchatel : With shading devices and open vents
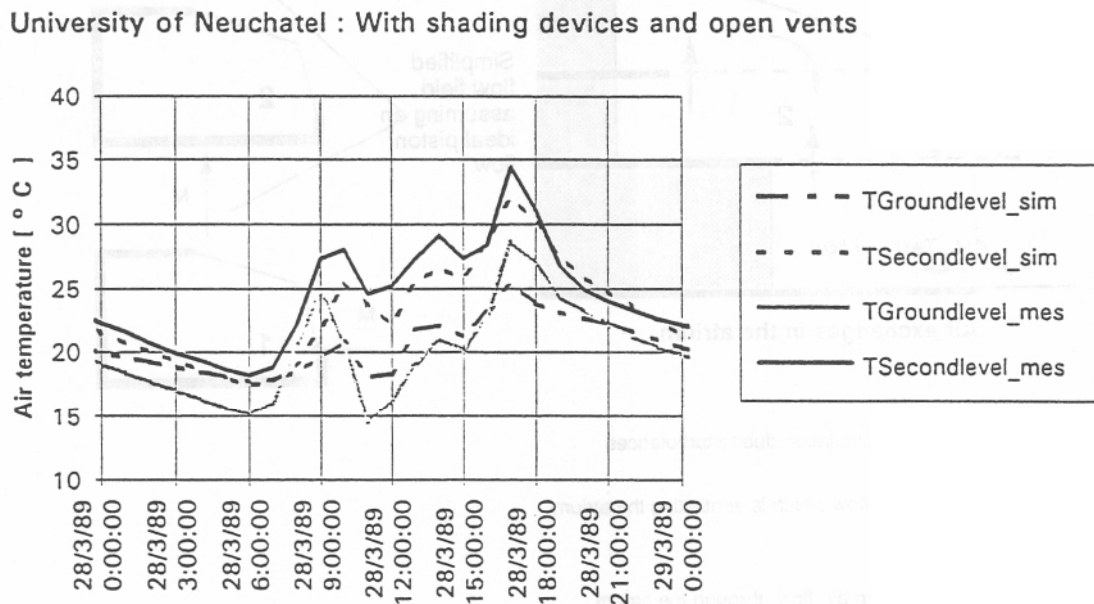
Fig. 32   Comparison of the calculated values with the measurements

The correspondence is good particularly when one think at the complicate air movements in reality and the assumption used in the model.

3.10.4 First   day   closed   hatches   without   internal   shading devices

In this typical situation there will not be any important temperature stratification so that there is no advantages in partitioning the space of the atrium in 3 different zones. With this kind of standard approach we will get a lot of stratification if the air movement between the zones is not implemented.

The problem in this case is to specify the air exchange between the different zones.
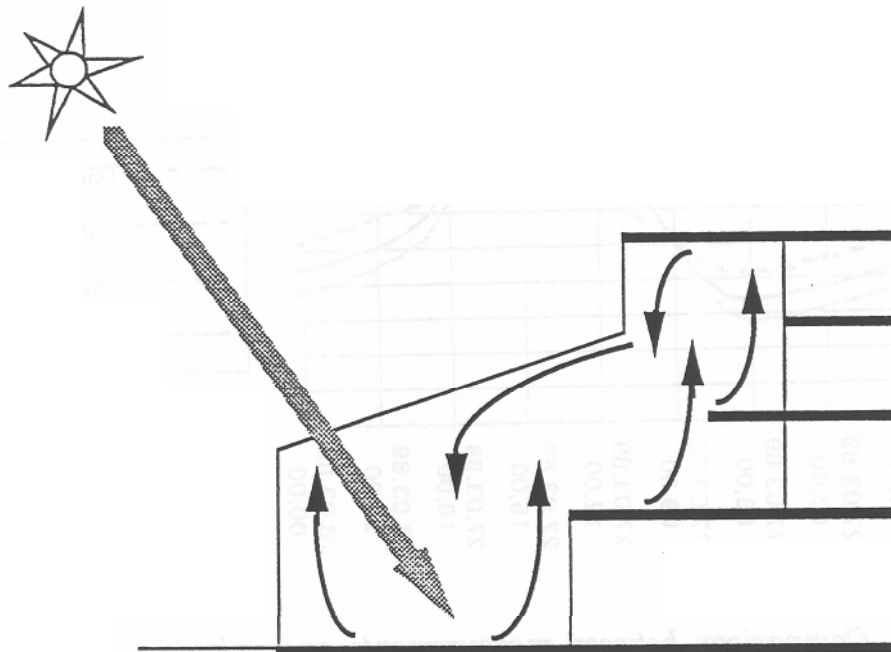
Fig. 33   Air movement in the atrium

In this case we use the relation giving the down draught volume flow created by a cold (or hot vertical) surface in order to make a first estimation of the air flow.

$$V = 0.0029 * \Delta T^{0.4} * B * Z^{1.2} \ m^3/s$$

where

> ΔT = the temperature difference between the air and the surface.
> B = the length of the surface
> Z = the height of the surface

In our case we assumed :

$$
\left.
\begin{array}{ll}
Z & = \quad 10 \ m \\
\Delta T & = \quad 10°C \\
B & = \quad 20 \ m
\end{array}
\right\} \quad V \quad = \quad 9000 \ kg/h
$$

3:37

This mass flow has been used in the simulation and has given good results, as one can see in the figure 34.

Fig. 34   Comparison between measurements and calculations, University of Neuchâtel with no shading devices and no open vents

3.10.5 First conclusion on the method

The method can be defined as satisfactory in two typical cases :

1. **No shading devices and no stratification.** By introducing the recirculation of the air the average temperature is well predicted.

2. **With opened vents (high and low position),** the model based on a piston flow is working and the errors due to the bad solar gain distribution are less predominant than in the case with stratification (internal shading devices used) and no opened vents.

Unfortunately this method cannot be defined as fully appropriate in the stratified case, because it is too sensitive to the zone partitioning (Z direction).

For the design phase, where no information are available, this method can lead to big uncertainties   but when some measurements are available and that a validation can be done (as in the case of' the university of Neuchâtel) it can be used for some sensitively studies (because   a reasonable partitioning can be found in comparison with the measurements).

3:38

3.11 ELA atrium of the University of Trondheim simulated with type 56 of TRNSYS

3.11.1 General approach

The same approach that has been used for the atrium of the University of Neuchâtel is tested on the geometry of ELA. The space is divided horizontally also here in three volumes.
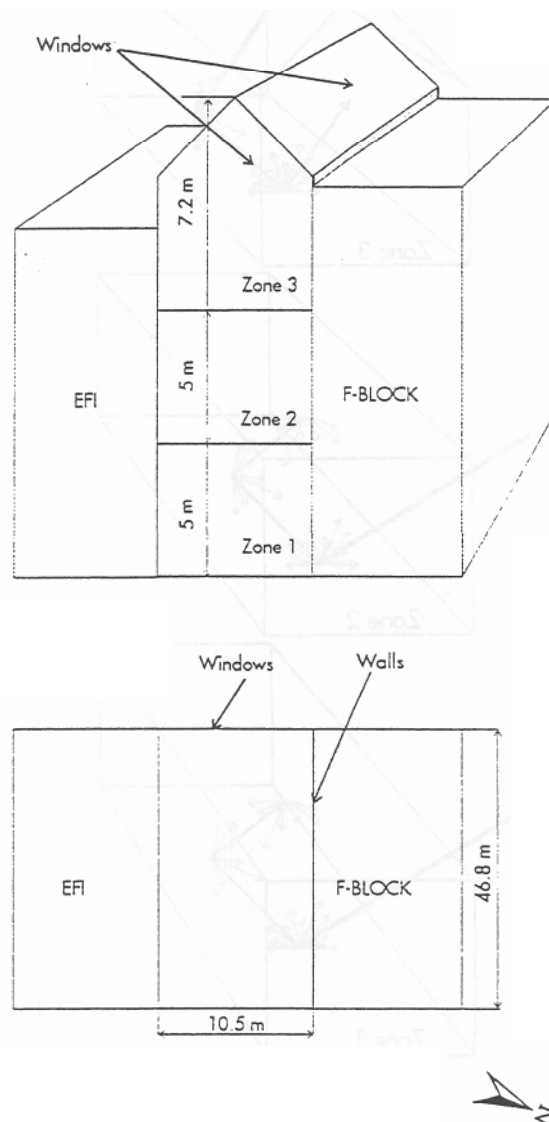

Fig. 35   Vertical Partitioning of the atrium ELA

Two types of calculations will be done on this example :

1. Solar gains distributed in each volume according to the surface ratio rate.

   The sun entering in the upper part is distributed only in the upper volume which is not accurate and can lead to problems (see 3.10).
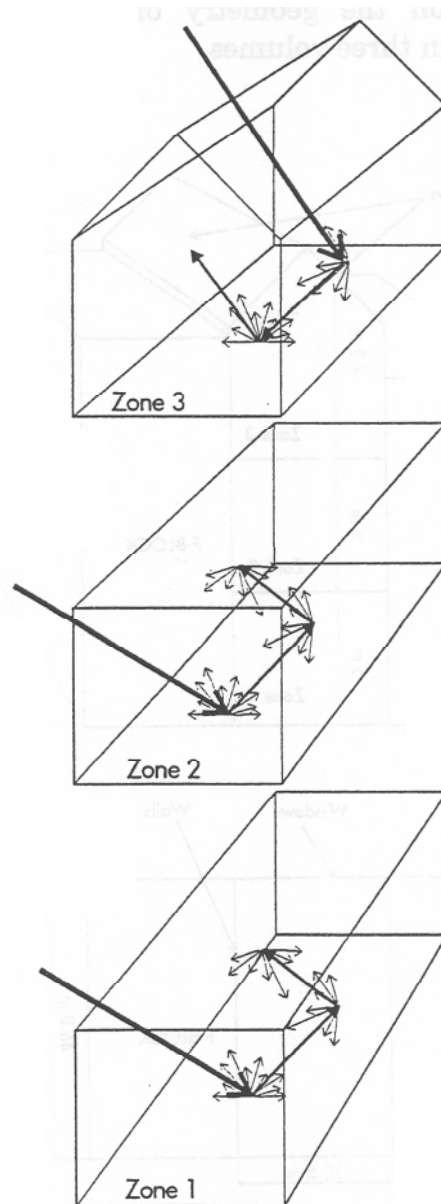
Fig. 36 Solar gains calculations and distribution with the TRNSYS standard model

3:40

2. Solar gains distributed according to a more sophisticate model (presented in the chapter 7) which take into account the real part of the sun rays with the first reflection both diffuse and specular.

   The solar model of the type 56 is not activated in TRNSYS and the solar gains are distributed in the volume were they hit the surfaces as radiative gains.

Two situations are calculated :

1. The vents are closed, the stratification is important.

2. The vents are opened, the stratification is less important as well as the average temperature.

3.11.2 Standard approach

Closed vents

The measurements are presented in the following figure :
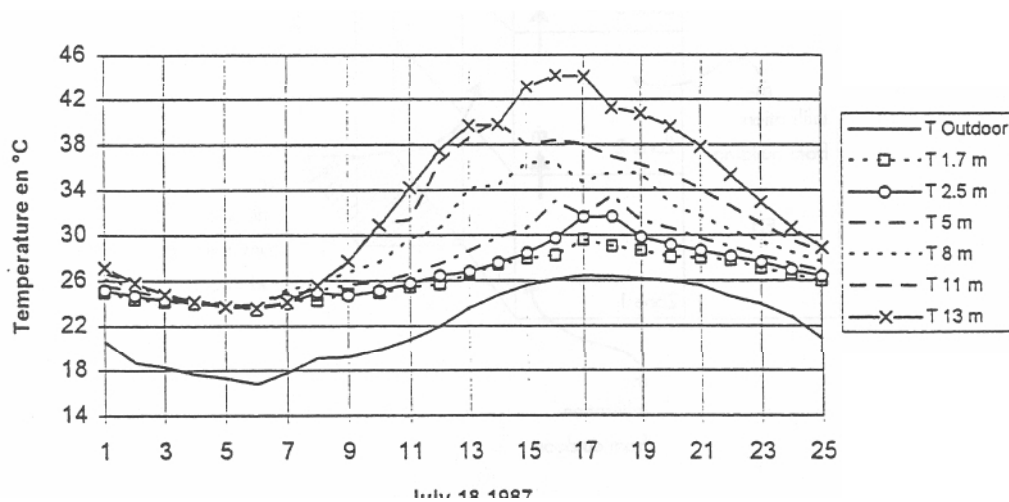
Fig. 37   Measured temperatures with closed vents in the summer

As one can see the stratification of the temperature is relevant.

The method used is described in chapter 3.10

The principal parameter which are important in order to get a good comparison with the measurements are .

- Estimation of the amount of solar gains which enter in the volume but do not stay in it because of the reflection on different surfaces, in that case we assumed that 20 % do not stay in the volume.

  Estimation of the air infiltration and exfiltration. In the case of ELA, the window of the offices can be opened in the atrium and there is an open link between the atrium and the office building (which is mechanically ventilated) we have assumed about 1.5 ach coming from outside and from the building, which are going out through the leakages of the roof of the atrium and to the adjacent
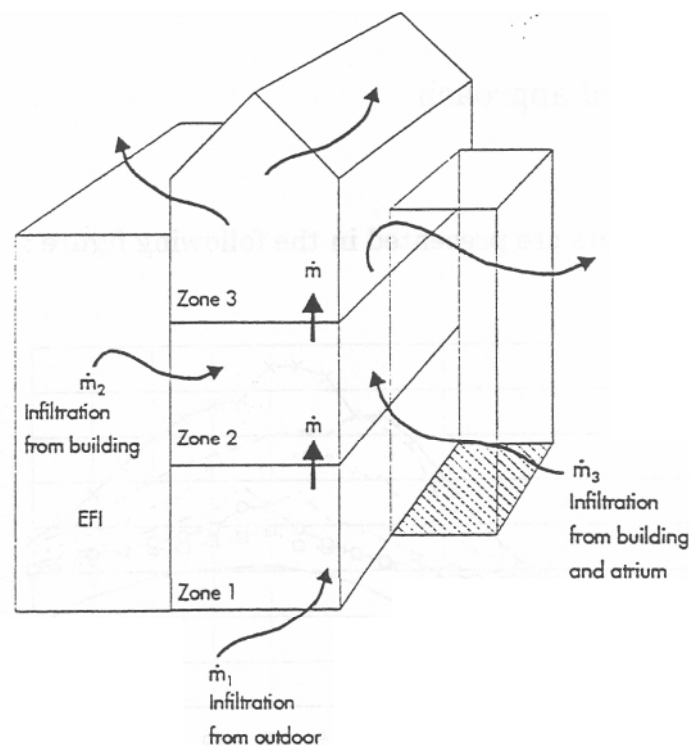
Fig. 38 Simplified infiltration and ex filtration flow field

The results are presented in the following figures. Figure 39 shows the three calculated temperatures.
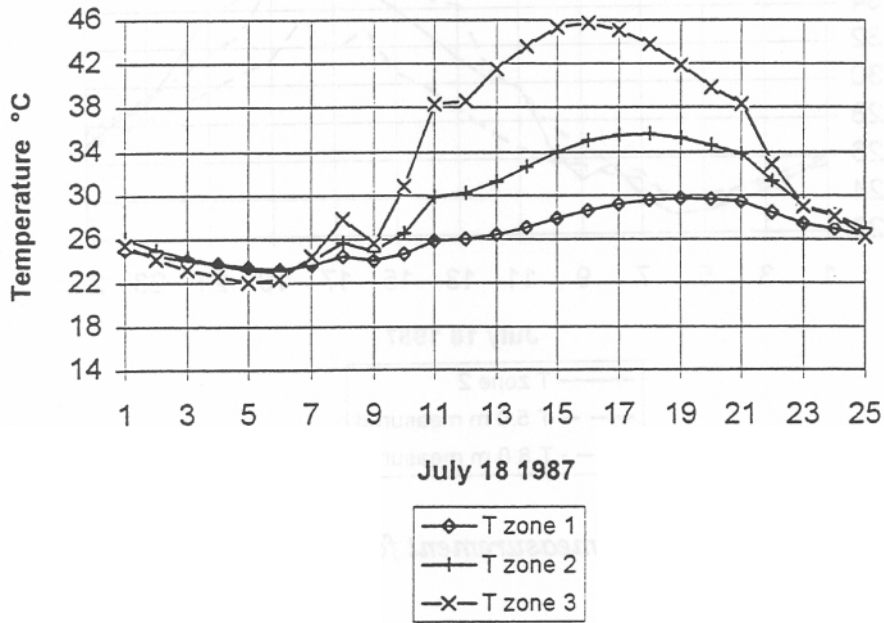
Fig. 39   Calculated average temperature in the 3 zones

The following figures show the comparison with the measured temperatures in the same zone
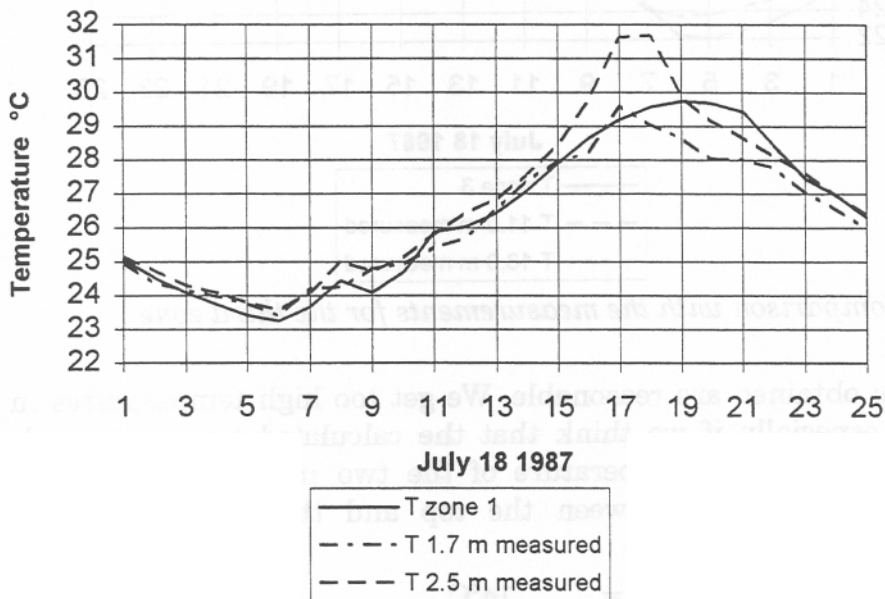

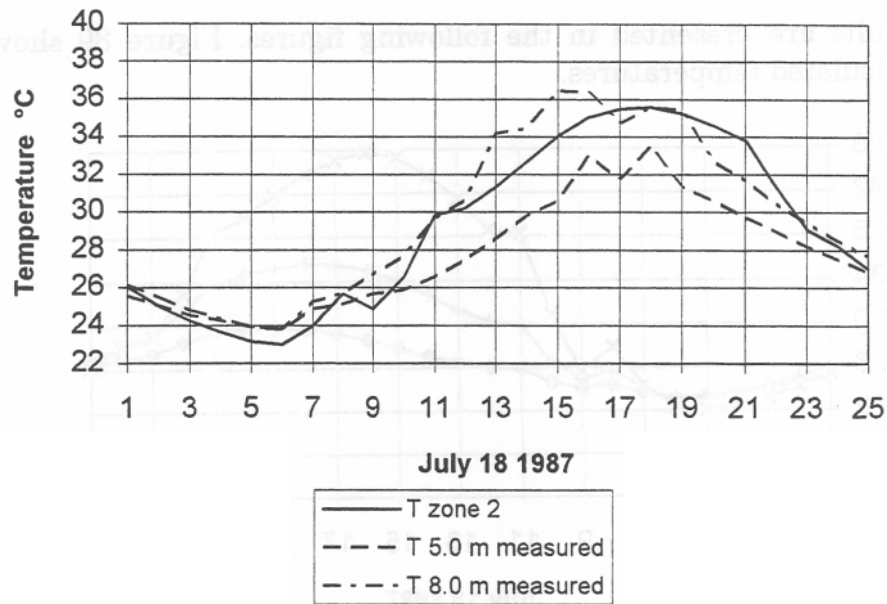*Fig. 40   Comparison with the measurements for the first zone : ground*

3:43

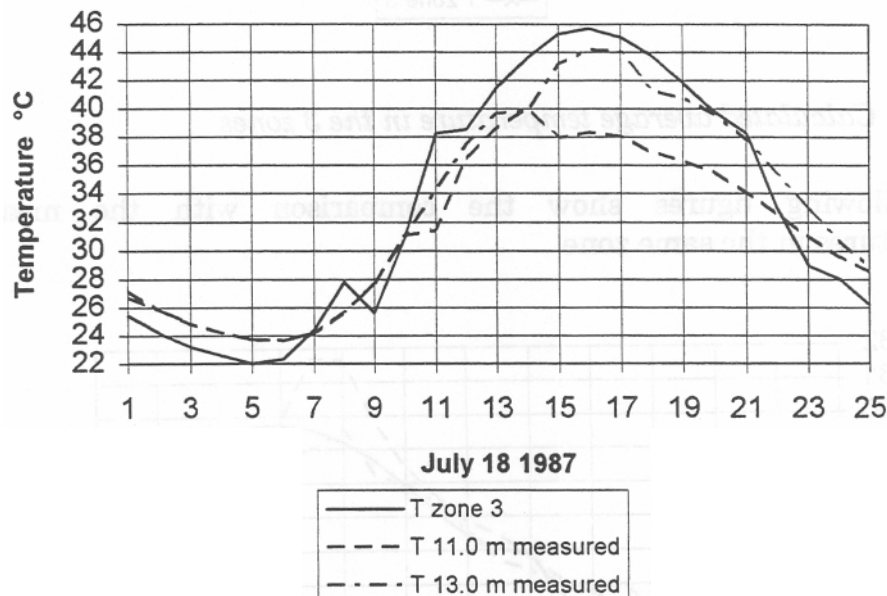*Fig. 41   Comparison with the measurement for the second zone*

Fig. 42   Comparison with the measurements for the third zone

The results obtained are reasonable. We get too high temperatures in the last zone, especially if we think that the calculated temperature should represent the average temperature of the two measured ones. But the temperature difference between the top and the ground is predicted reasonably.

- $\Delta T_{measured}$ = $14°C$
- $\Delta T_{calculated}$ = $16°C$

Opened vents

With the vent opened, the air exchange rate with the outside has been evaluated in the same way that has been done for the atrium of the university of Neuchâtel.

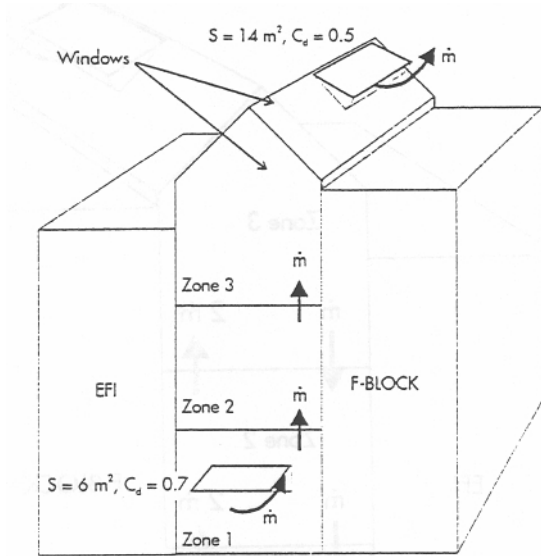The air flow field assumed for the first time is described in the next figure.

Fig. 43   Piston flow

The velocity of the wind has not been measured precisely, but has been estimated to 2 m/s and coming from the side of the gable which was opened (low : opening of the atrium). The exact opened surfaces of the vents are not clearly documented so that different assumptions have been done.

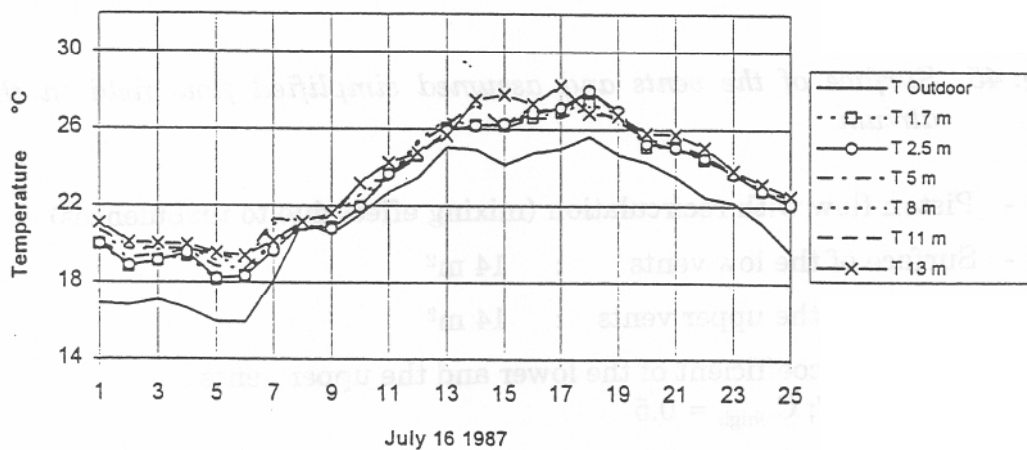The measurements of the air temperature in the atrium are presented in the next figure.

Fig. 44   Measured temperatures with opened vents in the summer.

3:45

As one can see there is no stratification any more (only 2 degrees). Except between 13.00 and 17.00 the air temperature in the atrium is well mixed.

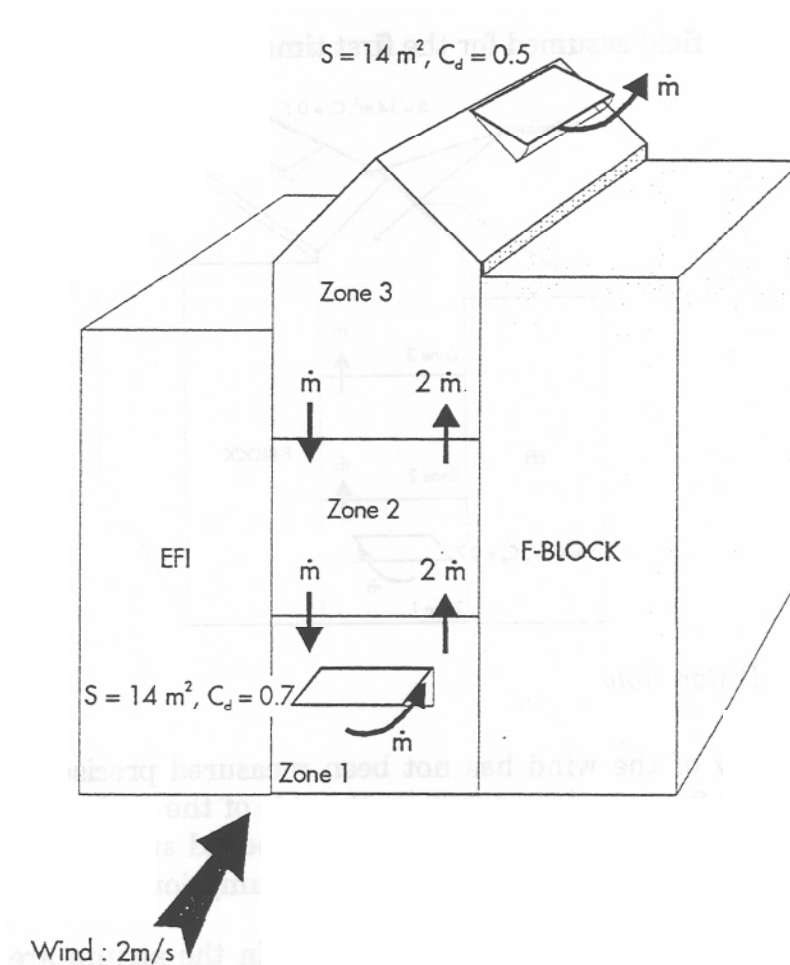The calculation is based on the assumption presented in the figure 45.

Fig. 45 Surface of the vents and assumed simplified flow field in the atrium

- Piston flow with recirculation (mixing effect due to turbulences)

  Surface of the low vents   14 m^2

  Surface of the upper vents :   14 m^2

- Discharge coefficient of the lower and the upper vents :
  $C_{Dlow} = 0.7$; $C_{Dhigh} = 0.5$

- 2 m/s of wind in the direction of the low opening

3:46

The results are presented in the next four figures
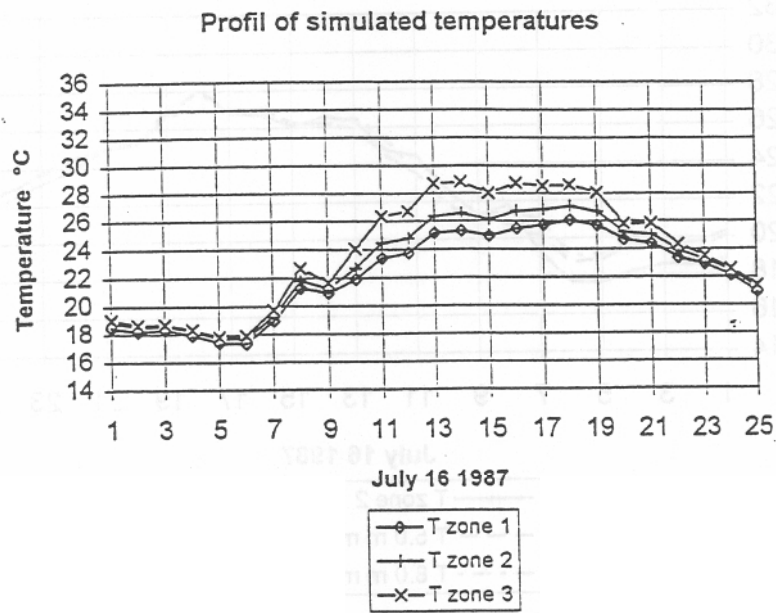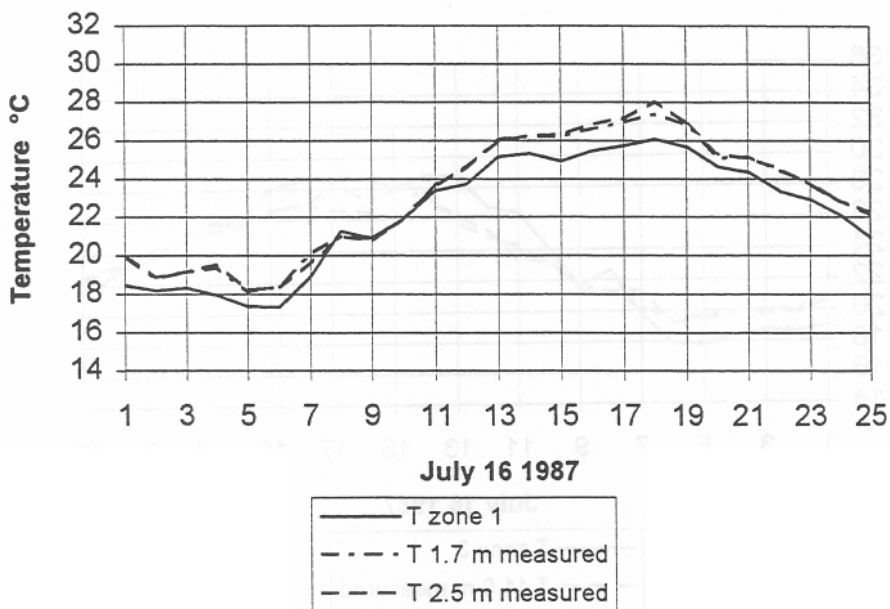

Fig. 46   *Calculated temperature in the 3 zones*

Fig. 47 Comparison with the measurements in the first zone : ground
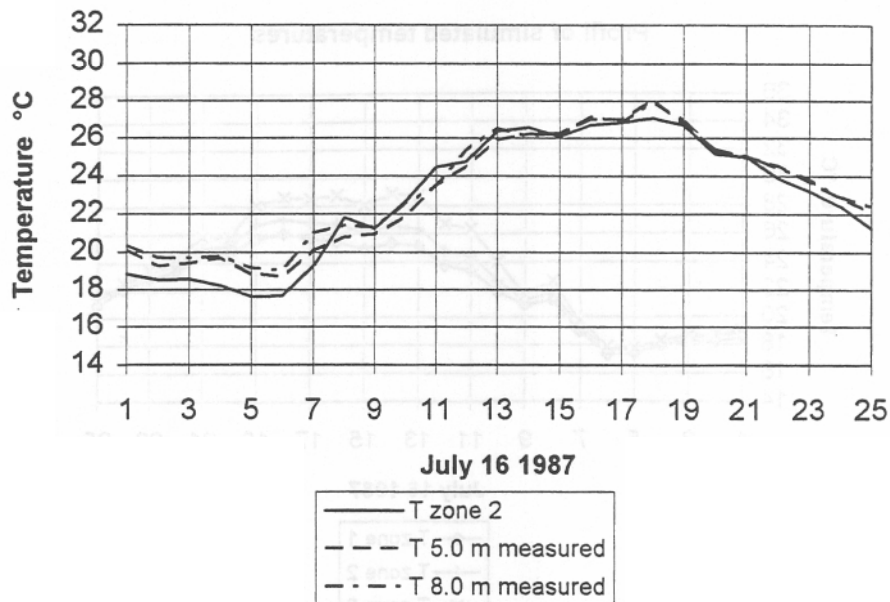
3:47

Fig. 48   Comparison with the measurements in the second zone
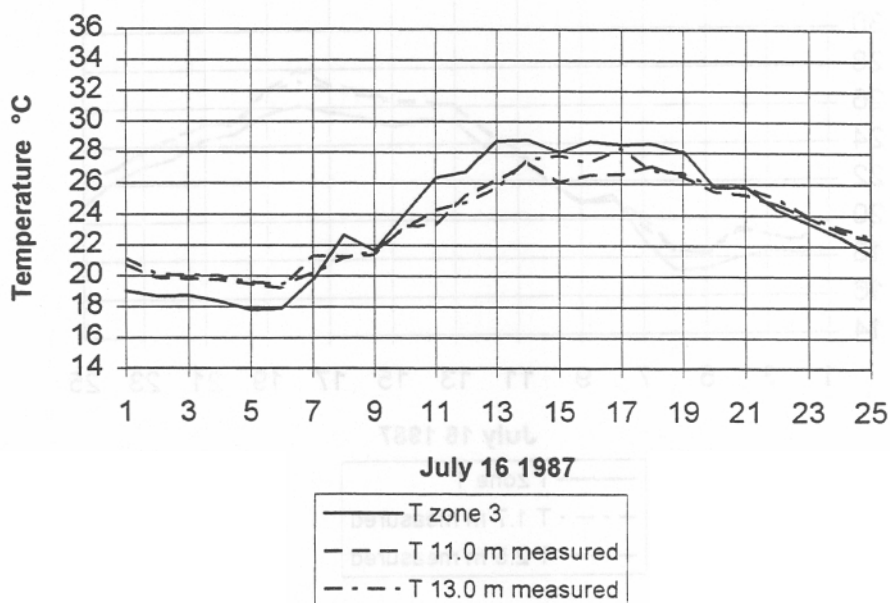

Fig. 49   Comparison with the measurements in the third zone

The results obtained with these new assumption are quite better than the first one. The average temperature and the stratification profile are much closer to the measured values.

3:48

3.11.3 Modified solar distribution approach

The standard distribution method of the solar gains of the program TRNSYS has been modified in the following way.

The first step is to calculate the total amount of the solar gains coming in the whole atrium, see figure 50.
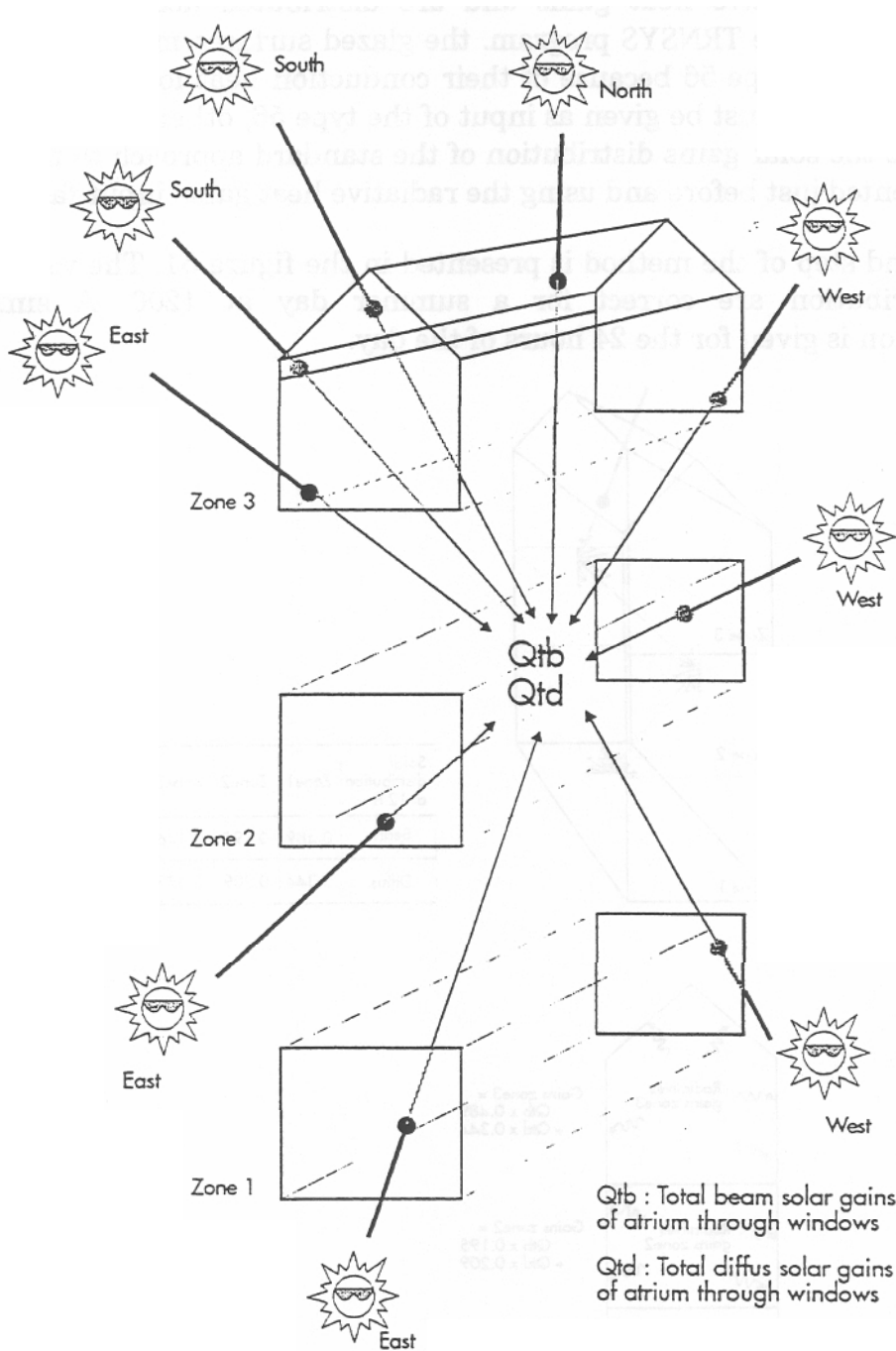

Fig. 50   Step one : calculation of the total amount of solar gain

3:49

The second step is using the solar gain distribution obtained with the program presented in chapter 6. The sun penetration in the space and the first reflections both specular and diffuse are calculated correctly. This lead to a power heat distribution on the surfaces of the atrium.

The sum of both the diffuse and the direct radiation which heat the surfaces of each zones is done. This gains are introduced in the Type 56 of TRNSYS as radiative heat gains and are distributed according to the surface ratio of the TRNSYS program. the glazed surfaces must be defined as before in the type 56 because of their conduction heat losses (or gains) but no radiation must be given as input of the type 56, otherwise we would superpose the solar gains distribution of the standard approach to the new one presented just before and using the radiative heat gains input facilities.

The second step of the method is presented in the figure 51. The values of the distribution are correct for a summer day at 1200. A similar distribution is given for the 24 hours of the day.

Solar distribution at 12 h.	Zone1	Zone2	Zone3
Beam	0.489	0.195	0.146
Diffus	0.344	0.209	0.173

Gains zone3 = Qtb x 0.489 + Qtd x 0.344

Gains zone2 = Qtb x 0.195 + Qtd x 0.209
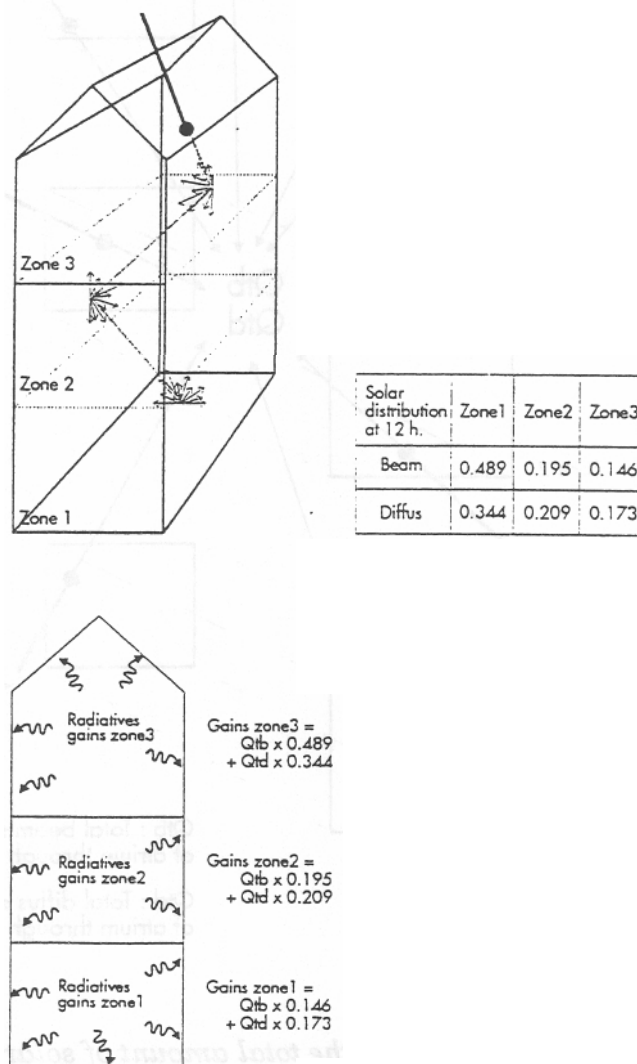
Gains zone1 = Qtb x 0.146 + Qtd x 0.173

Fig. 51   Second step of the method

3:50

With this method the solar gains which comes from the roof are not only active in the zone number 3 but can effect the ground and the zone 2 of the atrium.

We can also see from this distribution that 17 % of the incoming direct radiation do not stay in the atrium and that 28 % of the diffuse incoming radiation is also not absorbed by the surfaces of the atrium.

Closed vents

The same flow field due to infiltrations which has been used in the standard approach (Chap. 3.11.2) has been used here.

The results of the next figure show the calculated temperature.
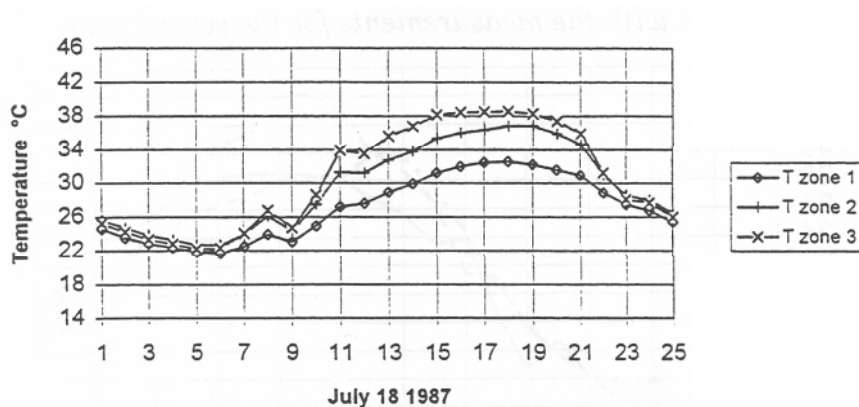

Fig. 52   Calculated average air temperatures in the 3 zones with the new method

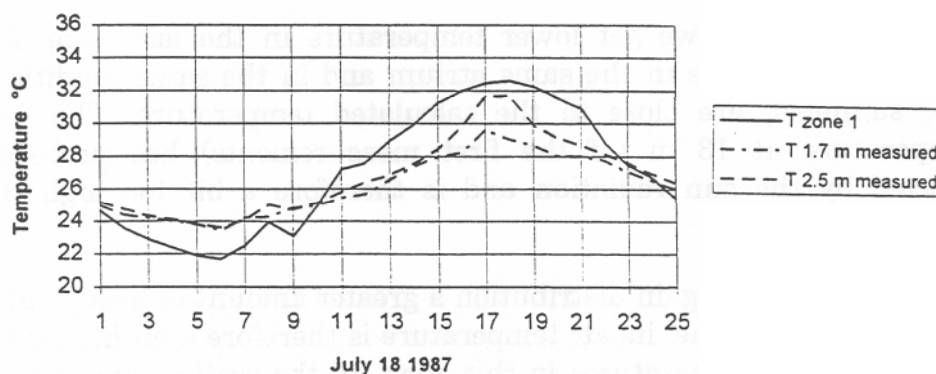The next figures show the comparison with the measured values in the same zones.

Fig. 53   Comparison with the measurements of the first zone : ground
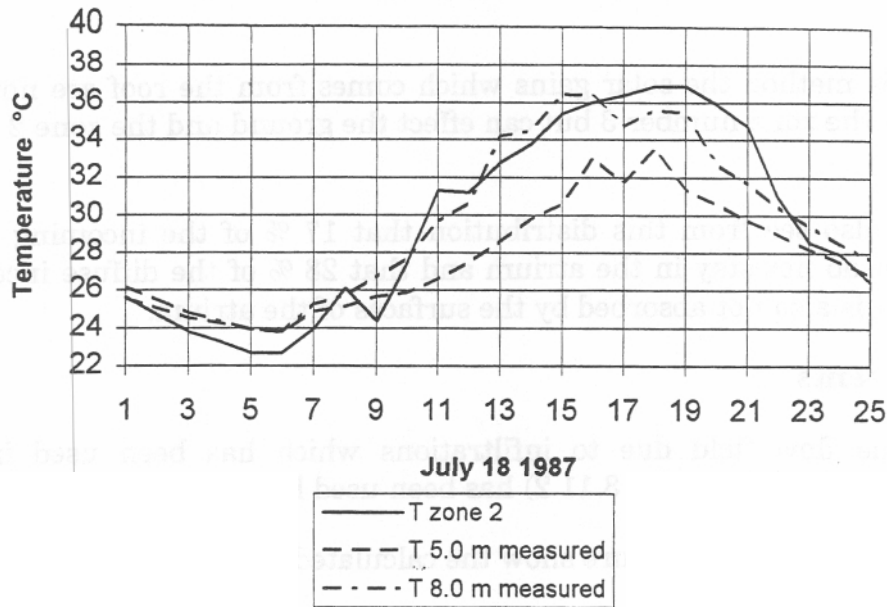
3:51

Fig. 54 Comparison with the measurements for the second zone

Fig. 55 Comparison with the measurements for the third zone

With this method we get lower temperature in the last zone. But new measurements done in the same atrium and in the same condition (clear day, summer), are close to the calculated temperature. The measured temperature at 13 m (of the first measurements) has probably been affected by the sun radiation and is therefore a bit too high than the reality.

With the new solar gain distribution a greater amount of heat is affected to the first ground zone, its air temperature is therefore a bit higher than the two measured temperatures in this zone. In the reality some interception effects as for example plants and trees which have not been taken into account here could lower the temperature in that zone.

3:52

Opened vents

The same distribution method is used here, and the condition of the flow field presented in figure 56 are used.
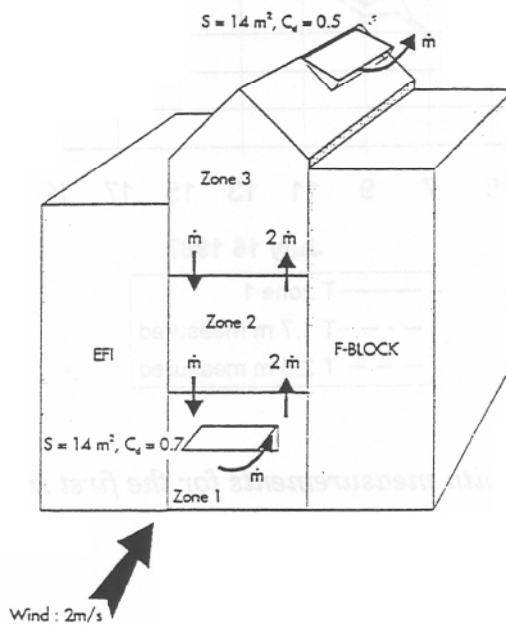
Fig. 56

Wind : 2m/s

- Piston flow with recirculation (mixing effect due to turbulences)
- Surface of the low vents :   14 m^2
- Surface of the upper vents   14 m^2
- Discharge coefficient of the lower and the upper vents :   CD$_{high}$= 0.5
                                        CD$_{low}$ = 0.7

- 2 m/s of wind in the direction of the low opening

July 16 1987

—◇—T zone1
—+—T zone 2
—×—T zone 3

Fig. 57   Calculated temperatures in the 3 zones

3:53

Fig. 58   Comparison with measurements for the first zone

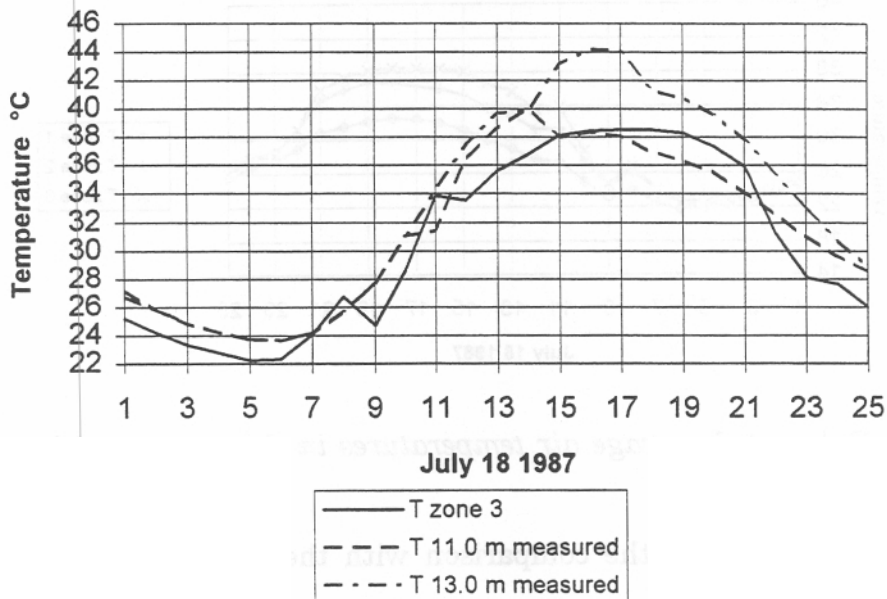*Fig. 59   Comparison with measurements for the second zone*

3:54

Fig. 60   Comparison with measurements for the third zone

The results obtained in this case are very good. Both the stratification and the average temperature in the atrium are predicted correctly.

3.11.4 Limits of the method

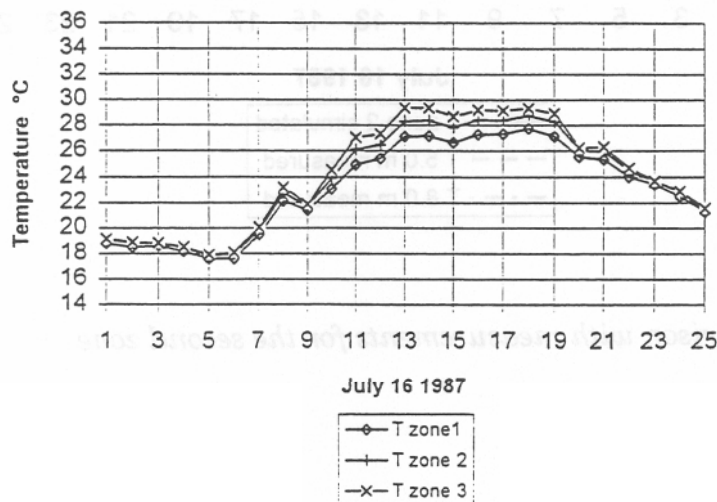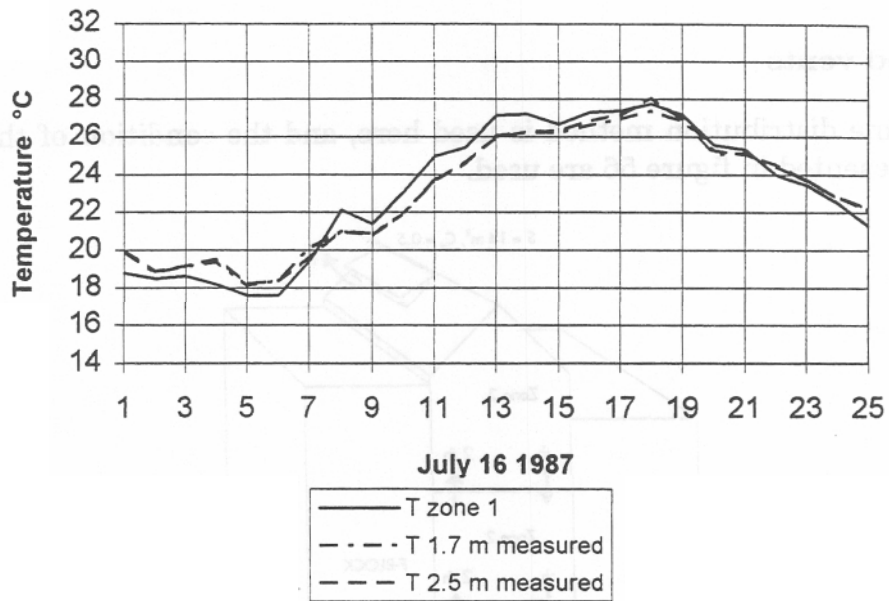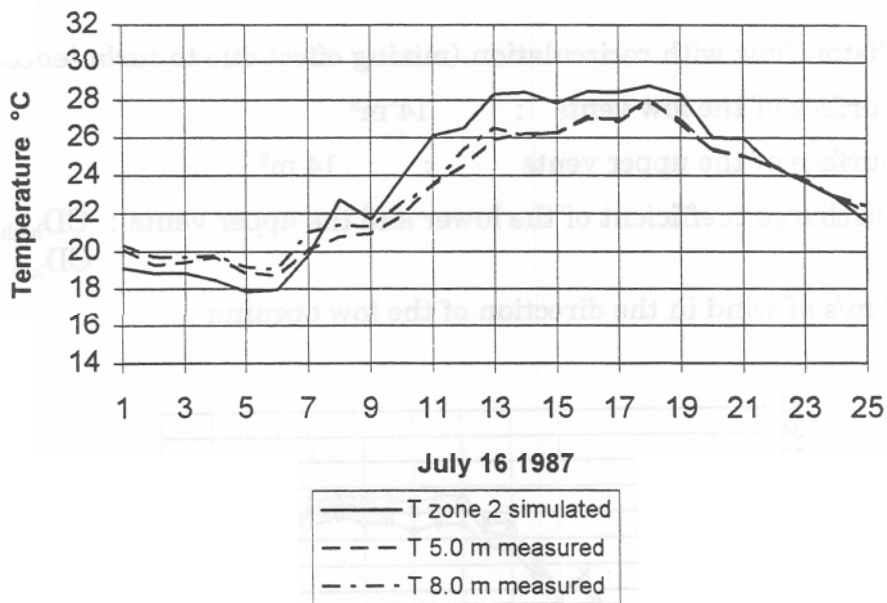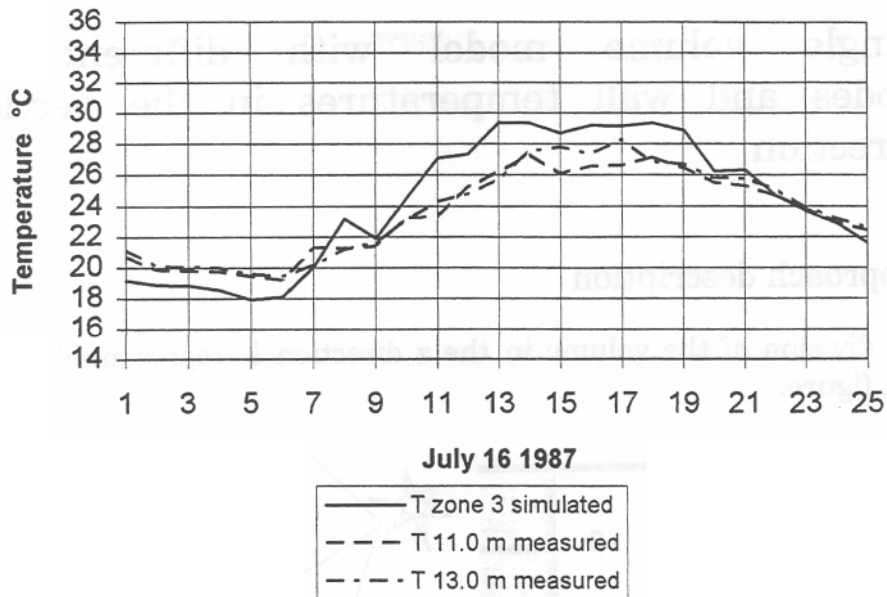The results obtained with this standard use of building simulation programs are not so bad in the case of the atrium similar to ELA although some important parameters must be assumed, as the amount of solar gain which enter in the volume but are reflected outside afterwards, or the air infiltration in the lower parts of the atrium coming from outside and from the adjacent building. The method can give the designer some important information about the amount of temperature stratification and the surface of vents which is needed in order to ventilate the atrium correctly in the summer.

The results obtained with the correct calculations of the solar gain distribution seem not to be much better than the first one. But they are much more appropriate for the designer because the assumption of the solar gain which are reflected outside the atrium is yet calculated correctly. This precalculation (solar gain distribution) will give much more appropriate results in the case of the atrium of the university of Neuchâtel (attached atrium) than the standard method of the building simulation program. This one is too much sensitive to the volume partitioning of the atrium, and therefore is not appropriate in the general design phase.

3:55

3.12 Single volume model with different air nodes and wall temperatures in the vertical direction

3.12.1 Approach description

The division of the volume in the z direction is represented in the next figure.
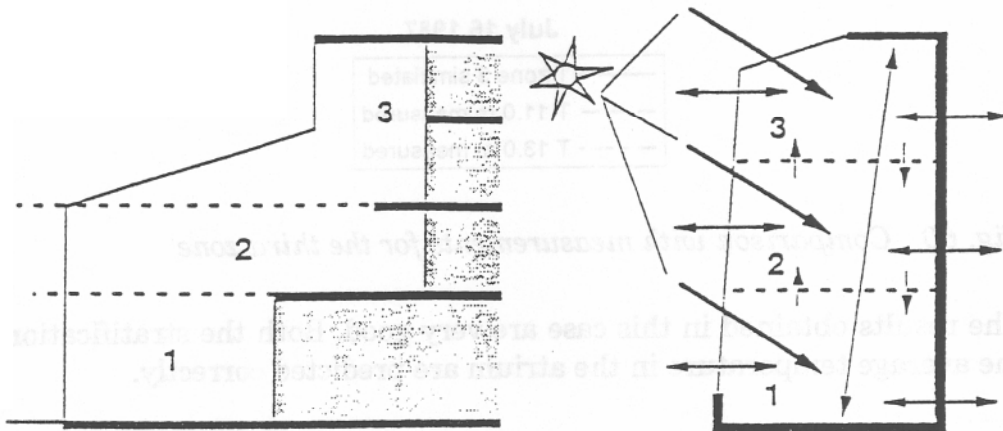
Fig. 61   Single volume model

With this approach the division in the vertical direction is less important because the solar gain distribution is done correctly.

The total amount of energy coming into the atrium is calculated and then distributed on the different surfaces and light elements (air) according to a solar distribution program.

Each hour of the day, a new solar distribution is used according to the season and orientation of the building. Such a distribution program is described in the report <u>dealing</u> with the short wave radiation (chapter 6).

The program used to model the atrium is called MODPAS and has been developed by Sorane SA. It uses a mesh of 40 temperature nodes. These nodes can be the air of a zone as well as the surface or element temperature of a wall. Each nodes is coupled with some other nodes by symmetrical connections (conduction, convection, I.R. radiative exchanges) by non-symmetrical connection (radiative exchanges as short wave (sun) and heat gains), or by connection with the outside.

The atrium is divided in three zones, the connection mesh is presented in the next two pages.

3:56

CONDUCTION ET CONVECTION CONNECTIONS

12   THICKNESS OF LAYERS

● 5   NUMBER OF THE NODES

↘   NODES RECEIVING SOME SUN

SOME NODES ARE INDICATED MORE TIMES IN ORDER TO MAKE THE
UNDERSTANDING EASIER.

3:57
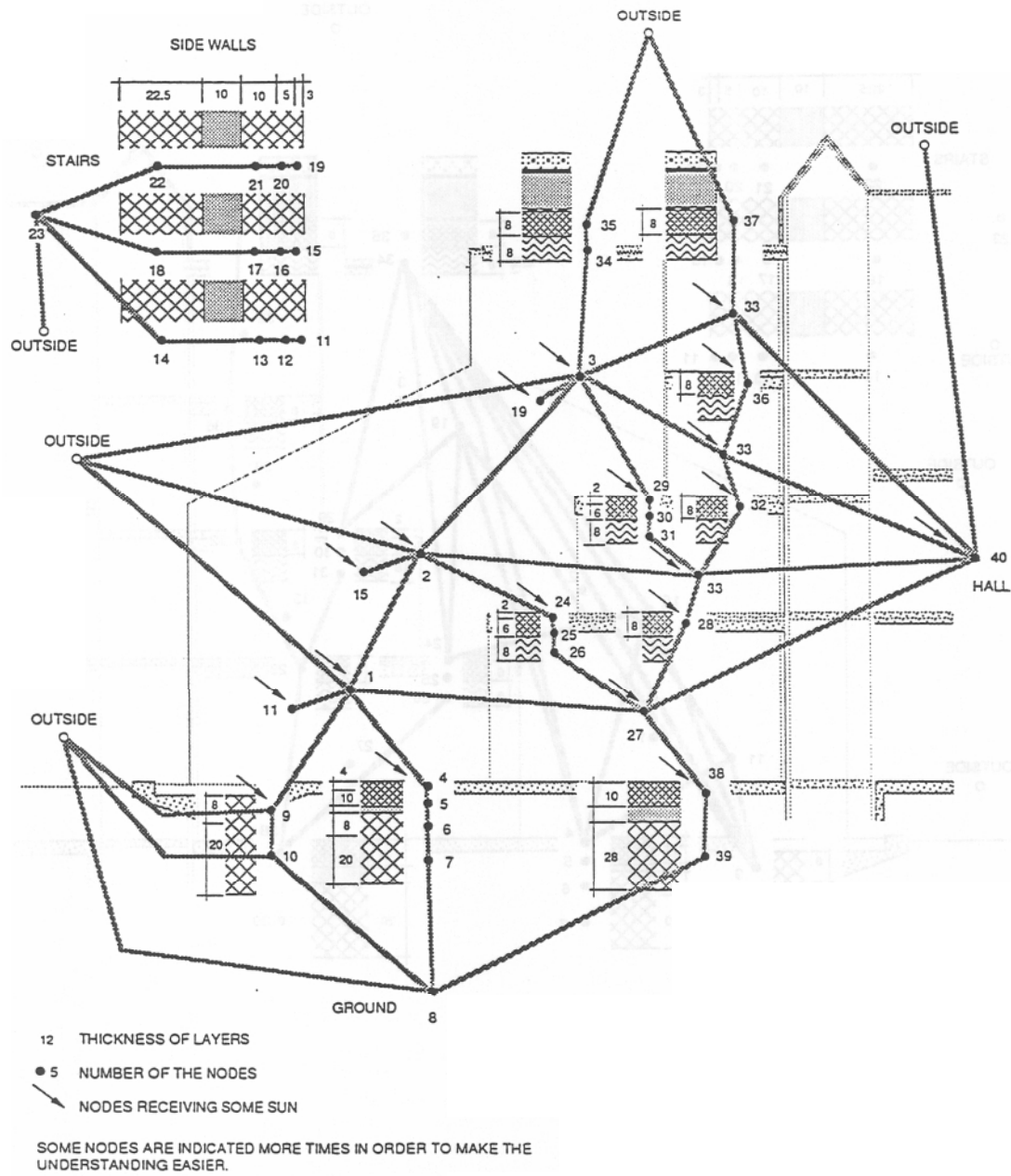
INFRARED RADIATION CONNECTIONS
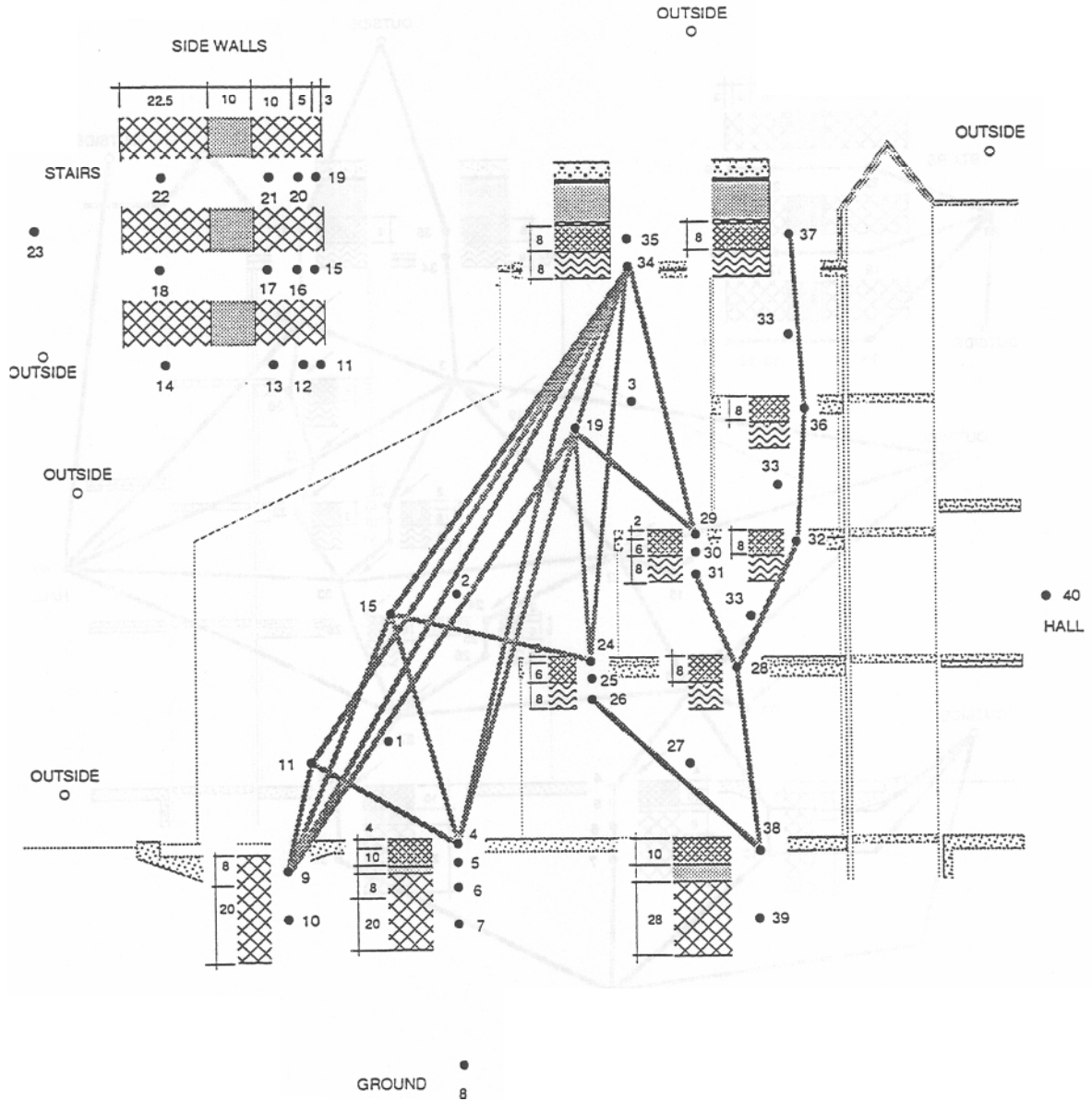
Two types of air movements are modelled in this program :

- Natural ventilation when the vents are opened

- Mixing due to buoyancy

a) Natural ventilation

When the vents are opened the flow field is assumed as in chapter 3.8 (Piston flow).
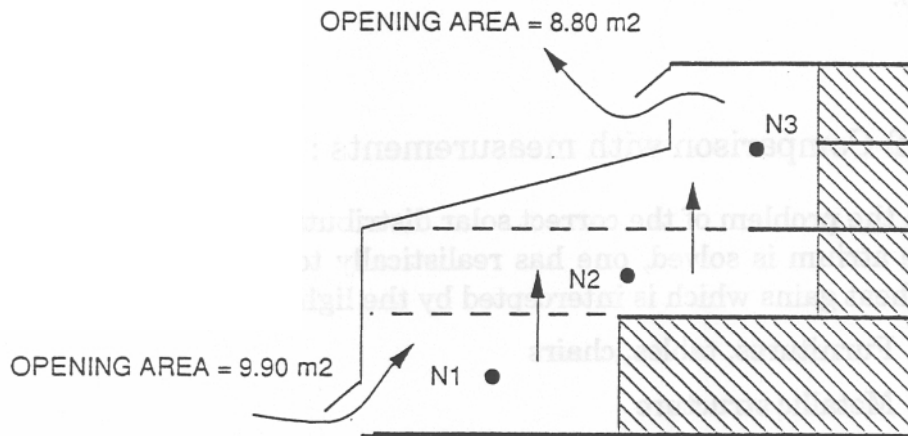
Fig. 62   Piston flow when the vents are opened

The air flow rate entering in the lower zone and going out on the top is calculated using the average air temperature in the atrium $((T1 + T2 + T3) / 3)$ and with the relation presented in chapter 6.4.2.3 $m = f$ (T_{int} and $T_{outside}$)

b) Mixing due to buoyancy

If a lower zone becomes hotter than the zone just above, a convection flow is calculated between the two zones.
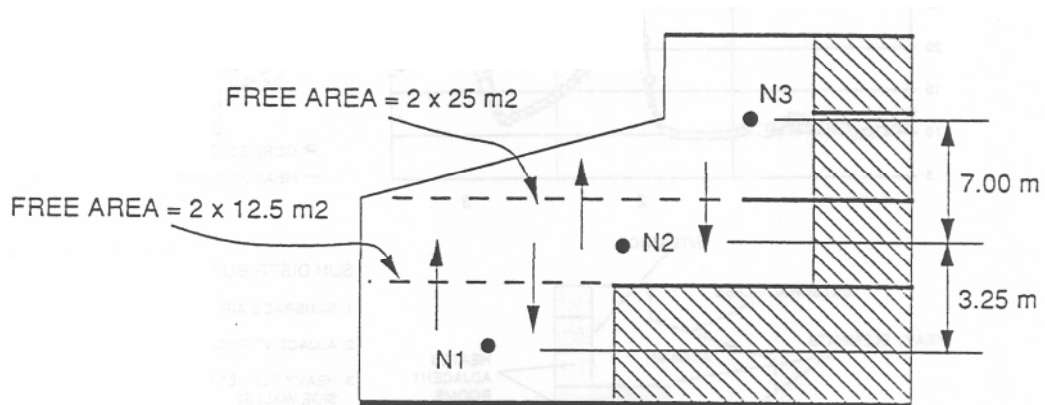
Fig. 63 Buoyant   flow

3:59

Connection   ***1-2*** :   S   =   25 m^2 $\Delta H = 3.25$ m
$$Cd = 0.5$$

Connection   ***2-3*** :   S   =   12 m^2 $\Delta H = 7$m
$$Cd = 0.5$$

The flow takes place only if T1 > T2 or T2 > T3, the mass flow is calculated with the formula based on Bernoulli   presented in chapter 3.10.3.

3.12.2 Comparison with measurements : Results

When the problem of the correct solar distribution on the different surfaces of the atrium is solved, one has realistically to evaluate the part of these solar heat gains which is intercepted by the light elements of the atrium :

-   Furnitures, tables, chairs

-   Metallic structure

-   Gates

The consequences of the underestimation of this intercepted part is that the calculated transient behavior and the peak temperature can be wrong.

In the next figure the **average air temperature** in the atrium has been calculated with two intercepted ratios. It can be seen that an error in this evaluation can lead to peak temperature underestimation of about 10°C.
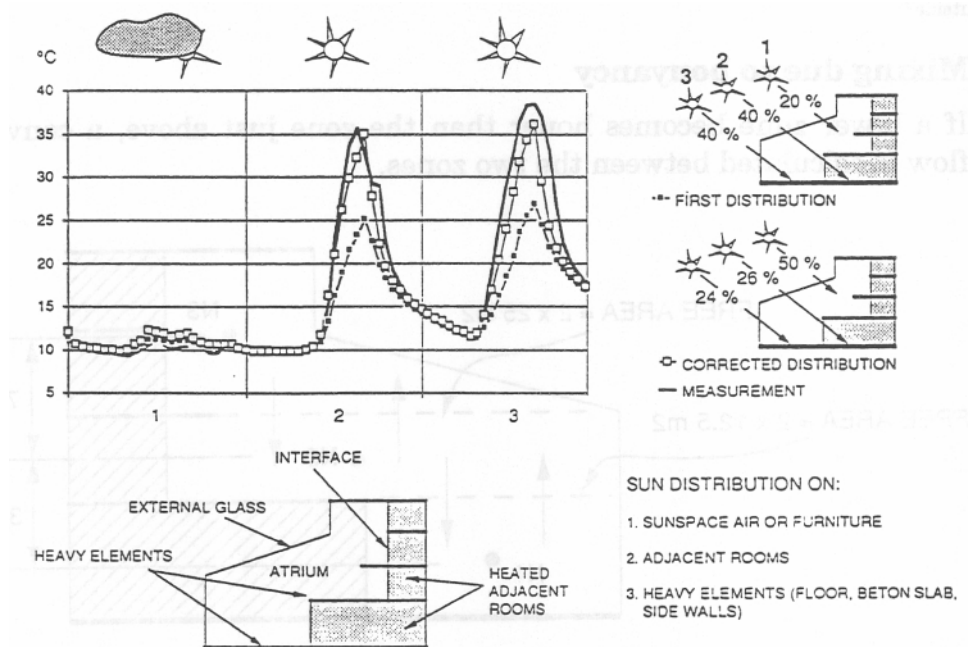
Fig. 64 Importance of the correct evaluation of the solar interception in the atrium

3:60

A first period of five days in March has been chosen for the comparison
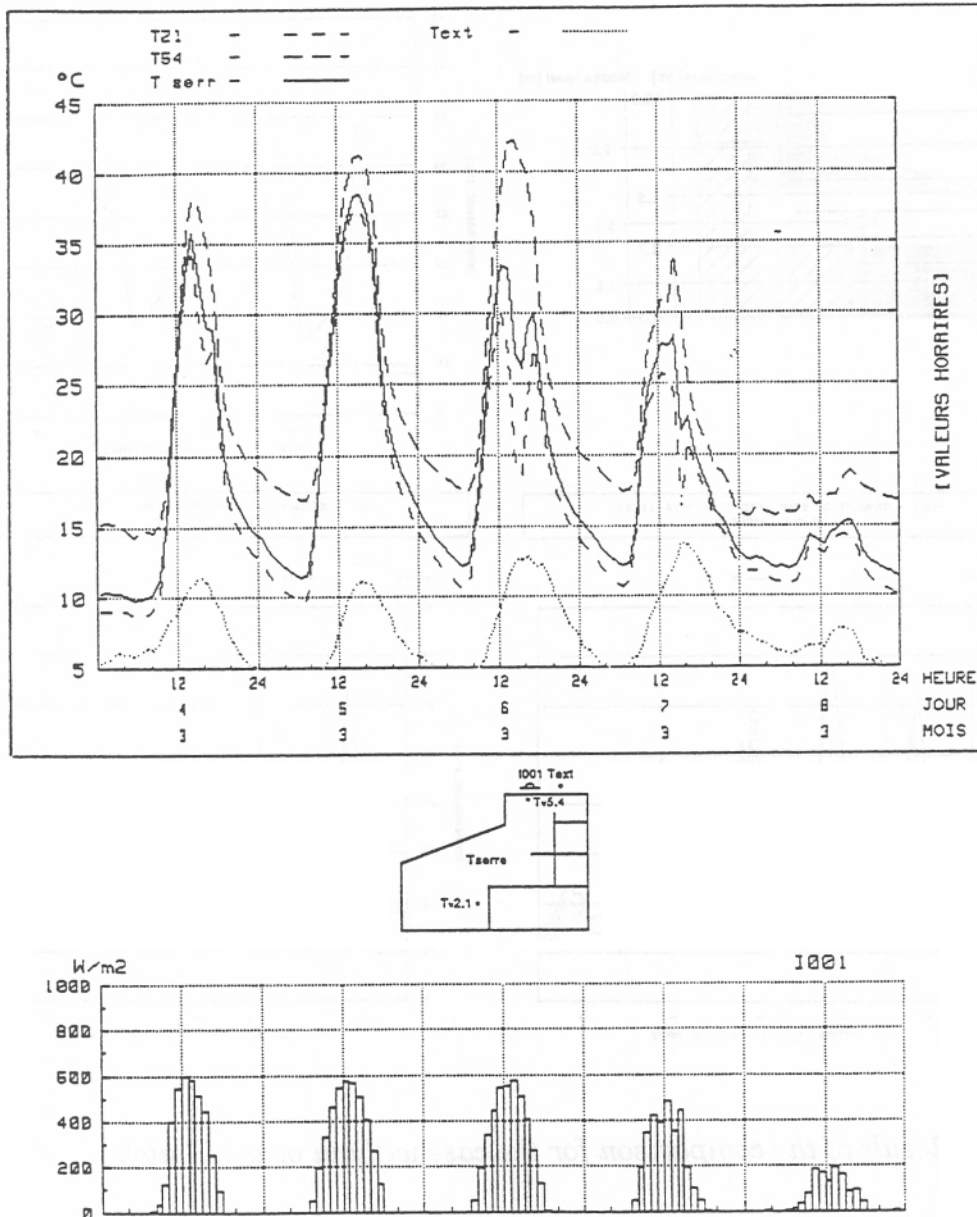
Fig. 65   Measured temperature evolution in the atrium from the 4th to 8th of March 1989

The results of the comparison are shown in the three following figures. The points S1 to S5 refers to measured values, the points N1, N2, N3 to calculated average air temperature in the three volumes.

3:61
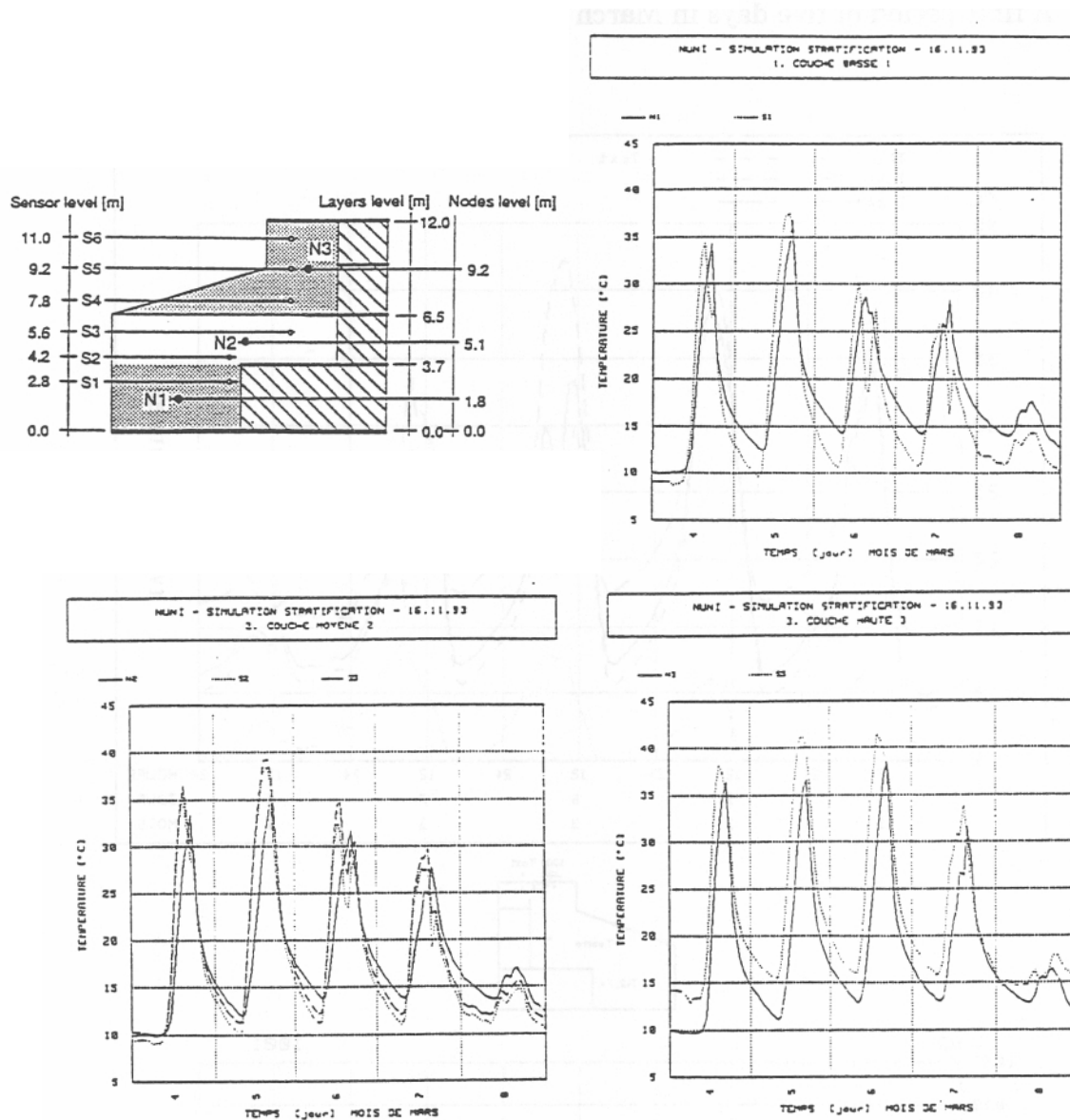
Fig. 66   *Result of the comparison for the case without opened hatches*

During the two first days the internal shading devices are not used, and the air temperature in the atrium is not stratified very much. During the two next days with the solar protection, the temperature stratification takes place. The calculated values of the different zones are in agreement with the measurements. Some discontinuities in the measured air temperature especially for the lower zone are due to punctual opening of the lower hatches. This small detail has not been taken into account in our calculations.

3:62

The second period used is the one already used in the case of the TRNSYS standard approach of chapter 3.10.

The first day (27 of March) is clear and the temperature of the atrium is mixed. No shading devices are used and no vents are opened.

During the second day the shading devices are used as well as the vents opened. The day is also clear (sunny).

During the last day the vents are closed (except the lower ones for about half an hour) and the shading devices are used.

The results of the calculation are presented in the next figure.
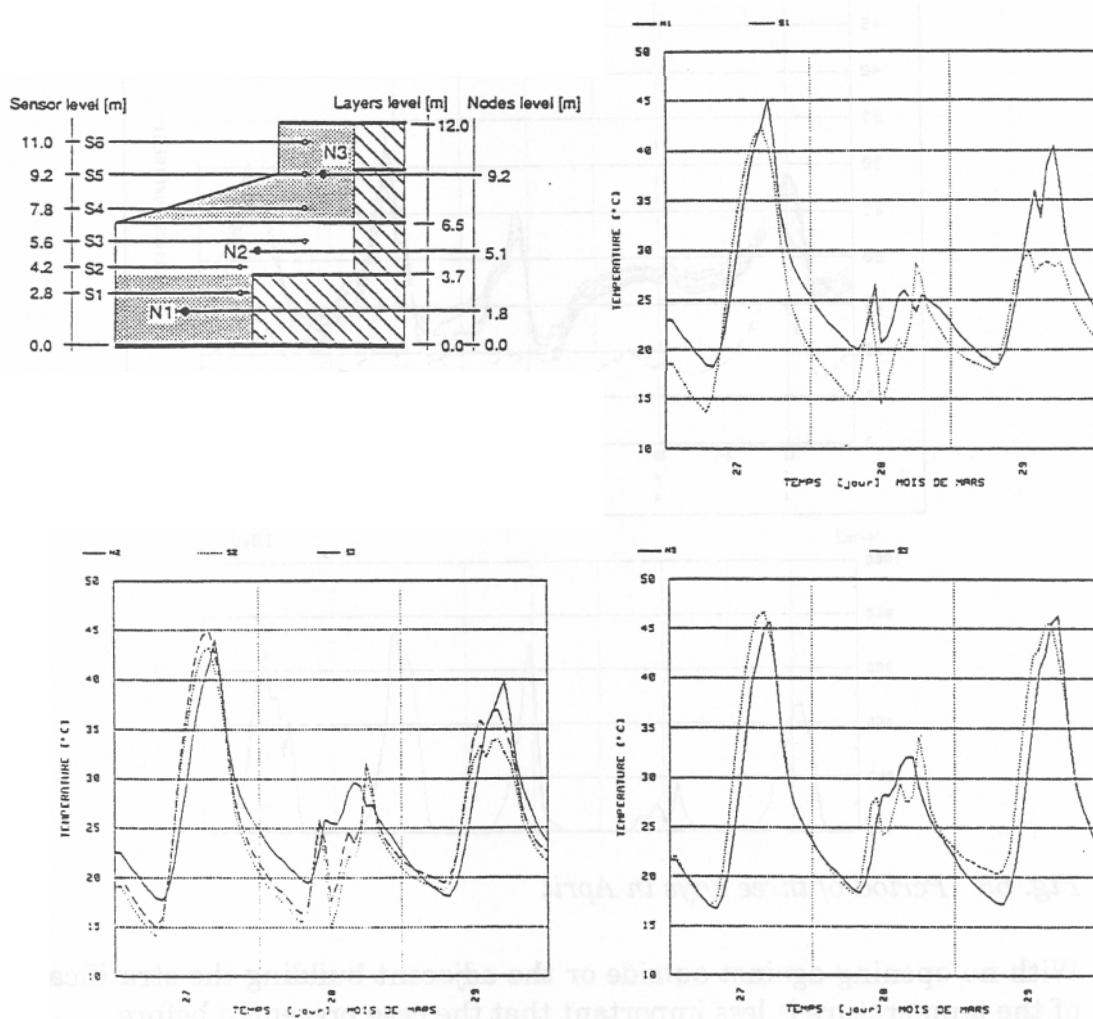
Fig. 67 Results of the comparison for the 27, 28, 29 of March

If the first two days are rather well predicted, the last one is not well predicted in the lower parts. This is not due to the model but simply to the fact that a mobil wall has been opened in the lower part of the atrium. This wall is in direct connection with the building which is at a temperature of 20°C. An important air exchange takes place so that the ground level is maintained at a temperature of 30°C. This effect is not introduced for the moment in the model so that the stratification is not calculated correctly.

The last period is a succession of three days in April. During these days the shading devices are used, the vents are closed and no doors or mobil walls are opened against the building.
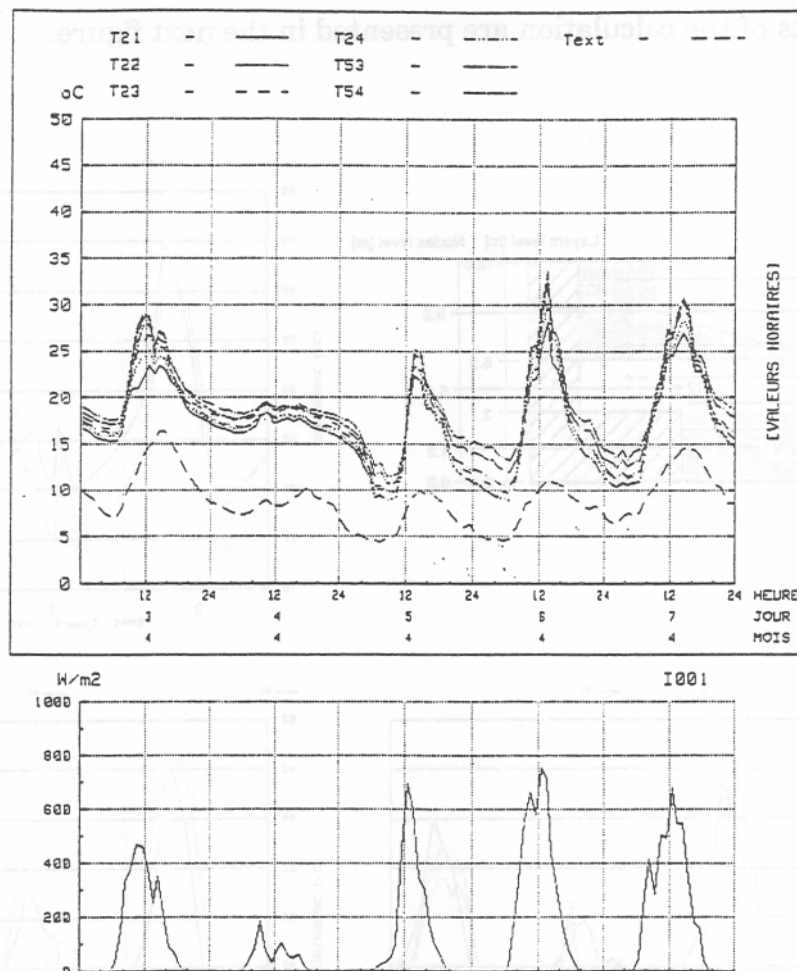
Fig. 68   Period of three days in April

With no opening against outside or the adjacent building the stratification of the temperature is less important that the case presented before.

The comparison of the calculated temperature with the measurements presented in figure 69 are very good and illustrate the validity of the method used.

3:64

Fig. 69

3:65
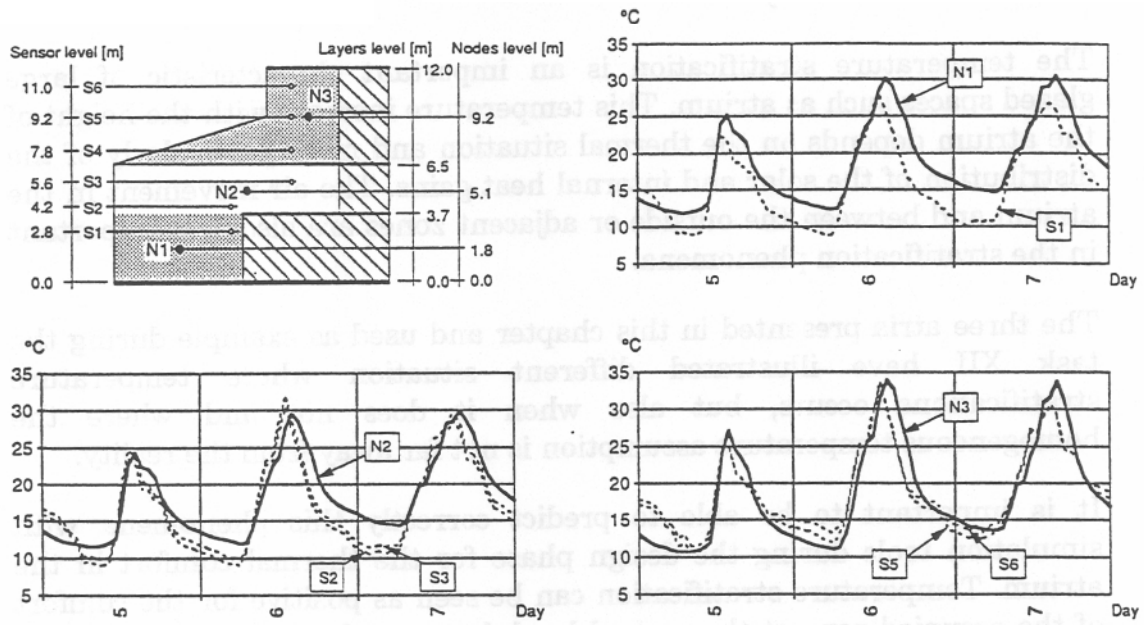
3.13 Summary and conclusions

The temperature stratification is an important characteristic of large glazed spaces such as atrium. This temperature increase with the height of the atrium depends on the thermal situation and more particularly of the distribution of the solar and internal heat gains. The air movement in the atrium and between the outside or adjacent zones are also very important in the stratification phenomena.

The three atria presented in this chapter and used as example during the task XII have illustrated different situation where temperature stratifications occurs, but also when it does not and where the homogeneous temperature assumption is not far away from the reality.

It is important to be able to predict correctly this phenomena with simulation tools during the design phase for the thermal comfort in the atrium. Temperature stratification can be seen as positive for the comfort of the occupied zone at the ground level, but can also lead to overheating problem if the upper part is also occupied or if adjacent offices are in contact with the upper part of the atrium. In winter time, especially in heated atria the situation is different. Temperature stratification is a disadvantage because it will require more heat in order to obtain comfortable conditions on the ground level.

In fact, the stratification of the temperature in the summer is not very often sufficient to provide comfortable condition at the ground level so that natural ventilation must be used. In that case the stratification decreased, and a simulation tool using the well mixed assumption (homogeneous temperature in the atrium) will give reasonable results.

For the energy consumption prediction it is note quite clear if it is very important to take into account the temperature stratification. Very often, but this is not a rule, heated glazed spaces are not stratified in an important manner, see for example ELA. The reason is that the convectors (heat sources) and the cold surfaces (glasses of the gable and the roofs) are creating a strong air movement which will mixed the air temperature.

In order to illustrate the problem some calculations have been performed on the atrium of the university of Neuchatel. In that case the differences (between the calculation with the all mixed and with the stratification model). In the annual energy consumption of the atrium were not important (maximum difference of 12 %) and the difference for the adjacent space less than 1/2 %. For other atrium and building configuration the result can be a bit different but more sensitivity studies about this subject must be done before a general conclusion can be drawn.

The studies done during the task XII about the modelling of the temperature stratification in an atrium with simplified models have pointed out the following points :

1. The linear temperature stratification model work well in the case of ELA. Of course it assumes a certain temperature profile which is not always valid in other cases. In addition when more opening at different levels are present its use can lead to some problems.

2. When no temperature profile is assumed but the volume simply divided in different horizontally partitioning, the correct distribution of the solar gains in the vertical partitioning is the most important parameter for the correct temperature calculation. Programs which are able in their standard form to predict this distribution correctly as DEROB gives already reasonable results. Other programs as TRNSYS must be corrected as it has been shown in chapter 3.11.3 if one wants to use them in the design phase.

3. Simple flow field assumption are able to give reasonable results, particularly when the vents are opened and the atrium naturally ventilated. Down draft problems cannot be pointed out with these simple flow field models.

4. **The effect of the temperature stratification on the energy** consumption seems not to be very important in most typical atrium. But more sensitivity studies about this subject must be done before a correct conclusion can be drawn.

3.14   List of symbols

T	=	Temperature	[°C] [°K]
V	=	Volume	[m^3]
S	=	Surface	[m^2]
p	=	Density	kg/m^2
g	=	Gravity	m/s^2
Z	=	Z coordinate, distance	[m]
B	=	Length	[m]
H	=	Height	[m]
t	=	Time	[s]
Q	=	Heat flux	[W]
X	=	Dimensionless temperature near the floor	[-]
U_i	=	Heat conductance from surface to nearest wall node	[W/°]
U_a	=	Convective heat transfer coefficient for the surface	[W]
C_a	=	Heat capacity rate of inlet air	[W/°]
F_r	=	Fraction of radiation for room heat load	[W]
γs	=	Local strafication number for surface S	
Ys	=	Mean height	[m]
C_D	=	Discharge coefficient	[-]
m	=	Mass floor	kg/s

3.15 References

Stein Are Kvikne.   1991.   Numerisk Simulering av Termisk Komfort i Glassgarder. Institutt for VVS-Teknikk

Maria Wall. 1992. Glazed courtyard at Taman : Thermal performance of the courtyard   and surrounding residential buildings   Measurements and calculations. Swedish Council for Building Research

Y. Brügger, P. Chuard and P. Jaboyedoff.   1990.   Nouvelle Université de Neuchâtel, mesure de la serre. Office fédéral de l'énergie

Kjell Kolsaker and Hans Martin Mathisen. 1992.   Computer simulation of energy use and thermal climate in glazed spaces. Roomvent'92 - Aalborg, Denmark.

3:69

4   Natural Ventilation

4.1   Introduction

The purpose of an atrium ventilation system is to ensure the comfort in summer and to remove moisture and other air pollutants in winter with the lowest possible energy consumption. These considerations will determine the maximum and minimum ventilation capacity respectively. Additionally, the inlets and outlets shall be placed and the inlet air velocities shall be chosen so that draft is avoided in the occupancy zone.

For a natural ventilation system, thermal buoyancy and wind are the driving forces, and these forces can effectively be used in atria if only the system is designed and executed in a proper manner as to obtain sufficient ventilation capacity and suitable regulation possibilities.

A natural ventilation system can be designed either as a displacement system or as a mixing system. It is mainly a question of choosing the right position and size of the inlets. With the right size, it is possible to obtain as low an inlet air velocity as 0.1-0.2 m/s for a displacement system.

The critical situation is the hot summer day with no wind. A sufficient ventilation capacity shall then be obtained by the buoyancy alone, and therefore the greatest importance will be attached to thermal buoyancy in this chapter. The wind will contribute to the ventilation capacity. On the other hand, it can give undesired high air velocities and this has to be taken into consideration when designing the control system.

4.2   Ventilation by Thermal Buoyancy

Natural ventilation by thermal buoyancy is the air exchange between two or more zones with different air densities. These differences can be due to different temperatures or different moisture contents. In an atrium the temperature differences will dominate, and therefore moisture differences

4:1

will not be taken into account in the following discussion of thermal buoyancy.

Ventilation by air exchange implies openings between the zones, and the opening arrangement can either be separate small openings in different levels or it can be a single large vertical or horizontal opening.

The temperature difference can occur due to heating one or more of the zones. After a period of time, steady state conditions will exist with a balance between the heat supply, the temperature difference, the resulting ventilation capacity and the heat losses. It is this steady-state situation, that will be dealt with in the following discussion.

4.2.1   Ventilation Through Two Separate Openings

The simplest   case involves only two small rectangular openings placed above each other as shown on figure 4.1. In both openings an air jet is created as shown on the figure.
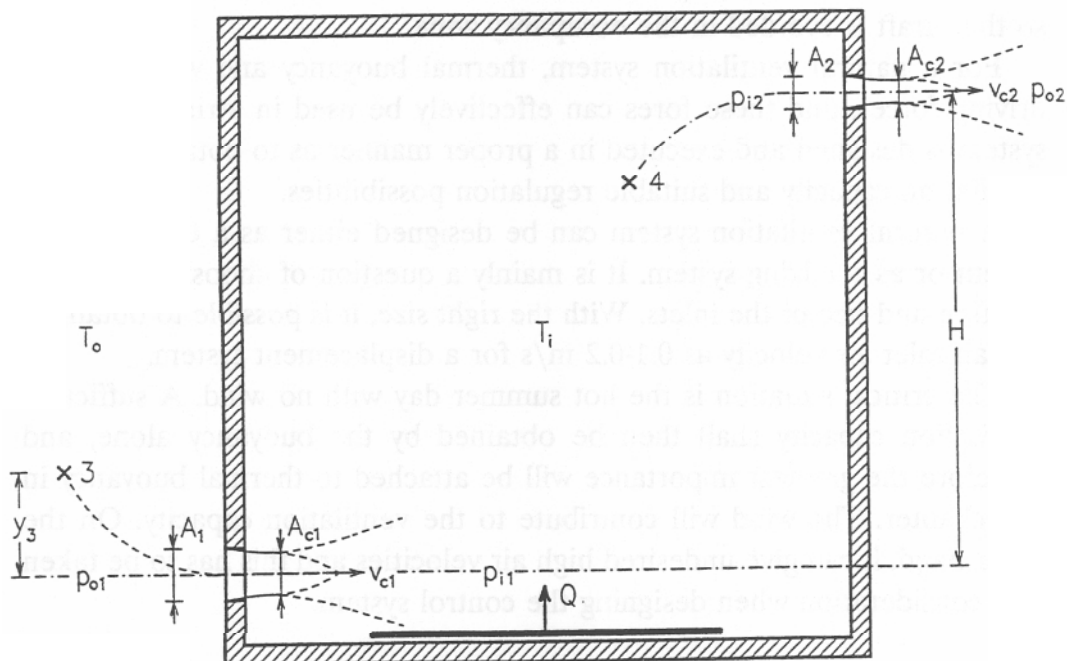

Figure 4.1   Natural ventilation through two openings by thermal buoyancy

The jet passes through the so-called constricted area, where the air pressure is equal to the surrounding pressure and where the air velocity corresponds to, that almost the whole pressure drop across the opening is converted to kinetic energy.

4:2

For the flow situation in question, the following equations can be set up:

$$\rho_o \, c_p \, A_{cl} \, v_{cl} \, \Delta T \, = \, Q_s \qquad \text{(energy conservation)} \qquad (4.1)$$

$$\rho_o \, A_{cl} \, v_{cl} \, = \, \rho_i \, A_{c2} \, v_{c2} \qquad \text{(mass balance)} \qquad (4.2)$$

$$\Delta p_1 \, + \, \Delta p_2 \, = \, \Delta \rho \, g \, H \qquad \text{(momentum in vertical direction)} \qquad (4.3)$$

$$\Delta p_1 \, / \rho_o \, = \, v_{cl}^2 / 2 \, + \, \zeta_1 \, v_{cl}^2 / 2 \, = \, \psi_1 \, v_{cl}^2 \, / 2$$

(modified Bernouilli equa-
tion across the inlet) (4.4)

$$\Delta p_2 \, / \rho_i \, = \, v_{c2}^2 / 2 \, + \, \zeta_2 \, v_{c2}^2 / 2 \, = \, \psi_2 \, v_{c2}^2 \, / 2$$

(modified Bernouilli equ-
ation across the outlet) (4.5)

where:

ρ_i and ρ_o are the indoor and outdoor air densities
c_p is the specific heat capacity of the air
A_{cl} and A_{c2} are the constricted inlet and outlet areas
v_{cl} and v_{c2} are the air velocities in the constricted areas
$\Delta \rho$ and ΔT are the differences between indoor and outdoor air density and air temperature
Δp_1 and Δp_2 are the pressure differences across the inlet and outlet
ζ_1 and ζ_2 are the resistance coefficients for the inlet and outlet
Q_s is the surplus heat, i.e. the heat available for heating up the indoor air.

Further relatinships are as follows:

$$A_{cl} \, = \, C_{cl} \, A_1 \quad and \quad A_{c2} \, = \, C_{c2} \, A_2$$

$$v_{cl} \, = \, C_{vl} \, v_{theo} \quad and \quad v_{c2} \, = \, C_{v2} \, v_{theo} \quad with \quad v_{theo} \, = \, (2 \, \Delta p / \rho)^{\frac{1}{2}}$$

4:3

$$\psi_1 = 1 + \zeta_1 \quad and \quad \psi_2 = 1 + \zeta_2$$

where:

C_{c1} and C_{c2} are the contraction coefficients for inlet and outlet
C_{v1} and C_{v2} are the velocity coefficients for inlet and outlet.

The unknown quantities are v_{c1}, v_{c2}, Δp_1, Δp_2 and ΔT or $\Delta \rho$. By using the following relationship between density and temperature:

$$\Delta \rho \sim \rho_i \, (\Delta T / T_o) = \rho_o \, (\Delta T / T_i) \tag{4.6}$$

where T_i and T_o are the indoor and outdoor temperatures, respectively, you get the following solution from the eqs. (4.2) - (4.5) :

$$v_{c1} = \left[\frac{2 \Delta \rho \, g \, H_1}{\psi_1 \rho_o} \right]^{1/2} = \left[\frac{2 \Delta T g \, H_1}{\psi_1 T_i} \right]^{1/2} \tag{4.7}$$

$$v_{c2} = \left[\frac{2 \Delta \rho \, g \, H_2}{\psi_2 \rho_i} \right]^{1/2} = \left[\frac{2 \Delta T g \, H_2}{\psi_2 T_o} \right]^{1/2} \tag{4.8}$$

$$\Delta p_1 = \Delta \rho \, g \, H_1 = \rho_o \Delta T g \, H_1 / T_i \tag{4.9}$$

$$\Delta p_2 = \Delta \rho \, g \, H_2 = \rho_i \Delta T g \, H_2 / T_o \tag{4.10}$$

where $H_1 + H_2 = H$, and where again:

$$H_1 = \frac{H}{1 + (T_i / T_o)(\psi_2 / \psi_1)(A_{c1} / A_{c2})^2} \tag{4.11}$$

$$H_2 = \frac{H}{1 + (T_o / T_i)(\psi_1 / \psi_2)(A_{c2} / A_{c1})^2} \tag{4.12}$$

4:4

Besides you get from equation (4.1):

$$\Delta T = \frac{Q_s}{\rho_o\, c_p\, A_{cl}\, v_{cl}} \qquad (4.13)$$

The result shows, that the aerostatic pressure distribution outside and inside will cross each other somewhere between the openings as shown on figure 4.2. In the crossing point, you have the so called neutral plane or axis where the inside and outside air pressures are equal. There will be an inward air flow through one of the openings and an outward air flow through the other one.
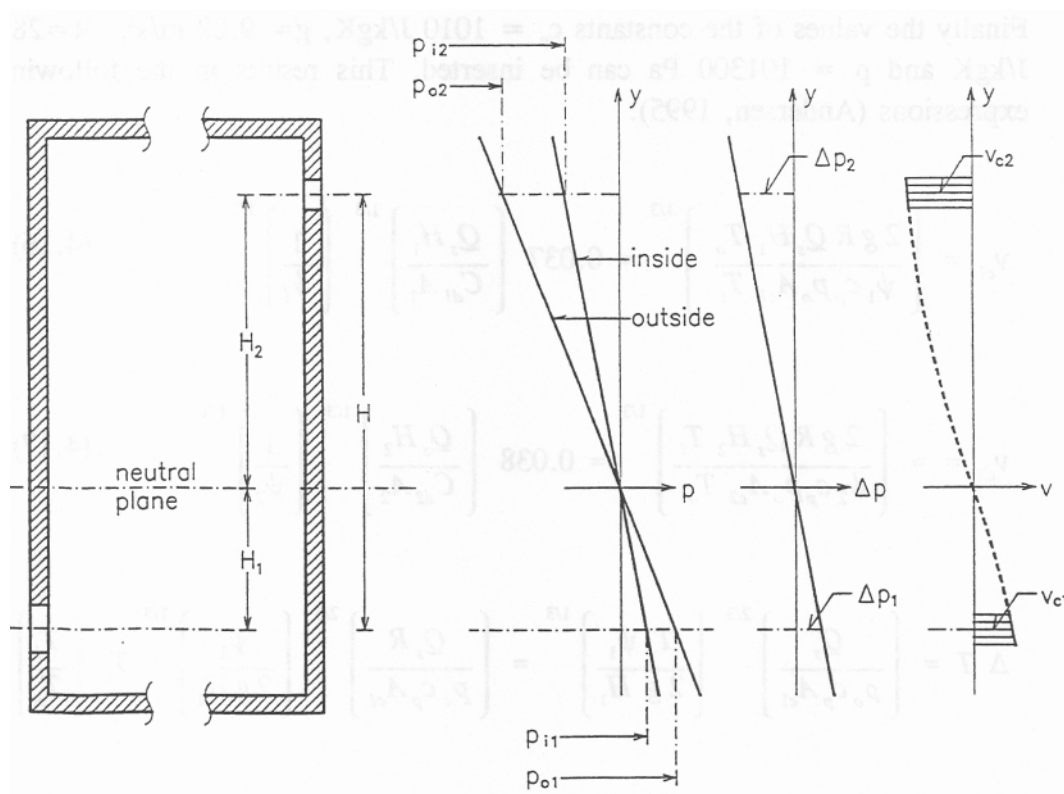

Figure 4.2   Pressures, pressure differences and air velocities at the two openings

The equation (4.13) can be used to eliminate ΔT from the eqs. (4.7) - (4.8). Additionally the following relations between pressure, density and temperature can be used:

$$\rho_i\, T_o = \rho_o\, T_o(\rho_i\, /\rho_o) = (p_o\, / R)\, (T_o\, /T_i) \qquad (4.14a)$$

4:5

$$\rho_o T_i = \rho_o T_o (T_i / T_o) = (p_o / R)(T_i / T_o) \qquad (4.14b)$$

where:

ρ_i and ρ_o are the indoor and outdoor pressures, respectively.

Besides the discharge coefficient can be introduced by (Andersen, 1995):

$$C_d = C_v \, C_c = C_c / (1 + \zeta)^{1/2} = C_c / \psi^{1/2} \qquad (4.15)$$

Finally the values of the constants $c_p = 1010$ J/kgK, $g = 9.82$ m/s², $R = 287$ J/kgK and $p = 101300$ Pa can be inserted. This results in the following expressions (Andersen, 1995):

$$v_{c1} = \left[\frac{2\,g\,R\,Q_s\,H_1\,T_o}{\psi_1\,c_p\,p_o\,A_{c1}\,T_i}\right]^{1/3} = 0.037 \left[\frac{Q_s\,H_1}{C_{d1}\,A_1}\right]^{1/3} \left[\frac{1}{\psi_1}\right]^{1/2} \qquad (4.16)$$

$$v_{c2} = = \left[\frac{2\,g\,R\,Q_s\,H_2\,T_i}{\psi_2\,c_p\,p_o\,A_{c2}\,T_o}\right]^{1/3} = 0.038 \left[\frac{Q_s\,H_2}{C_{d2}\,A_2}\right]^{1/3} \left[\frac{1}{\psi_2}\right]^{1/2} \qquad (4.17)$$

$$\Delta T = \left[\frac{Q_s}{\rho_o\,c_p\,A_{c1}}\right]^{2/3} \left[\frac{T_i\,\psi_1}{2\,g\,H_1}\right]^{1/3} = \left[\frac{Q_s\,R}{p_o\,c_p\,A_{c1}}\right]^{2/3} \left[\frac{\psi_1}{2\,g\,H_1}\right]^{1/3} T_i \left[\frac{T_i}{T_o}\right]^{2/3}$$

$$= 7.1 \cdot 10^{-5}\,T_i \left[\frac{Q_s}{C_{d1}\,A_1}\right]^{2/3} \left[\frac{1}{H_1}\right]^{1/3} \qquad (4.18)$$

It is here estimated that

$$T_o / T_i = 1 - \Delta T / T_i \sim 0.95$$

with an error less than 3% so that the expressions are valid with an error less than 2%.

4.2.1.1   Neutral Axis and Air Velocities.   The air velocities in the openings are determined by the position of the neutral axis, as can be seen for instance in eqs. (4.7) and (4.8). The position of the neutral axis is again determined by the following ratio, cf. eq. (4.11) and (4.12):

$$n^2 = \frac{T_i}{T_o} \frac{\psi_2}{\psi_1} \left[\frac{A_{c1}}{A_{c2}}\right]^2 = \frac{T_i}{T_o} \left[\frac{C_{d1} A_1}{C_{d2} A_2}\right]^2 \tag{4.19}$$

If for instance n=1, you get $H_1 = H_2 = H/2$, and for n=2 you get $H_1 = H/5$ and $H_2 = 4H/5$.

Concerning the quantities in eq. (4.19), it should be mentioned that:

- T_i/T_o is almost constant

- ψ_1/ψ_2 can vary a little if changes in A_1 and A_2 result in changes of the flow directions

- C_{c1}/C_{c2} can vary a little if changes in A_1 and A_2 result in changes of the flow through the openings

Changes of the position of the neutral axis is thus first of all dependent on changes of the ratio A_1/A_2.

If a small inlet velocity is desired in connection with a displacement system, this can be obtained by making H_1 small, and this can again be done by making the area ratio A_1/A_2 large.

A higher inlet air velocity is required by a mixing ventilation system and this can be obtained by increasing H_1. On the other hand, instability problems may occur near the outlet due to wind, if H_1 has a value close to H.

4.2.1.2   Ventilation Capacity and Opening Areas.   The ventilation capacity will be:

$$V = v_{c1} A_{c1} = A_{c1} (2 \Delta T g H_1 /(\psi_1 T_i))^{1/2} \tag{4.20a}$$

and by inserting eq. (4.8) you obtain:

$$V = 0{,}037 \, (Q_5 \; H^l)^{1/3} \; (C^{dl} \; A_l)^{2/3} \qquad\qquad (4.20b)$$

If the outlet area is kept fixed and the inlet area is varied, there will not be proportionality between the ventilation capacity and the inlet area. For instance, a doubling of the inlet area, so that $n = A_1/A_2 = 2$, will only increase the ventilation capacity by 26% if the temperature difference is kept constant and only by 17% if the net heat input is kept constant. By a six fold increase of the inlet area, the increase in ventilation capacity is 39% and 25% respectively. The reason is that by increasing the inlet area the neutral plane moves downward decreasing the pressure difference across the inlet and if the net heat input is kept constant, it results in a lower temperature difference which further decrease the pressure difference (or the "driving forces").

The ratio between a reference ventilation capacity V_{ref} with $A_1/A_2 = 1$ and fixed A_1 and the capacity with any other area ratio is, when ΔT is kept constant (cf. Equation (4.20a) together with Equations (4.11) and (4.19)) :

$$\frac{V_1}{V_{ref}} = \left[\frac{2}{1 + n^2}\right]^{1/2}$$

For fixed outlet area A_2 and constant ΔT you get similarly:

$$\frac{V_2}{V_{ref}} = \left[\frac{2}{1 + 1/n^2}\right]^{1/2}$$

These relationships between ventilation capacity and area ratio are illustrated on figure 4.3a.

The condition that ΔT is kept constant is not realistic in practice as it implies that the net heat input is increased with the same rate as the ventilation capacity. In practice the net heat input will rather be constant. This leads to, cf. Equation (4.20a) together with Equations (4.11) and (4.19):

$$\frac{V_1}{V_{ref}} = \left[\frac{2}{1 + n^2}\right]^{1/3}$$

$$\frac{V_2}{V_{ref}} = \left[\frac{2 \, n^2}{1 + n^2}\right]^{1/3}$$

This relationship is likewise shown in figure 4.3a
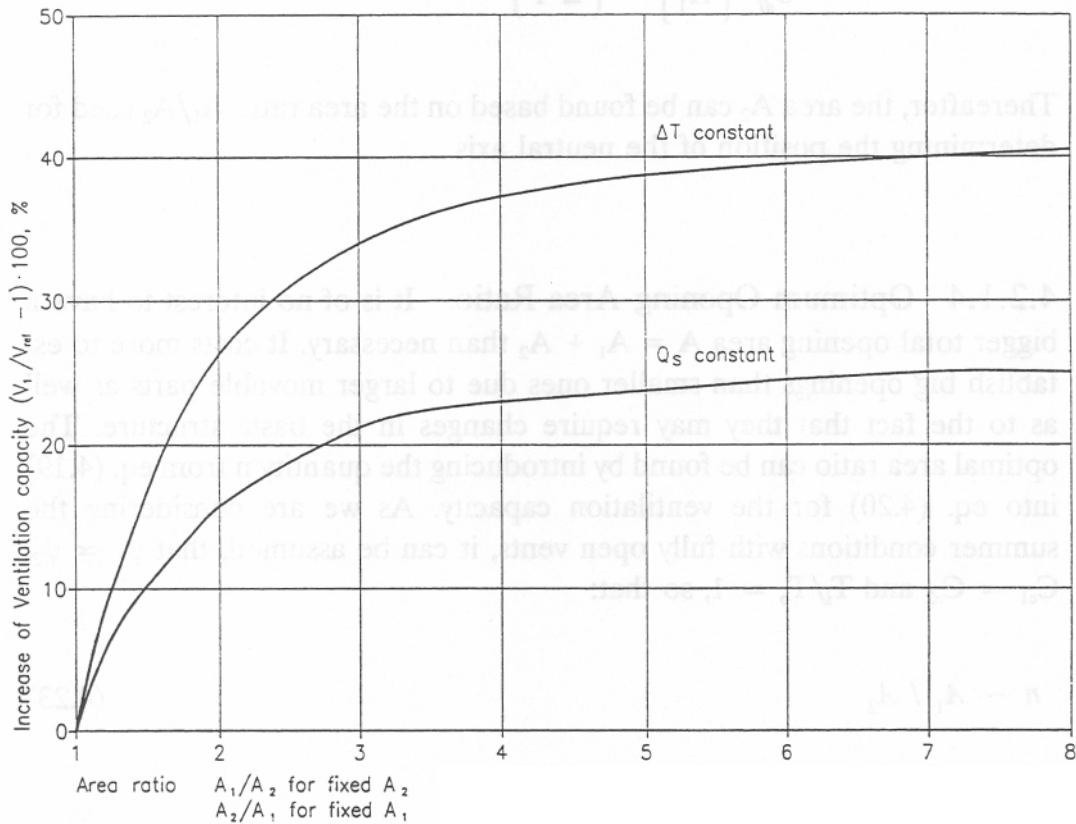
Figure 4.3a   Increase in flow for increased inlet or outlet area by constantly kept temperature difference or net heat input.

4.2.1.3   Required Opening Area.
The usual design task is to determine the opening areas so that a certain ventilation capacity or a certain temperature difference can be obtained under summer conditions. For this purpose, you get from the eqs. (4.20) and (4.18) the following expressions for the inlet area in dependence on either the ventilation capacity or the temperature difference:

$$A_1 = 140 \, \frac{V^{3/2}}{(Q_s \, H_1)^{1/2} \, C_{dl}} \tag{4.21}$$

4:9

$$A_1 = 6.0 \cdot 10^{-7} \frac{Q_s}{C_{dl}} \left[\frac{1}{H_1}\right]^{1/2} \left[\frac{T_i}{\Delta T}\right]^{3/2} \tag{4.22}$$

Thereafter, the area A_2 can be found based on the area ratio A_1/A_2 used for determining the position of the neutral axis.

4.2.1.4 Optimum Opening Area Ratio.

It is of no interest to have a bigger total opening area $A = A_1 + A_2$ than necessary. It costs more to establish big openings than smaller ones due to larger movable parts as well as to the fact that they may require changes in the basic structure. The optimal area ratio can be found by introducing the quantity n from eq. (4.19) into eq. (4.20) for the ventilation capacity. As we are considering the summer conditions with fully open vents, it can be assumed, that $\psi_1 \simeq \psi_2$, $C_{c1} \simeq C_{c2}$ and $T_i/T_o \simeq 1$, so that:

$$n \sim A_1 / A_2 \tag{4.23}$$

and besides you have, when $A_1 + A_2 = A$:

$$A_1 = \frac{A_1}{A_1 + A_2} A = \frac{A_1/A_2}{A_1/A_2 + 1} A = \frac{n}{n + 1} A \tag{4.24}$$

This results in:

$$V = 0.037 \left[\frac{n}{n + 1}\right]^{2/3} \left[\frac{1}{1 + n^2}\right]^{1/3} (C_{dl} A)^{2/3} (Q_s H)^{1/3} \tag{4.25}$$

As Qs is fairly constant, the only variable is n, and it can be found that there is only one extreme value, and that is for $n = 1$ resulting in a maximum value for V as shown on figure 4.3b If the inlet and the outlet have the same shape, the optimal opening ratio from a ventilation capacity point of view is thus obtained, when the two openings are of equal areas.

It should be mentioned that the ventilation capacity is not particularly sensitive to changes in n. It can thus be seen from figure 4.3b that:

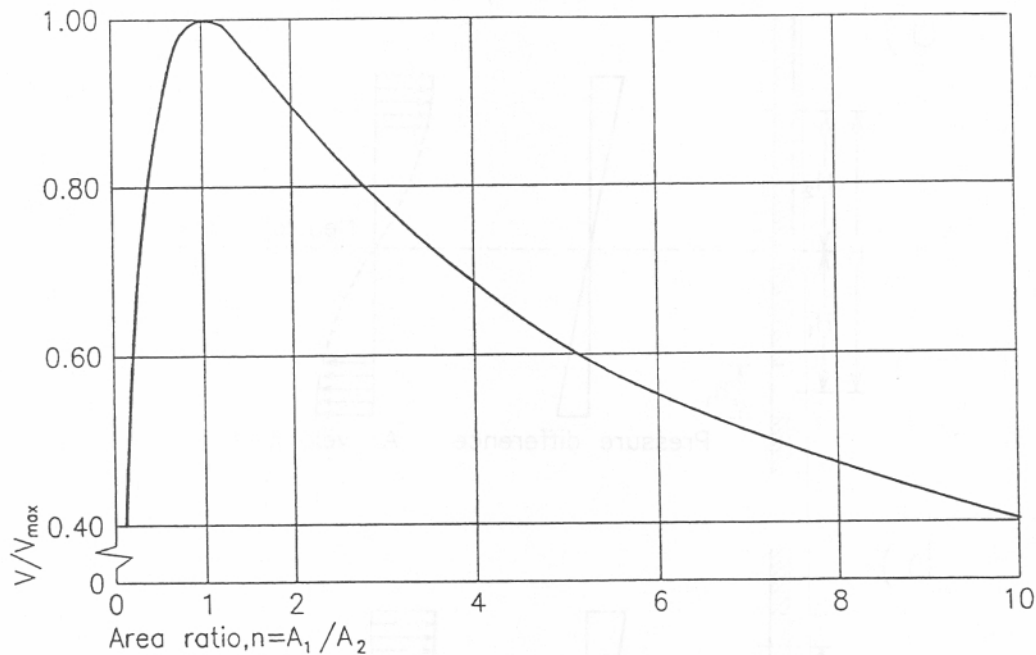$$V \geq 0.9V_{max} \text{ for } 0.5 \leq n \leq 2.0. \tag{4.26}$$

4:10

Figure 4.3b   *The ventilation capacity as a function of the area ratio when the total opening area is kept constant*

4.2.1.5   Threshold Position. Bidirectional Flow.   The neutral axis moves downward for increasing area ratio A_1/A_2, cf. eq. (4.11). At the same time the vertical velocity distribution over the opening goes from being almost constant to becoming more and more parabolic. When the neutral axis passes below the upper edge of the inlet, air starts to move outward through the part of the inlet between the neutral axis and the upper edge as shown on figure 4.4.

The neutral axis coinciding with the upper edge of the inlet is thus a threshold position for having an uni- or a bidirectional flow through the inlet. For this position the ventilation capacity can be determined by:

$$V_{thres} = \int_A v dA = \frac{2}{3} A_{cl} \, v_{cmax} = (2/3)C_{dl} \, A_1 \, (2 \Delta \rho \, g \, h_1/\rho_o)^{\frac{1}{2}} \tag{4.27}$$

If the air velocity is assumed constant and with a value corresponding to the pressure difference in the middle of the inlet you obtain the following capacity, c.f. eg. (4.7):

$$V = v_{cl} \, A_{cl} = C_{dl} \, A_1 \, (2 \Delta \rho \, g \, (h_1/2) /\rho_o)^{1/2} \tag{4.28}$$
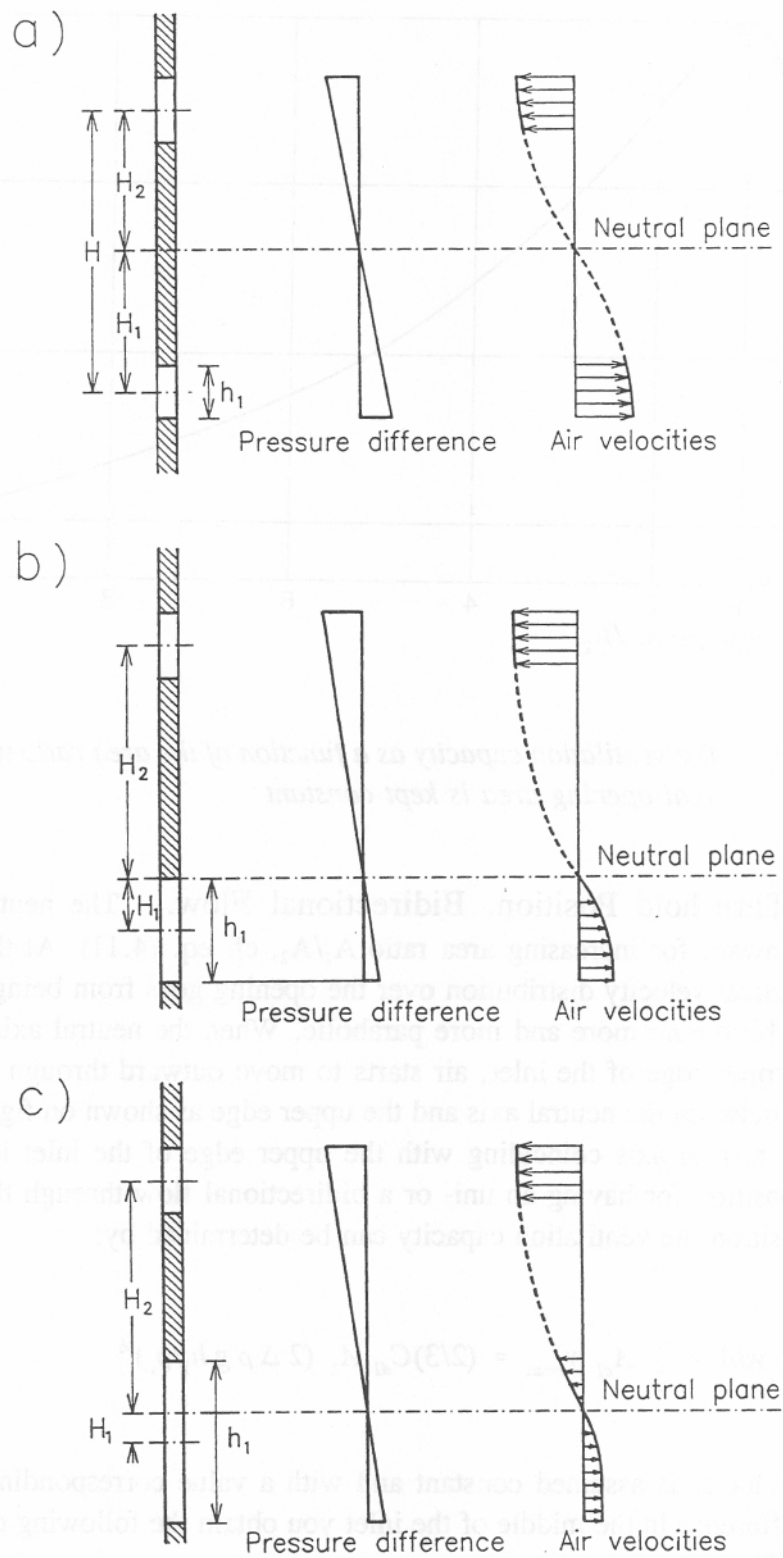
4:11

Figure 4.4   The position of the neutral axis by different area ratios with corresponding pressure differences and air velocities.

4:12

The ratio between the two capacities is:

$$\frac{V_{hra}}{V_{hra}} = 0,94$$

The error in using the ventilation capacity expression (4.20) is thus small and therefore the expressions derived so far can be used with good approximation as long as the neutral axis position is not below the threshold position, i.e. the upper edge of the inlet (or above the lower edge of the outlet).

In order to be sure beforehand that the neutral axis is above the threshold position, a certain requirement can be put on the opening height h_i of the inlet. This height shall be smaller than the height determined by the following mass balance equation:

$$(2/3)\ \rho_o\ C_{d1}\ (b_1\ h_1)\ (2\ \Delta\rho\ g\ h_1\ /\rho_o)^{1/2} = \rho_i\ C_{d2}\ A_2 (2\ \Delta\rho\ g\ (H - h_1\ /2)/\rho_i)^{1/2}$$

As $(\rho_i\ /\rho_o)^{1/2} \sim 1$ and by assuming that $C_{d1} \sim C_{d2}$, this can be reduced to:

$$2/3\ b_1\ h_1^{3/2} = A_2\ (H - h_1/2)^{1/2} \tag{4.29}$$

By squaring you get an equation in 3. degree for determining the threshold value of h_1. A first guess can be obtained by omitting $h_1/2$ from the parenthesis leading to:

$$h_1 \sim \left[\frac{3A_2}{2b_1}\right]^{3/2} H^{1/3} \tag{4.30}$$

A similar expressions can be derived for the threshold outlet height.

4.2.1.6 Temperature Stratification.
In a heated room, the air temperature can have one of the four vertical distributions as shown in figure 4.5.

- curve A, downward curved, by strong heating from a centrally placed, concentrated heat source
- curve B, a straight line, which is often used when only the temperature differences between inside and outside in top and bottom are known
- curve C, upward curved, when the heat source is close to the floor, and when there is a good mixing of the incoming air just above floor level.

4:13

curve D, constant temperature, used when all the incoming air becomes well mixed shortly after the entrance.
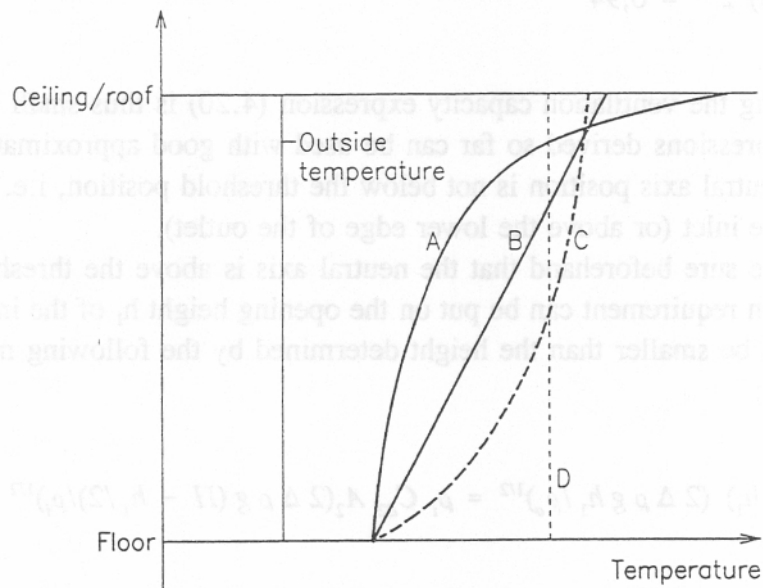

Figure 4.5   Possible vertical temperature distributions in a heated room represented by the curves A, B, C and D.

Temperature measurements in atria have shown a temperature distribution similar to curve A, when inlets and outlets are almost closed, similar to curve B, when they are slightly open and similar to curve D, when they are fully open.

For the straight line distribution, you in principle get pressure distributions as shown on figure 4.6. They will cross each other in order to get the mass balance fulfilled.

Taking the crossing point (or the neutral axis) as the starting point where $T_i = T_{io}$, the temperature distribution can be expressed by:

$$T_i = T_{io} + az \tag{4.31}$$

so that the density becomes:

$$\rho_i = \rho_{io} \, T_{io} / T_i = \rho_{io} \, T_{io} / (T_{io} + az) \tag{4.32}$$

The following pressure difference between outside and inside can then be derived (Andersen, 1995) :

4:14

$$\Delta p = p_o - p_i = (\rho_o - \rho_{io}) g \, y + 0.5 \, g \, \rho_{io}(a/T_{io})y^2$$

$$= \Delta \rho_o \, g \, y + b \, g \, y^2/2 \tag{4.33}$$

where:

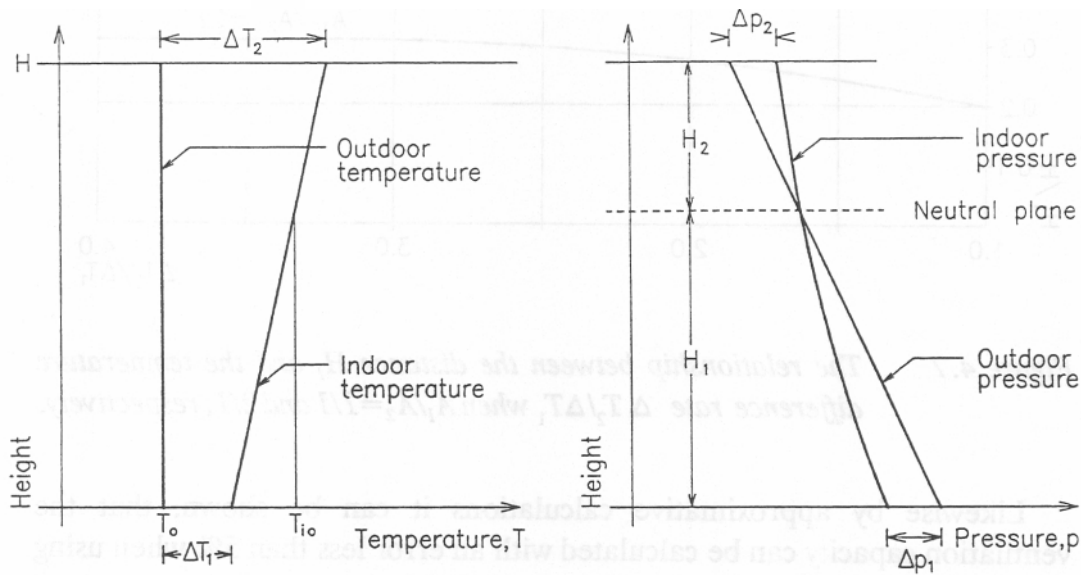$$b = \rho_{io} \, a/T_{io} = \rho_{io} \, (\Delta T_{12}/H) \, / \, T_{io} \tag{4.34}$$

Figure 4.6   Pressure conditions by linear indoor temperature distribution

By calculating first Δp_1 and Δp_2 across the two openings from eq (4.33), next the corresponding velocities by using eqs. (4.4) and (4.5) and then inserting these velocities into a squared mass balance equation, eq. (4.2), you get the following equation for determining the position of the neutral axis, when assuming $\rho_i/\rho_o \simeq 1$, $\psi_1 \simeq \psi_2$ and $C_{c1} \simeq C_{c2}$:

$$A_1^2 \, (\Delta \rho_o g H_1 - b g H_1^2/2) = A_2(\Delta \rho_o g H_2 + b g H_2^2/2) \tag{4.35}$$

As $H_2 = H - H_1$ this results in an equation of 2. degree in H_1, but with $\Delta \rho_o$ being dependent on H_1.

Approximate calculations with $A_1 = A_2$ and $A_1 = 2A_2$, respectively, result in the neutral axis position shown on figure 4.7 in dependence of the ratio $\Delta T_1/\Delta T_2$. For ΔT_1 moving towards zero (or $\Delta T_2/\Delta T_1$ moving towards infinity) you find $H_1/H = 0.71$ and 0.45 for $A_1/A_2 = 1/1$ and $2/1$, respectively. The

4:15

temperature stratification results in a bigger pressure difference at the outlet and a smaller one at the inlet, and this means again that the neutral axis moves above the position valid for constant indoor temperature.
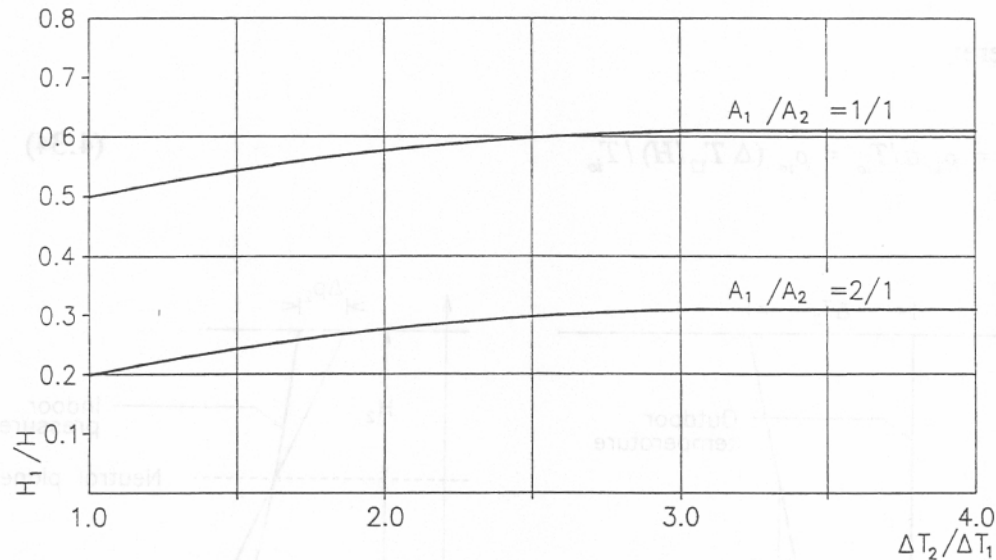

Figure 4.7   *The relationship between the distance H_1 and the temperature difference rate $\Delta T2/\Delta T1$ when $A_1/A_2 = 1/1$ and 2/1, respectively.*

Likewise by approximative calculations it can be shown, that the ventilation capacity can be calculated with an error less than 5% when using the eq. (4.20) with an indoor temperature (mean temperature) determined by:

$$T_i = T_o + (\Delta T_1 + \Delta T_2)/2 \qquad (4.36)$$

The reason for the good approximation is that the indoor pressure distribution is very close to a straight line even with a ratio $\Delta T_2/\Delta T_1 = 4/1$. The curved indoor pressure distribution shown on figure 4.6 is thus strongly exaggerated.

4.2.1.7   Opening Orientation.

The two openings may be placed horizontally or one may be placed vertically and the other horizontally, or they may be placed more or less sloped. The determining equations will remain unchanged, so that the same will be case for the solution. The air velocities, the ventilation capacities etc. are thus independent of the orientation of the openings, unless the orientation makes changes in the coefficients for velocity and contraction.

4:16

4.2.1.8 Surplus Heat.

The heat quantity Qs in eq. (4.1) is the amount of sensible heat available for creating the temperature difference between inside and outside. This amount can under steady state conditions be determined by a heat balance equation, which includes added heat from heating system, electrical equipment, people, adjacent rooms, sunshine etc and heat losses due to infiltration and heat transmission.

Some of the heat sources are dependent on the indoor temperature, and the heat losses are usually dependent on the temperature difference between inside and outside. The surplus heat thus becomes dependent on the inside as well as the outside temperature.

4.2.1.9 Coefficients of Interest.

In the equations derived above, coefficients are involved which take the friction loss into account (the velocity and the resistance coefficient) as well as the contraction of the jet (the contraction coefficient). Additionally, there is a coefficient taking both effects into account (the discharge coefficient).

The Velocity Coefficient C_v takes into account that the air velocity will not be completely constant across the contracted area due to friction along the opening edge. You get a mean velocity defined by:

$$C_v \qquad (4.37)$$

where $\qquad$ is the velocity obtained if the whole pressure drop is converted into kinetic energy. The coefficient $\qquad$ will be about 0.97 - 0.99 for sharp-edged openings, corresponding to a friction loss of 2 - 5 %. The coefficient may be markedly lower (Massey, 1989) for sharp-edged openings where the thickness is not negligible.

The Resistance Coefficient $\qquad$ describes the friction loss as a pressure drop defined by:

$$\Delta p_{fr} \qquad (4.38)$$

By using the modified Bernoulli equation (which takes the friction into account), you find the following relationship between the velocity and the resistance coefficient (Andersen, 1995) :

4:17

$$C_v = 1/(1 + \varsigma)^{1/2} \qquad (4.39)$$

or

$$v = (1/ \quad)^2 - 1 \qquad (4.40)$$

For C = 0.95, you get = 0.11.

In practice you may see resistance coefficient values of 1.8 - 2.8 or even higher for sharp-edged openings. These higher values include the contraction and/or the remaining kinetic energy. They may also include a vent that is partly closed, resulting in very high resistance coefficients. It is in fact artificial resistance coefficients, which are created with the purpose to simplify the calculations.

The Contraction Coefficient C_c takes the reduction of the flow cross section in the constricted area into account.
   The contraction coefficient has a value between 0.5 (for a so-called Borda opening) and 1.0 (for a well-curved opening). For a sharp-edged opening, the value will be about 0.6.

The Discharge Coefficient C_d is frequently used in practice. It is defined as the ratio between the actual flow (measured) and the theoretical one, i.e.:

$$C_d = \frac{V_{actuel}}{V_{theo}} = \frac{A_{cl}\, v_{cl}}{A_1\, v_{theo}} = \frac{A_1\, C_c\, C_v\, v_{theo}}{A_1\, v_{theo}} = C_c\, C_v \qquad (4.41)$$

By replacing the velocity coefficient with the resistance coefficient, you obtain, cf. eq. (4.39):

$$C_d = \frac{C_c}{(1 + \zeta)^{\frac{1}{2}}} = \frac{C_c}{\psi^{\frac{1}{2}}} \qquad (4.42)$$

4.2.1.10   Calculation Considerations.

The surplus heat Q_s will as mentioned before usually be dependent on the temperature conditions. Therefore, the calculation of the ventilation capacity often has to be carried out iteratively to get the heat balance equation fulfilled.
   In some cases the constant contributions to the heat balance are so dominating, that it is acceptable to consider Q_s as constant. This is for

4:18

instance the case in the summer situation when determining the necessary opening areas. The heat transmission and the infiltration losses can then be considered as so small that they can be omitted, and the surplus heat will be the sum of the heat from machinery, electrical equipment, people, the sun etc..

In winter the ventilation system should be designed to remove the air pollution.

If it for instance concerns removal of moisture in order to keep a certain moisture content or relative humidity of the indoor air, the necessary ventilation capacity is determined by:

$$ D = G $$

This gives a ventilation heat loss, when ρ   :

$$ Q_v = \rho i\, c_p\, V\Delta T = c_P G\Delta T/(x_i\text{-}x) $$

which has to be included in the heat balance equation. The heat balance may still be positive indicating that further ventilation is needed if an increased indoor temperature can not be accepted. It may also be negative and then more heat should be added if a lower indoor temperature is not acceptable.

4.2.2 Ventilation Through Several Separate Openings

Several separate openings will not change the inside linear pressure distribution. But you must know the position of the neutral axis to be able to calculate the air velocities through the openings. This position can be determined by the mass balance equation:

$$ \sum \rho_o A_{cr} v_{cr} - \sum \rho_i A_{cs} v_{cs} = 0 \qquad (4.43) $$

where index r and s indicates inlets and outlets respectively and where for instance the inlet velocities can be determined by:

$$ \Delta p_r/\rho_o = \Delta \rho\, g\, |y_r| = \psi_r v_{cr}^2/2 \qquad (4.44) $$

4:19

By inserting (4.44) into (4.43), you obtain the the following equation for determining the position of the neutral axis when assuming that

$$\rho_i \simeq \rho, \, \psi_r \simeq \psi_s \text{ and } C_{cr} \simeq C_{cs}:$$

$$\sum A_r |y_r|^{1/2} - \sum A_s y_s^{1/2} = 0 \tag{4.45}$$

For instance for four openings as shown on figure 4.8 you get:

$$A_1 H_1^{1/2} + A_2 (H_1 - L_1)^{1/2} - A_3 (H - H_1 - L_3)^{1/2} - A_4 (H - H_1)^{1/2} = 0 \tag{4.46}$$

where the neutral pressure plane height H_1 is the only unknown quantity. The equation can be solved iteratively. A good first guess can be obtained by solving the equation only taking the highest and lowest opening into account, as they usually contribute most to the equation.

In case the neutral axis goes through one of the openings, this opening can be omitted by the next step in the iteration, as the contribution from that opening to the equation will be almost zero.

When the position of the neutral axis is determined, you can find the air velocities and the ventilation capacity. For the above mentioned case with four openings, you obtain, when assuming that the neutral axis is placed between opening no. 2 and 3 and when using eq. (4.20a) on opening no. 1 and 2:

$$V = C_{d1} A_1 \left[\frac{2 \, g \, \Delta T H_1}{T_i} \right]^{1/2} + C_{d2} A_2 \left[\frac{2 \, g \, \Delta T (H_1 - L_1)}{T_i} \right]^{1/2} \tag{4.47}$$

By introducing:

$$A_2 = n \, A_1, \, y_2 = H_1 \text{-} L_1 = m_2 H_1, \text{ and } C_{d2} = q_2 C_{d1}$$

you obtain:

$$V = C_{d1} A_1 \left[\frac{2 \, g \, \Delta T H_1}{T_i} \right]^{1/2} (1 + n_2^2 \, m_2 / q_2)^{1/2} \tag{4.48}$$
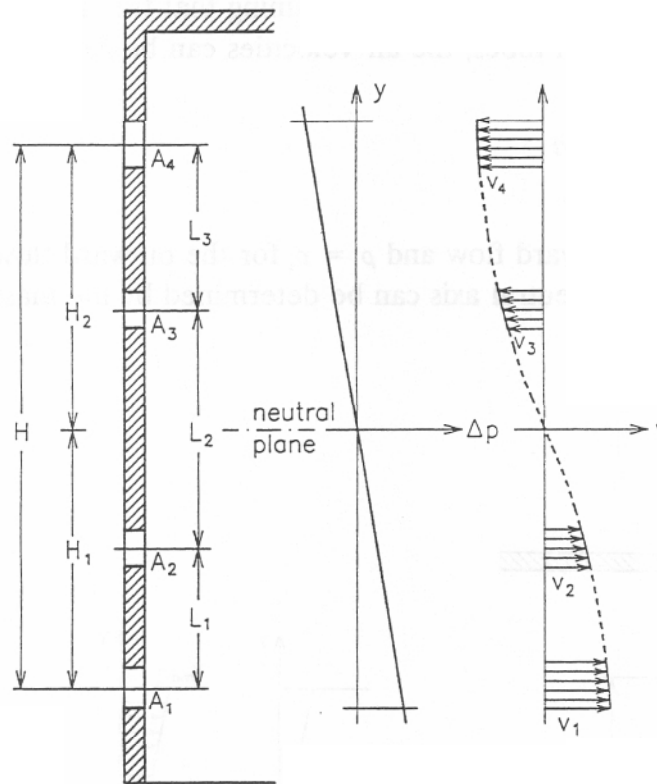
4:20

Figure 4.8 Pressure difference and air velocities by four openings

It is further possible to use the eqs. (4.18) and (4.20)-(4.22) for temperature difference, ventilation capacity, and opening areas, if only the quantity H_1 is replaced by:

$$H_1^{\bullet} = H_1 \, (1 + n_2^2 \, m_2/q_2) \tag{4.49}$$

More generally, i.e. for more than four openings, the same equations can be used by replacing H_1 with:

$$H_1^{\bullet} = H_1 \, (1 + n_2^2 \, m_2/q_2 + n_3^2 \, m_3/q_3 + ...) \tag{2.50}$$

where only openings with inward flow are included, and where H_1 is the distance between the neutral plane and the centre of the lowest opening.

4.2.3 Ventilation Through One Rectangular, Vertical Opening

For a large vertical opening as shown on figure 4.9, an aerostatic pressure will exist outdoors as well as indoors, and under steady state conditions, the inside and outside pressure distribution will cross each other somewhere in

4:21

the opening. This gives an inward air flow in the lower part of the opening and an outward flow in the upper part. Assuming that the flow takes place in thin, horizontal stream tubes, the air velocities can be determined by:

$$V = (2 \, \Delta \rho \, g \, |y| / (\rho \, \psi))^{1/2} \qquad (4.51)$$

where $\rho = \rho_o$ for the inward flow and $\rho = \rho_i$ for the outward flow.
   The position of the neutral axis can be determined by the mass balance equation, and you find:
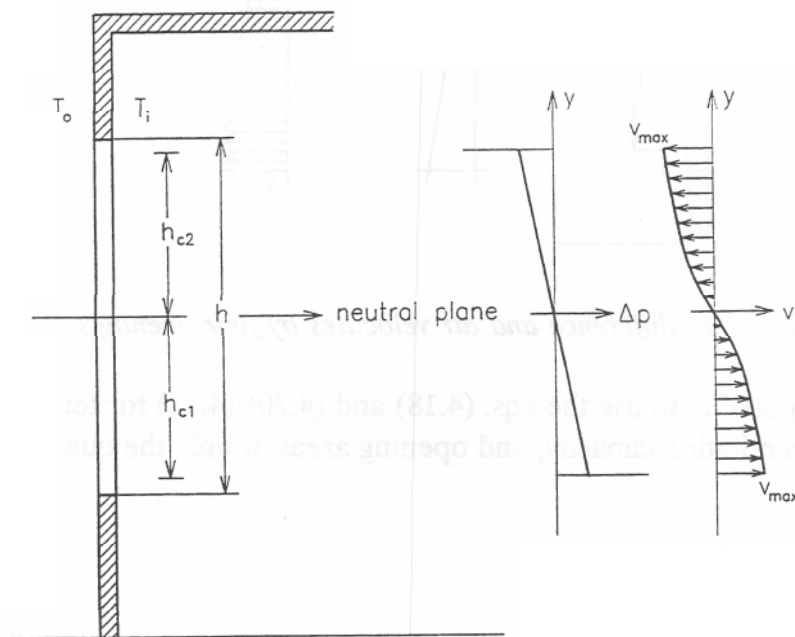
$$h_1/h_2 = (T/T)^{1/3} \qquad (4.52)$$

Figure 4.9 Distribution of pressure difference and air velocity by one vertical opening

As $(T \approx 1$ the position of the neutral axis will be close to the middle of the opening, and you obtain the following maximum velocities at the lower and upper edges of the opening:

$$v_{max} = \left[\frac{2 \, g \, \Delta \, T \, h_c \, /2}{T_i \, \psi} \right]^{1/2} = \left[\frac{g \, \Delta \, T \, h_c}{T_i \, \psi} \right]^{1/2} \qquad (4.53)$$

4:22